



Anion exchange polyelectrolytes for membranes and ionomers

Nanjun Chen, Young Moo Lee*

Department of Energy Engineering, College of Engineering, Hanyang University, Seoul04763, South Korea



ARTICLE INFO

Article history:

Received 12 May 2020

Revised 11 August 2020

Accepted 15 December 2020

Available online 29 December 2020

Keywords:

Anion exchange polyelectrolytes (AEPs)

Anion exchange membranes (AEMs)

Anion exchange ionomers (AEIs)

Anion exchange membrane fuel cells

(AEMFCs)

Peak power density

Durability

ABSTRACT

Anion exchange membrane fuel cells (AEMFCs) have attracted great interest as a low-cost fuel cell technology for clean energy conversion and utilization for the future. AEMFCs have been considered the most promising succedaneum to proton exchange membrane fuel cells (PEMFCs) for addressing the cost issues associated with PEMFCs due to utilizing non-platinum group metals as electrocatalysts under alkaline conditions (such as Ag, Ni, and Co). Herein, we focus on a critical topic of AEMFCs—*anion-exchange polyelectrolytes (AEPs)*—which are essential materials for low-cost AEMFCs. Specifically, AEPs have been used as anion-exchange *membranes (AEMs)* and *binders (or ionomers)* in AEMFCs. Years of study have allowed AEMFCs to recently achieve unprecedented progress, specifically in terms of power density and durability. These properties are comparable to or higher than PEMFCs due to the recent development of high performance AEPs. Currently, most AEPs focused on the application of AEMs, and the importance of ionomer research has not been widely recognized. Moreover, a comprehensive review involving a systematic performance comparison of the state-of-the-art AEMs and ionomers is still lacking, making future research on AEMFCs unclear. This review systematically and comprehensively summarizes the development of AEPs and highlights the importance of cationic species and polymer backbone structures on durability with an emphasis on the importance of ionomer research. We further describe the differences between AEMs and ionomers by comparing the advantages and disadvantages of the state-of-the-art AEMs and ionomers to accurately guide future research on AEMFCs. We cover synthetic methods, degradation mechanisms, strategies to enhance performance, water transport behaviors, structure design criteria, and new challenges for AEMs and ionomers. This review is expected to expand further understanding of AEMs and ionomers and provide a future direction for designing AEMs and ionomers for future AEMFCs.

© 2020 The Author(s). Published by Elsevier B.V.

This is an open access article under the CC BY-NC-ND license (<http://creativecommons.org/licenses/by-nc-nd/4.0/>)

Abbreviation: s: AEIs, Anion exchange ionomers; AEMFCs, anion exchange membrane fuel cells; AEMs, anion exchange membranes; AEPs, anion exchange polyelectrolytes; AFCs, alkaline fuel cells; ASR, area specific resistance; ASU, 6-azaspiro[5.5]undecanium; BPN, poly(biphenyl); BTEA, benzyl triethylammonium; BTMA-ETFE, benzyltrimethylammonium-functionalized poly(ethylene-co-tetrafluoroethylene); BTMA-HDPE, benzyltrimethylammonium-functionalized high-density polyethylene; BTMA-LDPE, benzyltrimethylammonium-functionalized low-density polyethylene; DFT, density functional theory; DHFC, direct hydrazine hydrate fuel cell; DMP, N,N-dimethyl piperidinium; DMSO, dimethyl sulfoxide; E2, Hofmann degradation; FLNs, polyfluorene; GDL, gas diffusion layer; HOR, hydrogen oxidation reaction; HTM, hexyltrimethylammonium; IEC, ion exchange capability; IM, Imidazolium (IM); MEA, membrane electrode assemblies; η , osmotic drag coefficient; ORR, oxygen reduction reaction; PAP, poly(aryl piperidinium); PBI, polybenzimidazole; PEEK, poly(ether-ether ketone); PEM, proton exchange membrane; PEMFCs, proton exchange membrane fuel cells; PEO, poly(ethylene oxide); PFSA, perfluorosulfonic acid; PMFCs, polyelectrolyte membrane fuel cells; PNB, polynorbornene; PPD, peak power density (PPD); PPO, poly(phenylene oxide); PS, polystyrene; PSF, polysulfone; PTFE, polytetrafluoroethylene; QA, quaternary ammonium; ROMP, ring-opening metathesis polymerization; SEBS, styrene-ethylene-butadiene-styrene; SN2, nucleophilic substitution; TAA, tetraalkylammonium; TB, Tröger's base; TFSA, trifluoromethanesulfonic acid; TMA, tetramethylammonium; TPB, three-phase boundary;

1. Introduction

Development of renewable and clean energy sources and energy-conversion technologies has become an urgent need for human society. Fuel cell technologies have been regarded as optimal energy conversion devices for utilizing hydrogen energy, and they have gained popularity in the past few decades since they can directly and efficiently transform the chemical energy of fuels (e.g., hydrogen, hydrazine, and methanol) into electricity in a completely eco-friendly way [1–3]. In the history of fuel cell development, alkaline fuel cells (AFCs) have been employed as the first fuel cell technology used in outer space. However, to explore the applications of fuel cells on earth, polyelectrolyte membrane fuel cells (PMFCs) have attracted the attention of the research com-

TPN, poly(terphenyl alkylene)s; VRFs, vanadium redox flow batteries; λ , hydration values.

* Corresponding author.

E-mail address: ymlee@hanyang.ac.kr (Y.M. Lee).

munity due to the introduction of ion-exchange polyelectrolytes (H^+/OH^-) as solid electrolytes, which address the issues associated with liquid-electrolyte leakage and the instability of electrolytes in AFCs [4–6]. PMFCs reached a milestone when the DuPont Company developed a perfluorosulfonic acid (PFSA) polymer, so-called Nafion®, in the 1970s. PFSA membranes possess excellent physical and electrochemical properties, such as high ion conductivity, mechanical properties and durability. Other commercial proton exchange membrane (PEMs) also have been developed, such as Aquivion® and Forblue®. Therefore, the PFSA membrane and ionomer provide excellent performance and durability for proton exchange membrane fuel cells (PEMFCs), making PEMFCs popular as a clean power generation technology in many fields, particularly in transportation application. Specifically, hydrogen fuel cell vehicles—Mirai and Nexo cars equipped with PEMFCs are currently being produced by Toyota and Hyundai Automotive companies, respectively. However, PEMFCs rely heavily on expensive platinum catalysts and PFSA polyelectrolytes, making the high-cost issues difficult to address, which limits the global applications [7–12].

1.1. Anion exchange membrane fuel cells

To address the cost issues associated with PEMFCs, anion exchange membrane fuel cells (AEMFCs) appeared on the scene in 2000 by operating under alkaline (or high pH) conditions [6–15]. AEMFCs have a distinguishable cost advantage due to the permission of utilizing non-noble metals (such as Ni, Co, Mn, and Fe) as electrocatalysts. AEMFCs pursue a parallel track to PEMFCs and intend to replace the high-cost PEMFCs in the near future. Although PEMFCs still dominate in low temperature fuel cells, some AEMFC prototypes have been currently seen, such as from Po-Celltech Ltd. Among the anion exchange cationic species, hydroxide ion transport membranes represent the majority of anion exchange membranes (AEMs) in AEMFCs compared with chloride, carbonate ions and many other larger cations than hydroxide ions. In this review, we will mainly deal with AEMs, anion exchange ionomers (AEIs) and AEMFCs to accommodate common recognition, although hydroxide ions are the major transporting species. By switching from an acid medium to an alkaline one, AEMFCs also have been endowed with a lot of valuable merits, such as higher oxygen reduction reaction (ORR) kinetics and the elimination of acid-corrosion issues [16–22]. Unfortunately, the insufficient lifetime and power efficiency of AEMFCs have severely hampered their commercial success so far.

In general, AEMFC consists of membrane electrode assembly (MEA), gas diffusion layers, flow field plates, and current collectors, and the MEA is the central component of the AEMFC, as shown in Fig. 1. MEA acts as a power generation device for the hydrogen oxidation reaction (HOR) and ORR, which consists of AEMs and catalyst layer electrodes containing AEIs [23–25]. An ideal MEA should possess high power density and long-term durability under alkaline conditions with an acceptable cost [26–32]. The electrochemical power density and durability of MEAs are primarily determined by the nature of anion exchange polyelectrolytes (AEPs)-based AEMs and AEIs. Technically, the same structure of AEPs can be utilized as both AEMs and AEIs. However, except for OH^- transport, the roles of AEMs and AEIs are different in AEMFCs [33–35]. AEMs are installed in the middle of AEMFCs and act as gas barriers to prevent hydrogen and oxygen cross-over. Nevertheless, AEIs are added in the anode and the cathode catalyst layers to bond well to AEMs and catalysts to decrease the interfacial resistance of MEA [36–38]. More importantly, a qualified ionomer can construct an effective three-phase boundary (TPB) between catalysts (solid), water-containing ionomers (liquid), and reactants (gas) in MEAs to boost the electrochemical performance of AEMFCs [39–42].

1.2. Challenges in anion exchange polyelectrolytes

Generally, AEPs are composed of polymer backbones with pendant cationic groups that transport OH^- and H_2O molecules, signifying that these cationic groups govern the transport of ions and the durability of the AEPs. On the other hand, the polymer backbone is used to house cationic groups and maintain the stability of the morphology of AEPs [43–47]. Note that ideal AEPs should possess high OH^- conductivity and sufficient durability under alkaline conditions. However, it is difficult to find ideal AEPs for AEMFCs due to the following complex challenges. Overall, AEPs face three main technical challenges in AEMFCs.

1.2.1. Insufficient ion conductivity

Compared to H^+ ($M=1$, diffusion coefficient $D=10\pm 2\times 10^{-5}$ cm^2/s) ions in PEMFCs, OH^- has a higher molecular weight and a lower mobility ($M=17$, $D=6\pm 1\times 10^{-5}$ cm^2/s) [6], making OH^- transport slow or difficult, which leads to the lower ionic conductivity of AEPs. Nafion membranes typically display a high proton conductivity of up to 200 mS/cm at 80 °C in water. Thus, a good ion conductivity is one in which the OH^- conductivity of AEMs is close to, or higher than this reference [48–52].

1.2.2. Insufficient durability

Unfortunately, AEPs suffer from an intrinsic drawback under alkaline conditions since most AEPs are easily degraded by OH^- , especially at elevated temperatures [53–58]. Numerous cationic species such as ammonium [59–62], phosphonium [63–65], sulfonium [66], and organic-metal cations [67–70] have been employed in AEPs, while only a few cationic species exhibit sufficient alkaline stability under alkaline conditions [61,71]. Moreover, some aryl ether-based polymer backbones such as poly(ether-ether ketone) (PEEK) [72,73], polysulfone (PSF) [74,75], and poly(phenylene oxide) (PPO) [76,77] could be attacked by OH^- ions as well, causing polymer chain cleavage and degradation of the mechanical properties. Even worse, most AEPs possess inferior oxidation resistance, making the durability situation more severe under the background of inevitable H_2O_2 generation during adverse ORR reactions in the cathode [78,79].

1.2.3. Trade-off between some properties of AEPs

Many properties of AEPs are mutually restricted by each other. In this case, it is a challenge to find an AEP having sufficient all-around physical properties. As a simple example, the ion conductivity of AEPs is mainly controlled by ion-exchange capacity (IEC). High IEC improves the ion conductivity of AEPs, while the water uptake and swelling ratio simultaneously increase, reducing the dimensional stability and mechanical properties of the AEPs [80–83].

On the other hand, there are still other underlying challenges in AEP applications. Most AEMFCs are operated under water-saturated conditions that increase the cell resistance. Therefore, low water permeability of AEMs and ionomers could be one of the critical issues in AEMFCs as the cells need to supply water to the cathode by water back diffusion. Moreover, the carbonation of AEMs and ionomers also could be issues when AEMFCs are operated with H_2 -air.

1.3. Recent developments and progress in AEPs

Researchers have proposed many strategies to boost the performance of AEPs and AEMFCs, including (1) the development of highly stable cationic groups and aryl ether-free polymer backbones [84–86], (2) the optimization of microphase morphologies of AEPs [87–89], (3) the introduction of crosslinking strategies [90–92] and composite methods [90,93–95], and (4) optimization of the water management of AEMFCs [96–100].

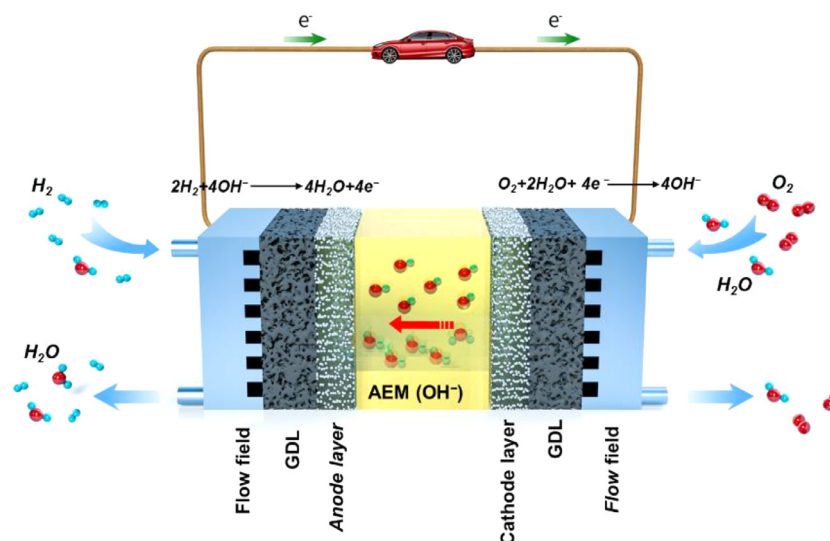


Fig. 1. Schematic representation of an AEMFC.

Years of study have revealed that AEMFCs have recently seen unprecedented progress due to the development of high-performance AEMs and ionomers, specifically in terms of power densities ($>3 \text{ W/cm}^2$) and long-term stability ($>500 \text{ h}$ under 0.6 A/cm^2 current density) [9,97]. The OH^- conductivity issues in AEPs have been well addressed in recent years. AEMFCs with state-of-the-art AEMs have comparable ohmic resistance to Nafion-based acid fuel cells. As a consequence, the durability issues associated with AEMs and ionomers have become a primary challenge in accelerating the commercialization of AEMFCs. Therefore, researchers have made efforts to find highly stable cationic groups and polymer backbones for AEPs.

1.4. Ionomers

Compared to AEMs, the research on ionomers is fairly limited in the literature. Up to 1st April 2020, there are only 45 publications on AEIs or binders or so based on a Web of Science search. So far, many researchers do not even know the importance of ionomers or how to obtain an efficient ionomer. In PEMFCs, ionomers are basically perfluorinated sulfonic acid polymers that have the same polymer structure as the membrane. Obviously, the requirements for the properties of AEMs and AEIs are not always the same due to their different roles. For instance, AEMs require good gas barrier properties and limited water contents and membrane swelling, while AEIs need high water permeability, minimal interaction with electrocatalysts, and sufficient electro-oxidative stability to improve the electrode reactions. Therefore, using the same AEPs as membranes and ionomers is not always a good choice for AEMFCs [101–103].

For these grounds, one should understand that the structural design for AEMs and AEIs may be different as well. As Kim and co-workers reported [104–106] that the phenyl groups and ammonium groups in some polyaromatic AEIs had adverse adsorption effects on electrode catalytic reactions. On the other hand, the water management of AEMFCs is more complicated compared to PEMFCs [98]. Note that there are four water molecules generated at the anode while two water molecules are consumed at the cathode for every four electrons transferred, which makes a water imbalance between the cathode and the anode (Fig. 2). Accordingly, the cathode is inclined to dry-out, while the anode is prone to flooding under high current density.

This review will comprehensively summarize the recent progress of AEPs and highlight the state-of-the-art AEMs and AEIs. Comparisons of these AEPs will also be covered, including synthetic methods, degradation mechanisms, strategies to enhance performance, and structure-property relationships. This review thus addresses what was lacking in reviews of AEPs in recent years. Moreover, this review will point out the right approaches for the structural design of AEMs and AEIs, highlighting the different structural-design criteria between AEMs and AEIs, emphasizing the importance of ionomer research and providing a comprehensive understanding of AEMs and AEIs.

2. Highly stable AEPs: effect of cationic species and polymer backbone

The majority of AEPs have been used as AEMs so far. Therefore, AEPs are often referred to as AEMs, hydroxide exchange membranes (HEMs), solid polymer electrolytes (SPEs), or alkaline polymer electrolytes (APEs) in the literature. Actually, the concept of SPEs was presented as early as the 1970s forelectrochemical device applications [107–110]. The most important example of SPEs is Nafion polyelectrolyte. In 2001, Ageland Fauvarque et al. [111] attempted to use KOH-doped poly(ethylene oxide) (KOH-PEO) and anionic membranes to overcome the problem of liquid electrolyte leakage and carbonate blocking in AFCs. Subsequently, numerous cationic groups and polymer species have been employed to prepare AEPs.

2.1. Ammonium-based AEPs

Ammonium groups have been most extensively investigated in AEPs due to the good nucleophilic activity and adjustability of amine groups. There were 2500 publications on quaternary ammonium (QA) and imidazolium (IM)-based AEPs in AEMFCs from 2000 to 2019 or so. However, most QA and IM groups are prone to degradation under alkaline conditions via the Hofmann degradation (E_2), nucleophilic substitution (SN_2), or ring-opening reaction, especially at elevated temperatures and high pH conditions [112–115], as shown in Fig. 3(a) and (b).

2.1.1. Quaternary ammonium-based AEPs

Focusing on the degradation mechanism of QA groups, the Hofmann degradation is mainly triggered by the elimination of β -hydrogen via an anti-coplanar intermediate. Thus, the degradation

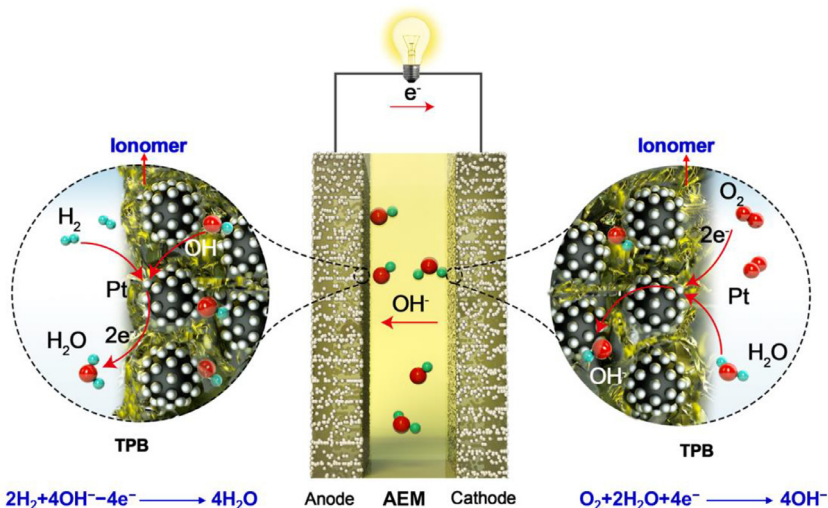


Fig. 2. Schematic representation of three-phase boundaries between fuel gas, ionomer and catalyst in MEA.

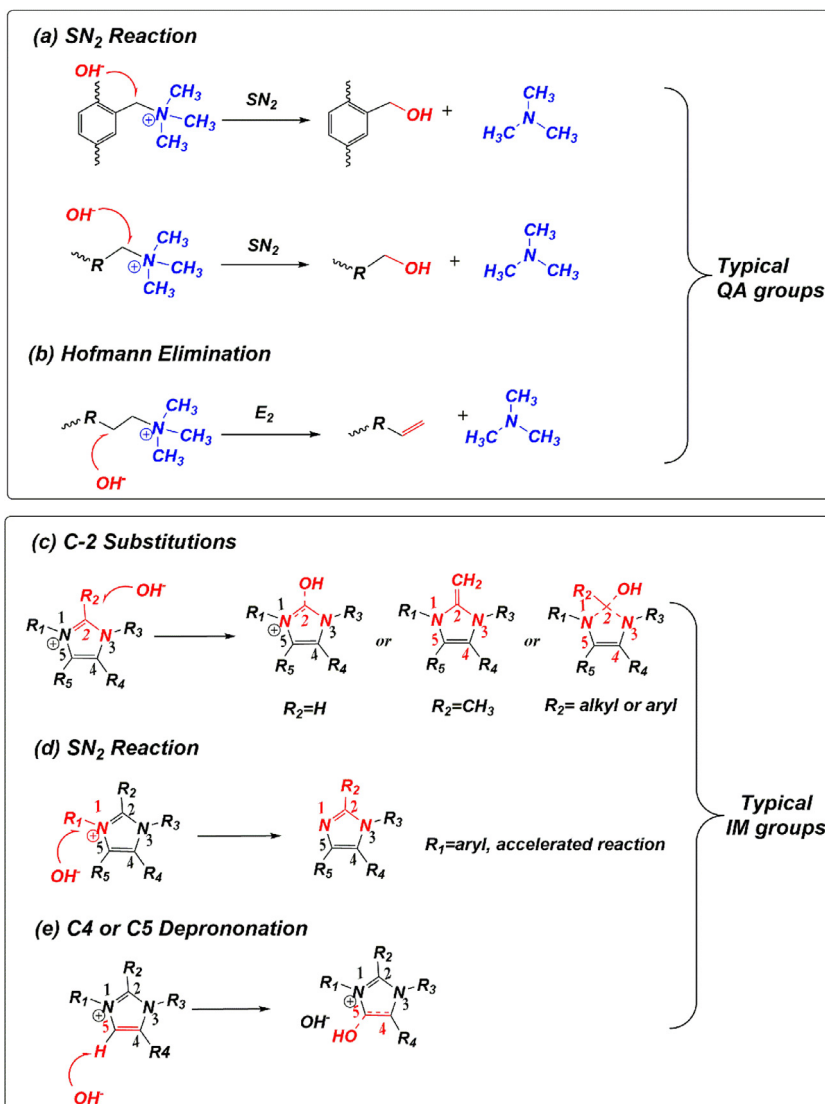


Fig. 3. The degradation pathway of QA and IM groups under alkaline conditions [113-115].

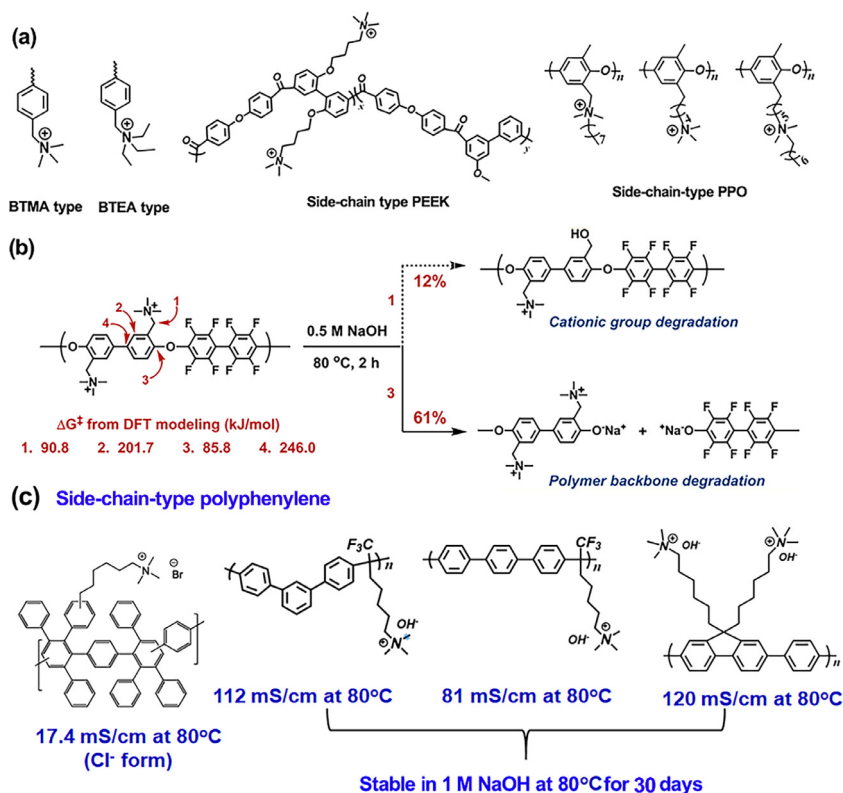


Fig. 4. (a) The chemical structure of BTMA-type AEPs, BTEA-type AEPs, side-chain type PEEK, and side-chain-type PPO [124,125]. (b) The degradation of BTMA-type polyaromatics with DFT calculation. [120], Copyright, 2014. Adopted from with permission from the American Chemical Society. (c) Side-chain-type polyphenylenes along with OH⁻ conductivity [27,47,122].

rate is mainly determined by the reactivity of dehydrogenation and the rate of formation of the intermediate. On the other hand, SN₂ degradation is conducted by a direct nucleophile attack from behind. Therefore, the reaction kinetics are mainly determined by the steric hindrance of QA groups. Hence, the synthesis of specific QA without a β -hydrogen is a typical way to avoid the Hoffmann degradation and improve the alkaline stability. Tetramethylammonium (TMA) was considered to be the most stable QA early on due to the absence of the β -hydrogens [71]. Nevertheless, it is theoretically impossible to directly introduce the TMA in AEPs because the cationic groups are grafted on the polymer backbone. Since most of the currently available AEPs contain phenyl groups, the most popular way to prepare AEPs is by functionalizing halogenated polymers with different tertiary amines. Therefore, benzyl trimethylammonium (BTMA)-based AEPs have been extensively developed [116–118]. In 2002, Danks et al. [119] prepared a series of BTMA-functionalized poly(vinylidene fluoride) (PVDF) and poly(tetrafluoroethylene-co-hexafluoropropylene) (FEP) membranes for direct methanol fuel cells (DMFCs) via a radiation-grafting method, where these AEMs exhibited ion conductivities of ~20 mS/cm at room temperature at that time. BTMA groups have been regarded as more stable than other alkyl benzyl ammonium (BA) such as benzyl triethylammonium (BTEA) under alkaline conditions since the BTMA does not contain any β -hydrogens. However, because of the withdrawing effect of phenyl group on benzyl hydrogen (α -H), BTMA-based AEPs exhibit accelerated SN₂ degradation at the benzyl position, especially at elevated temperatures [120–123].

Zhang, et al. [124] developed a series of side-chain-type PEEK membranes without BA structures, and these membranes showed enhanced alkaline stability in 6 M NaOH at 60 °C for 40 days compared to BA-type AEMs (Fig. 4(a)). Dang et al. [125] prepared a se-

ries of PPO membranes tethered with flexible cationic alkyl side chains. They found that placing QA groups on the flexible spacer units tethered to the PPO backbone facilitated the alkaline stability and ion conductivity (Fig. 4(a)). Kim's group [120] systematically investigated the alkaline stability of BTMA-functionalized polyaromatic membranes by computational modeling and experimental methods. The computational modeling study suggests that the aryl-ether backbone is easy to be cleaved under alkaline conditions due to the electron-withdrawing effect of BTMA groups. Their experimental methods showed that aryl-ether groups degraded after only 2 h of treatment in 0.5 M NaOH at 80 °C, while BTMA-type poly(phenylene) membrane was much stable in some cases (Fig. 4(b)). Based on these results, BTMA groups in aryl-ether backbones have been regarded as unstable for AEPs.

Hibbs [122] presented a series of poly(phenylene) (PP) AEMs with five different cationic head-groups and evaluated their alkaline stability in 4 M KOH at 90 °C. He found that BTMA-type PP exhibited over 30% loss in ion conductivity, while side-chain-type PP with six-carbon spacer showed only 5% ion conductivity loss. After that, many side-chain-type AEPs have been developed. Park et al. [27] also investigated the alkaline stability of side-chain-type PP membranes under various stability testing conditions. They found that side-chain-type PP membranes exhibited a slight degradation in 0.5 M NaOH at 80 °C after 11,000 h.

Lee et al. [47] developed a series of side-chain-type poly(terphenylene) (TPN) AEMs, and these membranes exhibited excellent alkaline stability in 1 M NaOH at 80 °C for 30 days. Bae and coworkers [28] also presented a side-chain-type polyfluorene membrane that possessed an ion conductivity over 100 mS/cm and stable in 1 M NaOH at 80 °C for 30 days (Fig. 4(c)).

Pivovar's group [29] studied the degradation pathways of tetraalkylammonium hydroxides and discussed their degrada-

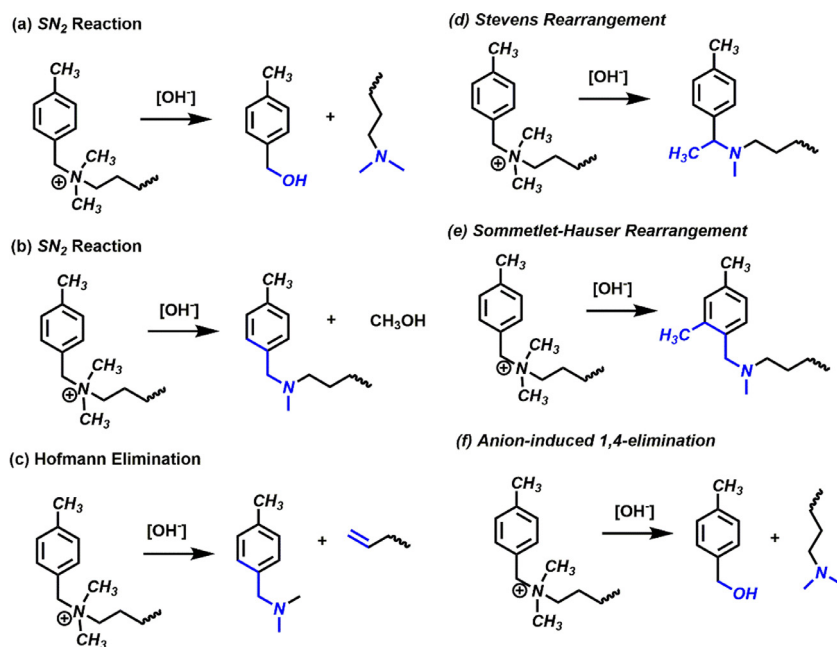


Fig. 5. Chemical degradation mechanisms of BA groups under alkaline conditions [29,126].

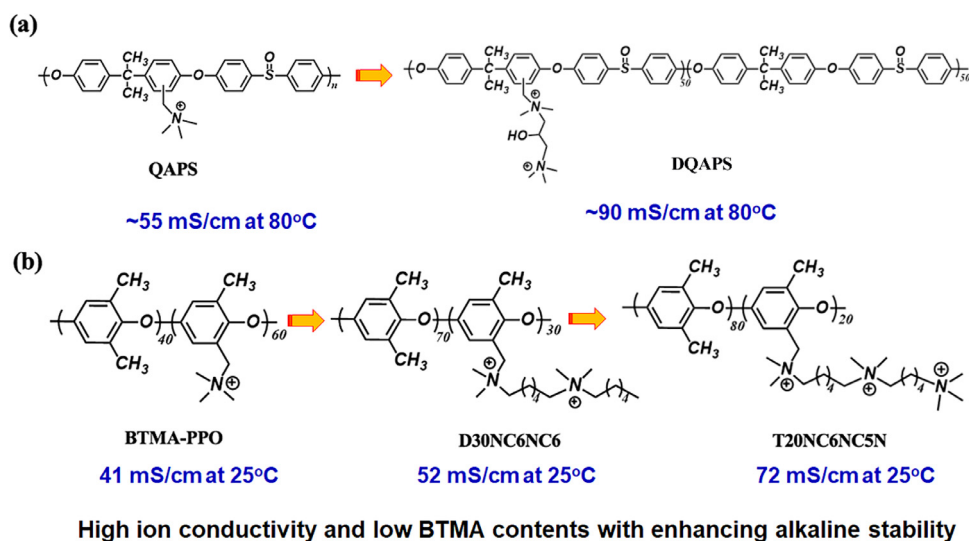


Fig. 6. (a) The chemical structure and OH^- conductivity of QAPS and DQAPS membranes. (b) The chemical structure and OH^- conductivity of multi-cation side chain PPO [127,128].

tion pathways by density functional theory (DFT) calculation. Four degradation pathways ($\text{S}_{\text{N}}2$ substitution, Hofmann elimination, Stevens and Sommelet-Hauser rearrangements) can be found in tetraalkylammonium hydroxides. The degradation pathways of tetraalkylammonium hydroxides are summarized in Fig. 5. Nuñez et al. [126] also studied on the alkaline stability of *n*-alkyl spacer tetraalkylammonium cations in various AEMs and small molecule analogues at 80 °C and 120 °C. They found that BA and benzyl dimethylammonium analogues were more labile than an *n*-alkyl interstitial spacer cation.

On the other hand, Pan et al. [127] presented a dual-ammonium side-chain PSF (DQAPS) membrane to reduce the BA content in the polymer backbone (Fig. 6(a)). They found that DQAPS membranes possessed higher ion conductivity and alkaline stability than QAPS. Hickner and co-workers [128] also prepared a series of multi-cation side chain PPO membranes (Fig. 6(b)). They found that a triple-ammonium based PPO (T25NC6NC5N) membrane simultane-

ously possessed higher ion conductivity, alkaline stability and dimensional stability compared to BA-type PPO. T25NC6NC5N displayed a high OH^- conductivity of 99 mS/cm at room temperature along with 31% in-plane swelling. Overall, multi-cation side chain AEMs cannot completely prevent the degradation of BA groups in the polymer backbone, and more effective approaches are needed to be developed.

Although alkyl spacers and multi-cation side chain strategies have been revealed to have a positive effect on the comprehensive properties of AEMs, the alkaline stability of the AEMs is still a considerable challenge for AEMFC applications. In 2014, Kreuer and co-workers [71] systematically investigated the alkaline stability of 26 different QA groups in 6 M NaOH at 160 °C. The results demonstrated that *N*-heterocyclic 6-azonia-spiro[5.5]undecanium (ASU) and *N,N*-dimethyl piperidinium (DMP) exhibited higher alkaline stabilities among these QA groups. The half-lives of ASU (110 h) and DMP (87.3 h) exceeded the TMA (61.9 h) benchmark.

Consequently, the appearance of ASU and DMP groups opened up newly recognized QA research since there are four β -hydrogens in DMP and eight in ASU, as shown in Table 1. They pointed out that the outstanding alkaline stability of ASU and DMP groups was attributed to the geometry conformation of the ring that constrained the transition state of SN_2 or E_2 reactions. On the other hand, propyltrimethyl ammonium (PTM, 33.2 h) and hexyltrimethylammonium (HTM, 31.9 h) groups exhibited much higher alkaline stability than BA groups (1.38 to 16.6 h), and these results essentially agreed with the previous reports.

However, the utilization of DMP and ASU in AEPs is not easy to be realized due to the lack of effective grafting sites. Olsson et al. [86] reported a series of PAP-based AEMs via a super-acid polycondensation, effectively incorporating DMP in aryl ether-free polymer backbone, as shown in Fig. 7(a). Poly(terphenyl piperidinium) (PTP) membranes were stable in 2 M NaOH at 90 °C for 15 d and exhibited a OH^- conductivity of 89 mS/cm at 80 °C. Subsequently, Peng et al. [129] also reported the same structure of PTP membrane (QAPPT) that possessed the higher OH^- conductivity of 137 mS/cm at 80 °C and were almost stable in 1 M NaOH at 80 °C for 210 days, as shown in Fig. 7(b). QAPPT membrane (thickness: $30 \pm 5 \mu\text{m}$)-based fuel cells reached a peak power density (PPD) of 1.5 W/cm^2 at 80 °C under H_2 - O_2 conditions. Recently, Wang et al. [96] presented a series of PAP copolymers (PAP-TP-x) by introducing a 2,2,2-trifluoroacetophenone block to adjust IEC values, as shown in Fig. 7(c). They pointed out that the inherent viscosity of PAP-TP-x polymers was about 12 times higher than Olsson et al.'s PTP (4.71 dL/g vs. 0.39 dL/g). These PAP-TP-x membranes (thickness: 25 μm) showed a high OH^- conductivity of 193 mS/cm at 95 °C, and were stable in 1 M KOH at 100 °C for 2000 h. PAP-TP-x based fuel cells achieved a PPD of 0.92 W/cm^2 with a Ag cathode under H_2 -air conditions.

However, the production of these PAP-based AEMs highly rely on an excess of trifluoromethanesulfonic acid (TFSA) that is one of the strongest acids known [pK_a (TFSA): -14.6 vs. pK_a (pure H_2SO_4): -11.93].

Compared to DMP-based AEPs, research work on ASU-based AEPs is relatively less common in recent literature. Fig. 8 summarizes current *N*-spirocyclic QA-based AEPs. Olsson et al. [83] reported a series of poly(*N,N*-diallylazacycloalkane)s with different *N*-spirocyclic QA groups. Poly(*N,N*-diallylpiperidinium) showed the

highest alkaline stability in 2 M KOH at 120 °C, while morpholine and azepane-based polyelectrolytes clearly degraded. Unfortunately, these *N*-spirocyclic polyelectrolytes were dissolved in water, which was detrimental to the application of AEPs. At the same time, Jannasch and co-workers [130] reported a series of *N*-spirocyclic QA ionenes that were stable in 1 M NaOH at 80 °C for 1800 h. Similar to the poly(*N,N*-diallylazacycloalkane)s, these spiroionene AEPs also faced water solubility issues.

Chen et al. [131] presented a side-chain-type ASU-PPO via nucleophilic substitution. These ASU-PPO membranes exhibited unacceptable OH^- conductivity of 92 mS/cm at 80 °C and were stable in 1 M NaOH at 80 °C for 1500 h. Subsequently, Li et al. [132,133] also reported a series of ASU and DMP-based polystyrene (PS) membranes via a click reaction. PS-ASU membranes exhibited an 8% loss in ion conductivity after alkaline treatment in 1 M NaOH at 80 °C for 900 h. However, PPO-ASU and PPO-DMP membranes were unstable after alkaline treatment for 900 h.

Pham et al. [134] reported a series of poly(arylene alkylene)s with pendant *N*-spirocyclic QA groups. The results demonstrated that the ring directly attached to the biphenyl backbone degraded significantly faster than the pendant ring in the spirocyclic cations. ASU-based AEMs exhibited a maximum ion conductivity of 102 mS/cm at 80 °C. However, the alkaline stability of ASU-based membranes was lower than that of DMP-based membranes in 2 M NaOH for 720 h at 90 °C. On the other hand, ASU-based AEMs are brittle in these reports [131–134] due to the rigidity of the ASU ring, making their applications difficult. Recently, Zhu et al. [135] presented a physical crosslinking method to improve the film-forming properties of ASU-based AEMs. After crosslinking, the ion conductivity and mechanical properties of ASU-based AEMs can be improved.

Recently, Pham et al. [136] presented four types of PTP membranes with pendant DMP and ASU groups, as shown in Fig. 9. They found that the alkaline stability of DMP-pendant PTP membranes was higher than aforementioned PTP membranes. Besides, DMP attached in different PTP backbones also exhibited large difference in ion conductivity. Moreover, DMP-pendant PTP exhibited higher ion conductivity and alkaline stability than ASU-pendant PTP. Only 5% degradation of DMP groups was found in DMP-pendant PTP after alkaline treatment in 2 M NaOH at 90 °C for 2900 h. Notably, the alkaline stability of ASU and DMP-based PAP membranes was inconsistent with Kreuer's results [71] in

Table 1

Summary of typical cationic groups with currently reported durability at different hydration number (λ =number of water molecules per OH^-).

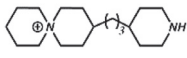
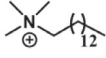
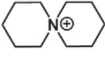
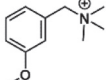
Cationic groups (Abbreviation)	Durability or half-life ($t_{1/2}$)	Alkaline conditions	Cationic groups (Abbreviation)	Durability or half-life time ($t_{1/2}$)	Alkaline conditions
Ammonium groups					
 P-ASU	(1) Stable for 2500 h [131]	1 M NaOH 80 °C ($\lambda=56$)	 TDTM	(1) 6% deg 720 h [61]	1 M KOH 80 °C ($\lambda=56$)
	(2) Stable for 2000 h [131]	5 M NaOH 80 °C ($\lambda=11.2$)		(2) 11% deg 720 h [61]	2 M KOH 80 °C ($\lambda=28$)
	(1) $t_{1/2}=110$ h [71]	6 M NaOH 160 °C ($\lambda=9$)		$t_{1/2}=16.6$ h [71]	6 M NaOH 160 °C ($\lambda=9$)
 ASU	(2) $t_{1/2}=49.5$ h [182]	$\lambda=4$ at RT	 MBTM		
	(3) $t_{1/2}=0.9$ h	$\lambda=0$ at RT			

Table 1
(continued)

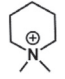

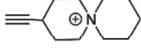
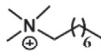
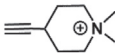
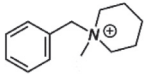
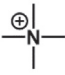
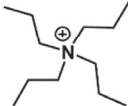

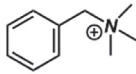
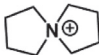
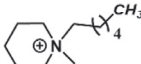
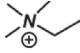
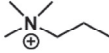
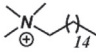
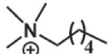
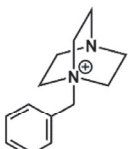
	[182]					
	$t_{1/2}=87.3$ h [71]	6 M NaOH 160°C ($\lambda=9$)			$t_{1/2}=13.5$ h [71]	6 M NaOH 160°C ($\lambda=9$)
DMP				MAABCO		
	None [132,133]	None			$t_{1/2}=12.7$ h [71]	6 M NaOH 160°C ($\lambda=9$)
E-ASU				OTM		
	None [132,133]	None			$t_{1/2}=7.26$ h [71]	6 M NaOH 160°C ($\lambda=9$)
E-DMP				BDMP		
	(1) $t_{1/2}=61.9$ h [71] (2) $t_{1/2}=2080$ h [154] (3) $t_{1/2}>600$ h [154]	6 M NaOH 160°C ($\lambda=9$) 3 M NaOD/ D ₂ O/CD ₃ OD at 80°C ($\lambda\approx 4.8$) $\lambda=1$ at RT			$t_{1/2}=7.19$ h [71]	6 M NaOH 160°C ($\lambda=9$)
TMA				TPA		
	$t_{1/2}=37.1$ h [71]	6 M NaOH 160°C ($\lambda=9$)			(1) $t_{1/2}=4.18$ h [71]	6 M NaOH 160°C ($\lambda=9$)
DMPy				BTMA		
	$t_{1/2}=28.4$ h [71]	6 M NaOH 160°C ($\lambda=9$)			(2) $t_{1/2}>180$ h [154]	$\lambda=1$ at RT
ASN						
	(1) 3% deg 720 h [61] (2) 7% deg 720 h [61]	1 M KOH 80°C ($\lambda=56$) 2 M KOH 80°C ($\lambda=28$)			$t_{1/2}=2.8$ h [71]	6 M NaOH 160°C ($\lambda=9$)
HDMP				ETM		
	$t_{1/2}=33.2$ h [71]	6 M NaOH 160°C ($\lambda=9$)			(1) $t_{1/2}=1.9$ h [71]	6 M NaOH 160°C ($\lambda=9$)
PTM				HDTM		
	$t_{1/2}=31.9$ h [71]	6 M NaOH 160°C ($\lambda=9$)			$t_{1/2}=1.38$ h [71]	6 M NaOH 160°C ($\lambda=9$)
HTM				BAABCO		

Table 1
(continued)

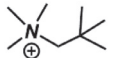
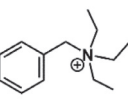
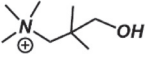
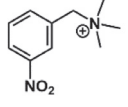
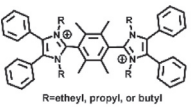
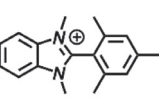
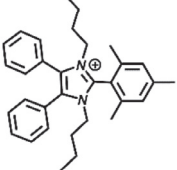
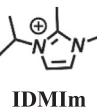
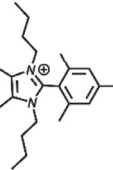
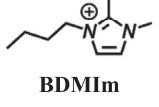
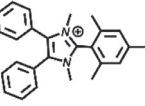
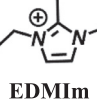
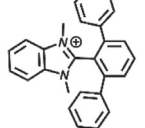
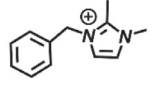
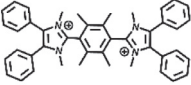
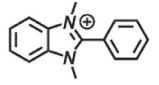
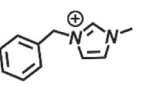
	$t_{1/2}=20.7$ h [71]	6 M NaOH 160°C ($\lambda=9$)		$t_{1/2}=0.68$ h [71]	6 M NaOH 160°C ($\lambda=9$)
	$t_{1/2}>1000$ h [150]	1 M NaOH 88°C ($\lambda=56$)		$t_{1/2}=0.66$ h [71]	6 M NaOH 160°C ($\lambda=9$)
Imidazolium groups					
 R=ethyl, propyl, or butyl	$t_{1/2}\geq 10000$ h [154]	3 M NaOD/ D ₂ O/CD ₃ OD at 80°C ($\lambda\approx 4.8$)		$t_{1/2}=436$ h [154]	3 M NaOD/D ₂ O/ CD ₃ OD at 80°C ($\lambda\approx 4.8$)
	(1) <1% deg 720 h [151] (2) $t_{1/2}\geq 10000$ h [154]	5 M KOH at 80°C ($\lambda=11.2$) 3 M NaOD/ D ₂ O/CD ₃ OD at 80°C ($\lambda\approx 4.8$)		(1) 15% deg 720 h [151] (2) 100% deg 720 h [151]	1 M KOH at 80°C ($\lambda=56$) 5 M KOH at 80°C ($\lambda=11.2$)
	<1% deg for 720 h [151]	5 M KOH at 80°C ($\lambda=11.2$)		(1) 28% deg 720 h [151] (2) 100% deg 720 h [151]	1 M KOH at 80°C ($\lambda=56$) 5 M KOH at 80°C ($\lambda=11.2$)
	$t_{1/2}=7790$ h [154]	3 M NaOD/ D ₂ O/CD ₃ OD at 80°C ($\lambda\approx 4.8$)		(1) 32% deg 720 h [151] (2) 100% deg 720 h [151]	1 M KOH at 80°C ($\lambda=56$) 5 M KOH at 80°C ($\lambda=11.2$)
	$t_{1/2}=3240$ h [154]	3 M NaOD/ D ₂ O/CD ₃ OD at 80°C ($\lambda\approx 4.8$)		(1) 65% deg 720 h [151] (2) 100% deg 720 h [151]	1 M KOH at 80°C ($\lambda=56$) 5 M KOH at 80°C ($\lambda=11.2$)
	$t_{1/2}=2330$ h [154]	3 M NaOD/ D ₂ O/CD ₃ OD at 80°C ($\lambda\approx 4.8$)		$t_{1/2}<0.1$ h [154]	3 M NaOD/D ₂ O/ CD ₃ OD at 80 °C ($\lambda\approx 4.8$)
	$t_{1/2}=1370$ h	3 M NaOD/ D ₂ O/CD ₃ OD at		(1) 100% deg 720 h [151]	1 M KOH at 80°C ($\lambda=56$)

Table 1
(continued)

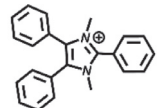
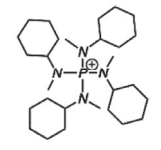
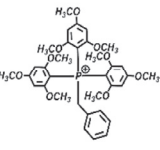
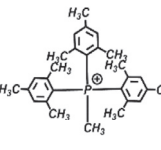
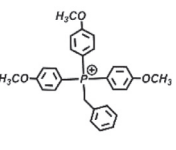
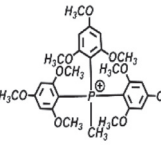
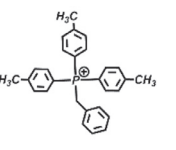
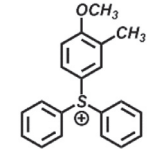
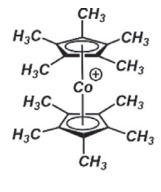
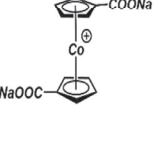
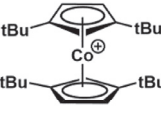
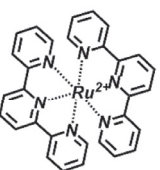
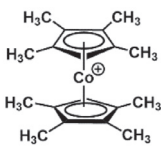
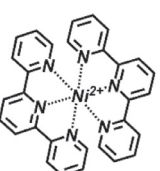

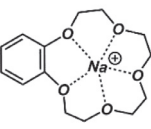
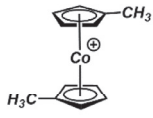
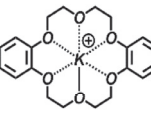
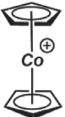
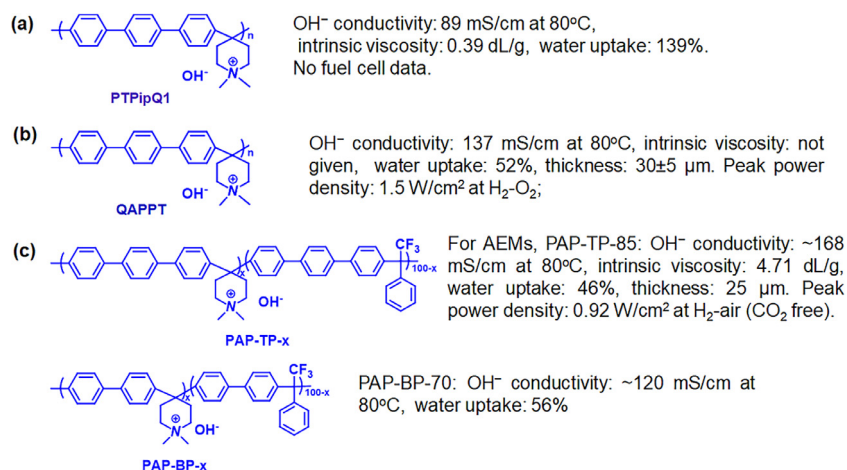
 TPIIm	[154] 80°C ($\lambda \approx 4.8$)	BMIm (2) 100% deg 720 h [151] 2 M KOH at 80°C ($\lambda = 28$)	
Phosphonium groups			
 [P(N(Me)Cy)₄]⁺	(1) <1% deg for 720 h [61] 1 M KOH 80°C ($\lambda = 56$) (2) <1% deg for 720 h [61] 2 M KOH 80°C ($\lambda = 28$)	 BTTP-(2,4,6-MeO)	1 M KOD 80% deg 1000 h [159] CD ₃ OD/D ₂ O (5:1 v/v) at 80°C ($\lambda = 9.25$)
 MTPP-(2,4,6-Me)	1 M KOD 10% deg for 2000 h [159] CD ₃ OD/ D ₂ O (5:1 v/v) at 80°C ($\lambda = 9.25$)	 BTTP-(p-MeO)	1 M KOD 100% deg 170 h [159] CD ₃ OD/D ₂ O (5:1 v/v) at 20°C ($\lambda = 9.25$)
 MTPP-(2,4,6-MeO)	1 M KOD 73% deg for 1000 h [159] CD ₃ OD/D ₂ O (5:1 v/v) at 80°C ($\lambda = 9.25$)	 BTTP-(p-Me)	1 M KOD 100% deg 20 h [159] CD ₃ OD/D ₂ O (5:1 v/v) at 20°C ($\lambda = 9.25$)
Sulfonium group			
	NA NA		
Organometallic-cation groups			
	8.5% deg 1000 h [68] 1 M NaOD/D ₂ O 140°C ($\lambda = 56$)	 ~15% deg after 48 h [69] 1 M KOH/D ₂ O 80°C ($\lambda = 56$)	
	8.2% deg after 1025 h [160] 5 M KOH/CD ₃ OH 80°C ($\lambda = 11.2$)	 NA [67] NA	
	19.5% deg for 1025 h [160] 5 M KOH/CD ₃ OH 80°C ($\lambda = 11.2$)	 NA [70] NA	

Table 1
(continued)

	26.6% deg for 1025 h [160]	5 M KOH/CD ₃ OH 80°C ($\lambda=11.2$)		NA [164]	NA
	(1) ~10% deg after 240 h [69]	1 M KOH/D ₂ O 80°C ($\lambda=56$)		NA [162,163]	NA
	~15% deg for 240 h [69]	5 M KOH/CD ₃ OH 80°C ($\lambda=11.2$) 1 M KOH/D ₂ O 80°C ($\lambda=56$)			

**Fig. 7.** (a) Olsson et al.'s PAP polymer along with basic physical performance [86]. Peng et al.'s PAP membrane with physical properties and fuel cell performance [129]. (c) The performance of PAP-TP-x and PAP-BP-x membranes [96].

DMP and ASU monomers, suggesting that the alkaline stability of AEPs is more complicated than small ammonium hydroxide groups. A detailed comparison of the alkaline stability between DMP and ASU groups with different substituents should be further conducted.

2.1.2. Imidazolium-based AEPs

With regard to IM species, the investigation of IM-based AEMs is still popular in current research. Lin et al. [137] prepared a series of cross-linked AEMs based on ionic liquids (ILs) in 2010. The resulting cross-linked copolymer membranes exhibited a OH⁻ conductivity of 55.8 mS/cm at 60°C. Guo et al. [138] reported a series of IM-typed AEMs that exhibited a OH⁻ conductivity of 48.4 mS/cm at 60°C. Subsequently, Thomas et al. [139] reported a poly(dialkyl benzimidazolium) (PDMBI) membrane based on *meta*-PBI. Actually, PBI-conducting membranes have been widely developed in other fields [140–144], particularly in high temperature PEMFCs. Henkensmeier et al. [145] also reported a *meta*-PBI-based AEMs, as shown in Fig. 10(a). This *meta*-PBI membrane exhibited a OH⁻ conductivity of 58 mS/cm at 60°C, while the membrane quickly degraded under alkaline conditions. The expected degradation mech-

anisms of the PBI membrane were assumed to be nucleophilic substitution and hydrolysis, which were triggered by hydroxide attack at the methyl groups and at the C-2 position, respectively. Later, Henkensmeier et al. [146] introduced an ether group in the para-position of the 2-phenyl substituent to improve the mesomeric stabilization of imidazolium cations (Fig. 10(b)). They found O-PBI was more stable and flexible than meta-PBI under alkaline conditions. Unfortunately, the durability of these polyelectrolytes was still far away from applications due to the existence of labile imidazolium rings. In 2012, Holdcroft et al. [147] indicated that benzimidazolium salt can be stabilized by steric crowding around the labile benzimidazolium C-2 position (Fig. 10(c)). They presented a stable poly[2,2'-(*m*-mesitylene)-5,5'-bis(*N,N'*-dimethylbenzimidazolium)] (Mes-PDMBI) membrane by shielding the C-2 position with a 2,4,6-trimethylphenyl group. The Mes-PDMBI membrane was nearly stable in 2 M KOH at 60°C for 300 h. However, the OH⁻ conductivity of the PDMBI (13.2 mS/cm at 21°C) exhibited a decreasing trend with C-2 steric hindrance compared to a *meta*-PBI membrane. The success in the steric-crowding strategy to stabilize the C-2 position made PBI species attract widespread attention in AEPs at that time.

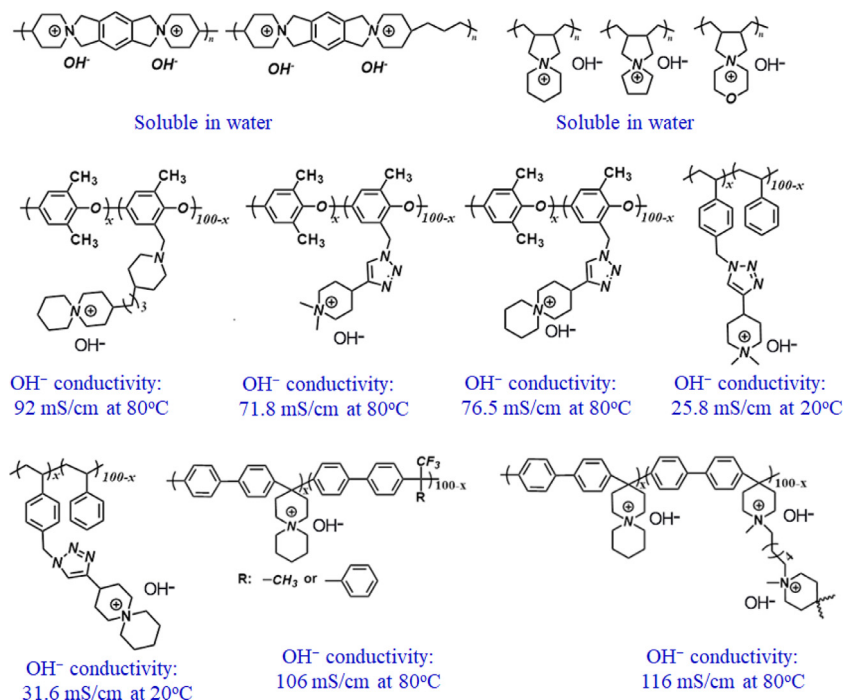


Fig. 8. Summary of N-heterocyclic ammonium-based AEPs along with the comparison of OH^- conductivity [83,130-135].

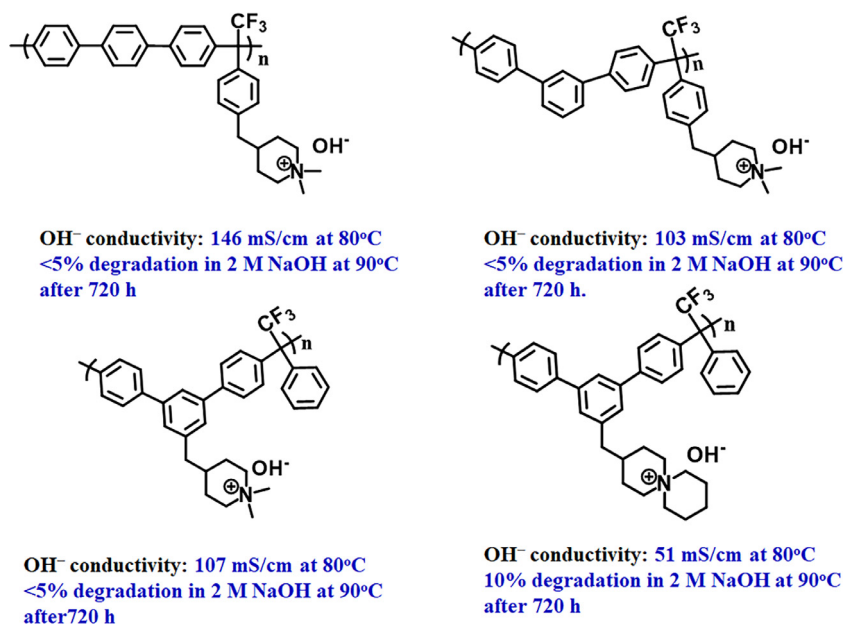


Fig. 9. DMP and ASU-pendent PTP membranes along with performance comparison [136].

After that, Lin et al. [148] investigated the effect of C2-substituents on the alkaline stability of imidazolium salts and AEMs, as shown in Fig. 11(a). Compared to the C2-unsubstituted imidazolium (EMIm), the alkaline stability of C2-substituted imidazolium salts was significantly enhanced at elevated temperatures due to the steric hindrance of the substituents. The alkaline stability of C2-substituted imidazolium salts followed the order (EDMIm) > (EIMIm) > (EMPhIm). Then, they [149] focused on the N3 position of imidazolium salts, and systematically investigated the effect of N3-substituents on the alkaline stability, as shown in Fig. 11(b). They found that the isopropyl substituted imidazolium cation (DMIIIm) showed the highest LUMO energy value and thus exhibited the highest alkaline stability in aqueous NaOH. Price

et al. [150] observed that the steric hindrance is the least effective strategy to stabilize imidazolium cations. They proposed that the most important stabilizing factor for an imidazolium was the ability to provide alternative and reversible deprotonation reactions with hydroxides. The following represents the order of effectiveness of increasing alkaline stability of imidazolium cations: (1) competing deprotonations, (2) electronic stabilization of the C-2 position through resonance such as other aromatic substituents, and (3) steric stabilization of the C-2 position.

To thoroughly understand the character of IM groups, Coates' group [151] systematically evaluated the alkaline stability of IM groups in 1, 2, or 5 M KOH/ CD_3OH at 80°C, and they investigated the effect of C-2, N-1, N-3, C-4, and C-5 substituents on the al-

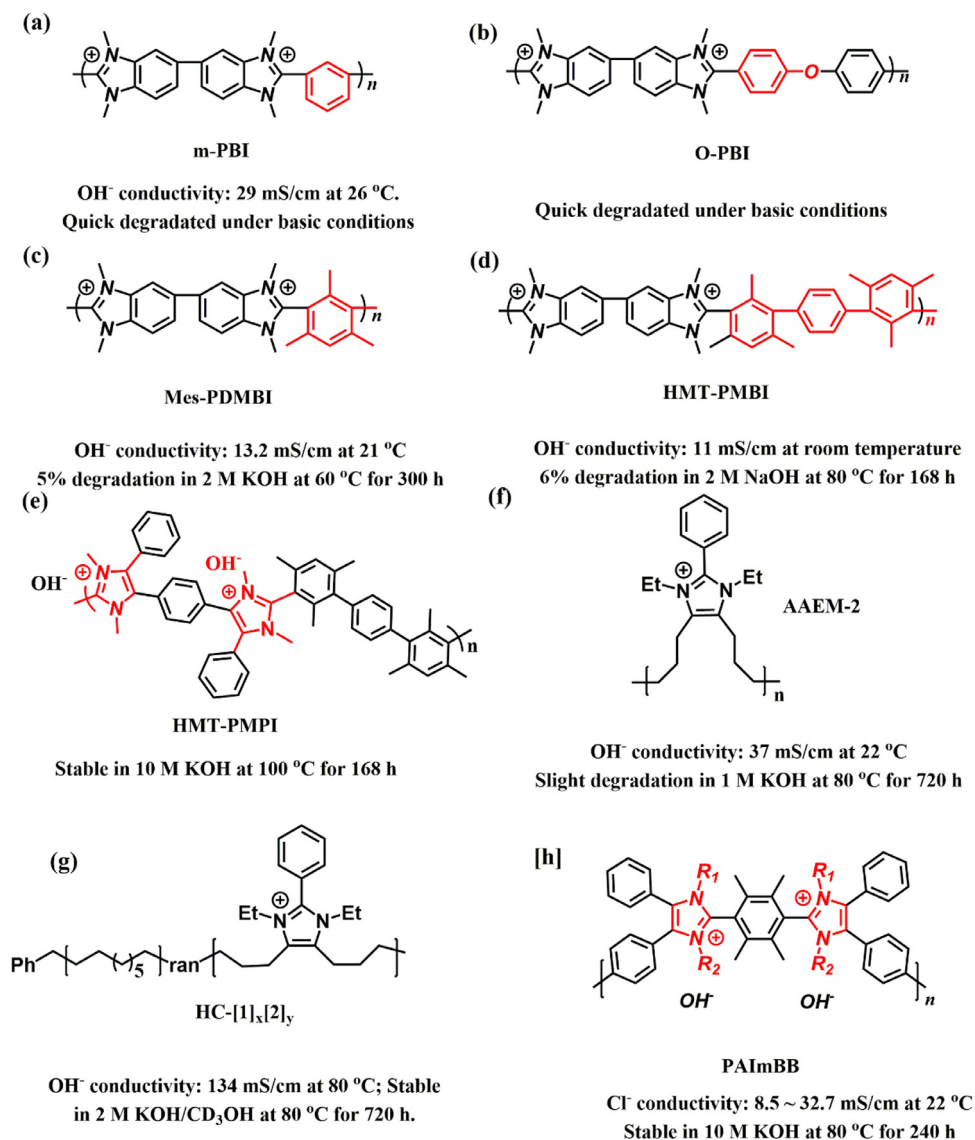


Fig. 10. The structures and a comparison of conductivity and stability in PBI-based AEMs [145-147, 152-156].

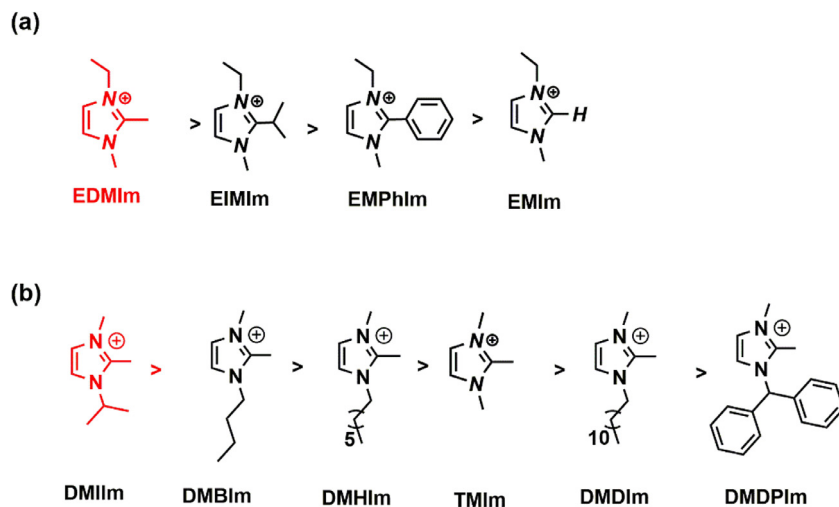


Fig. 11. (a) Alkaline stability comparison between C2-substituted imidazolium in 1 M KOH at 80 °C [148]. (b) Alkaline stability comparison between N3-substituted imidazolium in 2 M NaOH at 80 °C [149].

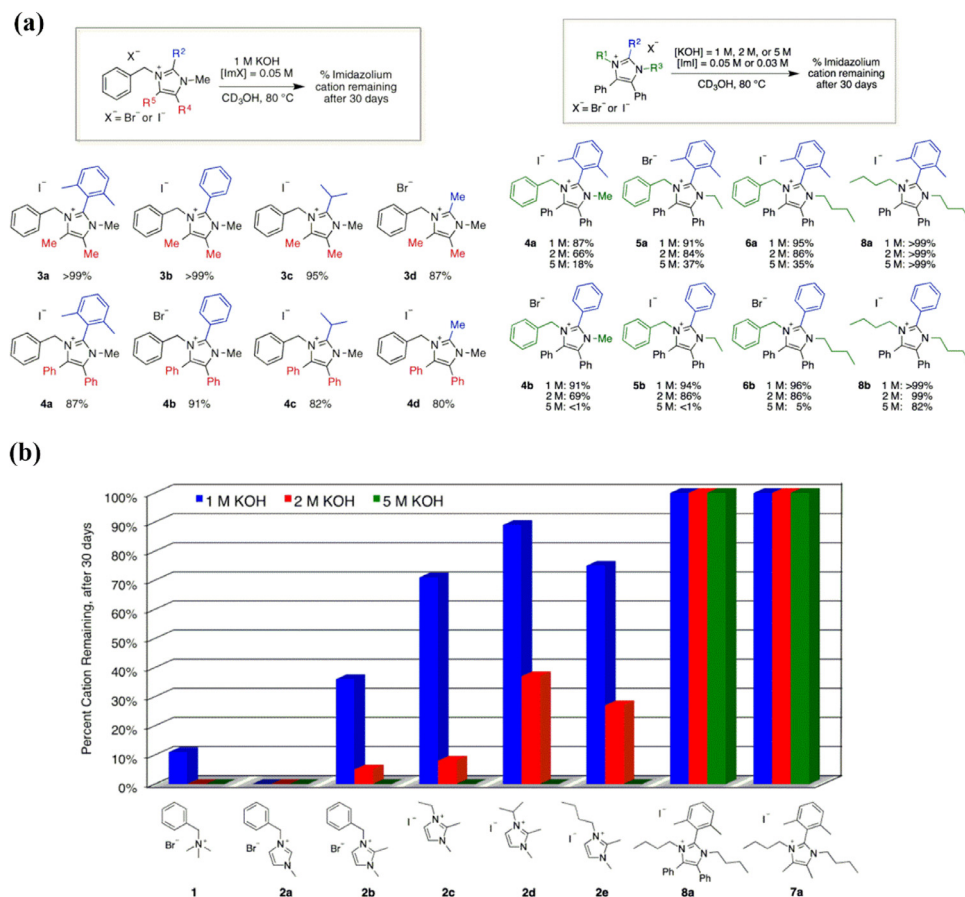


Fig. 12. (a) The effect of different substituents on the alkaline stability of IM groups and (b) an alkaline stability comparison of IM groups in 1, 2, or 5 M NaOH at 80 °C for 30 days. [151], Copyright 2015. Adopted with permission from American Chemical Society.

alkaline stability of the IM groups, as shown in Fig. 12. They found that the substituent identity at each position of the imidazolium ring had a dramatic effect on the overall cation stability, including C-4 and C-5 positions, which were previously unexplored. Subsequently, they noticed that 7a and 8a groups with substituted C-4 and C-5 were very stable in 5 M KOH/CD₃OH at 80 °C for 30 days.

Nevertheless, the utilization of these large IM groups with steric hindrance was still a challenge for researchers due to the complicated and time-consuming synthesis process. Wright et al. [152] prepared a poly[2,2'-(2,2'',4,4'',6,6''-hexamethyl-p-terphenyl-3,3'-diyl)-5,5'-bibenzimidazole] (HMT-PMBI) that exhibited enhancing alkaline stability, as shown in Fig. 10(d). Then, Fan et al. [153] described a step-growth polycondensation method to incorporate multi-substituted IM cations in AEPs (Fig. 10(e)). The resulting polyelectrolytes were stable in 10 M KOH at 100 °C for 168 h. Very recently, Fan et al. [154] renewed interest in these PBI polymers, and presented a series of large-hindrance poly(bis-arylimidazoliums) for AEPs (Fig. 10(h)). These AEMs exhibited acceptable ion conductivity and were stable in 10 M NaOH at 80 °C for 240 h. They investigated the half-lives of different IM groups in 3 M NaOD/D₂O/CD₃OD (hydration level: $\lambda=4.8$), demonstrating that ethyl, propyl, or butyl-functionalized bis-arylimidazoliums possessed long half-lives over 10,000 h.

Coates' group [155] presented a series of macrocycle-imidazolium AEMs based on polyethylene backbones by ring-opening metathesis polymerization (ROMP), as shown in Fig. 10(f). Using a bifunctional imidazole cross-linker, these AEMs exhibited a OH⁻ conductivity of 59 mS/cm at 50 °C but excellent alkaline stability in 5 M KOH at 80 °C for 30 days. Subsequently, they [156] further optimized these ROMP polyelectrolytes by the living

polymerization of trans-cyclooctenes, as shown in Fig. 10(g). The resulting random copolymers demonstrated a high OH⁻ conductivity of 134 mS/cm at 80 °C and were stable in 2 M KOH/CD₃OH at 80 °C for 30 days.

2.1.3. Outlook of QA and IM groups

With the development of AEPs, some of cationic groups exhibited promising alkaline stability. Unfortunately, researchers have not systematically compared the alkaline stability of QA and IM groups under the same conditions. Therefore, based on TMA as a benchmark, we summarize the half-life time of the promising QA and IM groups at two different conditions as shown in Fig. 13. Obviously, DMP and ASU groups exhibited an outstanding alkaline stability in ammonium species (Fig. 13(a)). On the other hand, the half-life time of some large hindrance IM groups can also exceed TMA benchmark (Fig. 13(b)). However, the OH⁻ ion conductivity of IM-based AEPs is relatively lower than QA-based AEPs.

2.2. Phosphonium and sulfonium-based AEPs

Compared to ammonium-based AEPs, there are relatively fewer works on phosphonium-based AEPs up until now. As early as 1990, Bauer et al. [157] found that the QA groups possessed a considerably higher thermal and chemical stability than quaternary phosphonium and tertiary sulfonium groups. However, systematic comparisons of the chemical stability of QA and phosphonium groups are still lacking to date. In 2009, Gu et al. [63] reported a soluble tris(2,4,6-trimethoxyphenyl) quaternary phosphonium-based polysulfone ionomer (TPQPOH), as shown in Fig. 14(a). TPQPOH ionomers exhibited higher ion conductivity (27

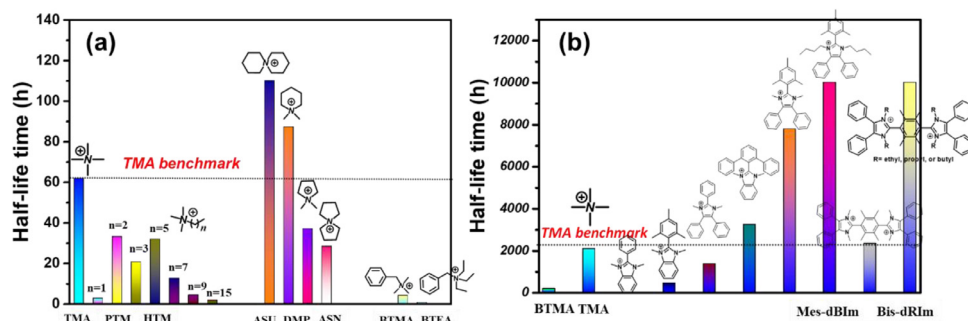


Fig. 13. Half-life comparison of (a) QA groups in 6 M NaOH at 160 °C ($\lambda=9.25$) and (b) IM groups in 3 M NaOD/D₂O/CD₃OD at 80 °C ($\lambda=4.8$) based on TMA benchmark [71,151,154].

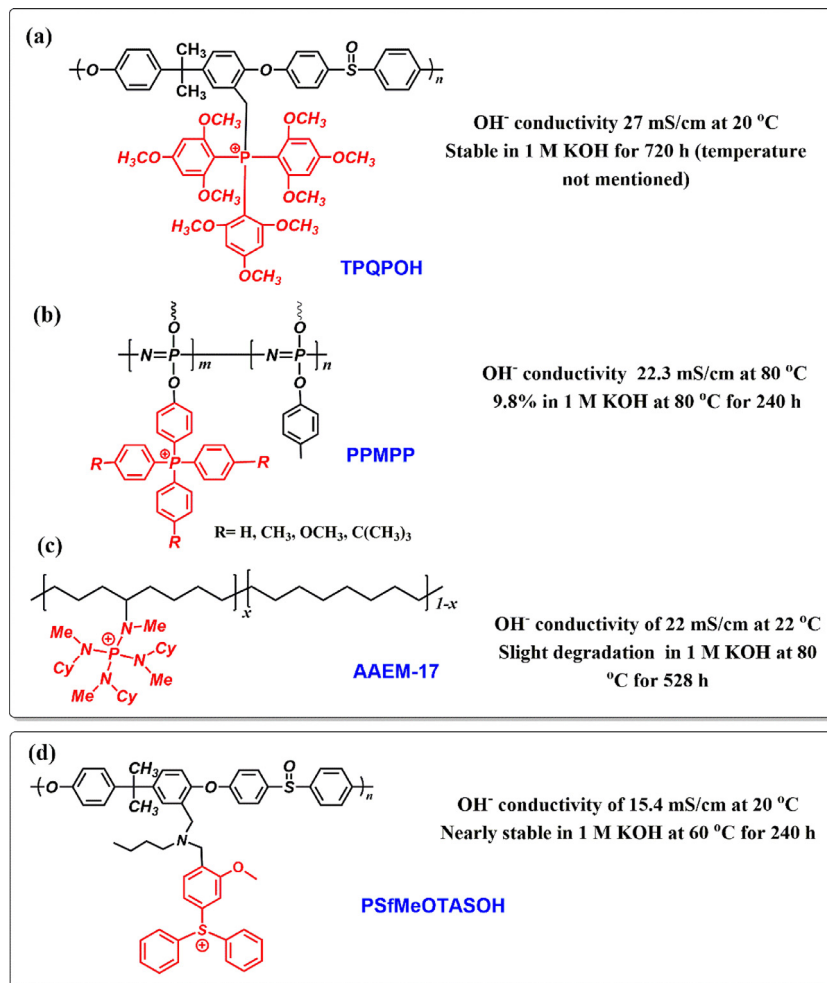


Fig. 14. (a), (b), and (c) the performance comparison of phosphonium-based AEPs and (d) sulfonium-based AEMs [63,64,66].

mS/cm at 20 °C) than a commercial FAA membrane (17 mS/cm at 20 °C, Fuma-Tech GmbH, Germany), A3Ver2 (2.6 mS/cm, Tokuyama Corporation, Japan) and AS-4 (13 mS/cm, Tokuyama Corporation, Japan) ionomers. Moreover, the TPQPOH membrane was stable in 1 M KOH for 30 days. Then, Han et al. [64] prepared a series of tetraphenylphosphonium functionalized polyphosphazene (PPMPP) membranes (Fig. 14(b)) that exhibited OH⁻ conductivities of 22.3 mS/cm at 80 °C and 9.8% degradation after alkaline treatment in 1 M KOH at 80 °C for 240 h. Hugar et al. [65] introduced a new class of tetrakis(dialkylamino) phosphonium (P(NR₂)₄⁺) cations, and they prepared a P(N(Me)Cy)₄⁺-based polyethylene membrane (Fig. 14(c)). The P(N(Me)Cy)₄⁺ cation was

stable in 1 M NaOD/CD₃OD at 80 °C for 20 days, and no significant loss of ion conductivity was found in P(N(Me)Cy)₄⁺-based AEMs after exposure in 15 M KOH at 20 °C for 138 days or in 1 M KOH at 80 °C for 25 days. Compared to QA-functionalized polyethylene AEMs [158] (69 mS/cm at 22 °C), these P(N(Me)Cy)₄⁺-based AEMs exhibited lower ion conductivity (22 ± 1 mS/cm) and IEC (0.67 mmol/g). After that, Zhang et al. [159] an ultra-stable methyl tris(2,4,6-trimethylphenyl)phosphonium [MTPP-(2,4,6-Me)] that exhibited only 20% degradation in 1 M KOD/CD₃OD/D₂O at 80 °C for 5000 h. Unfortunately, MTPP-(2,4,6-Me) groups have not been utilized in AEPs due to their complicated and low-efficiency utilization process.

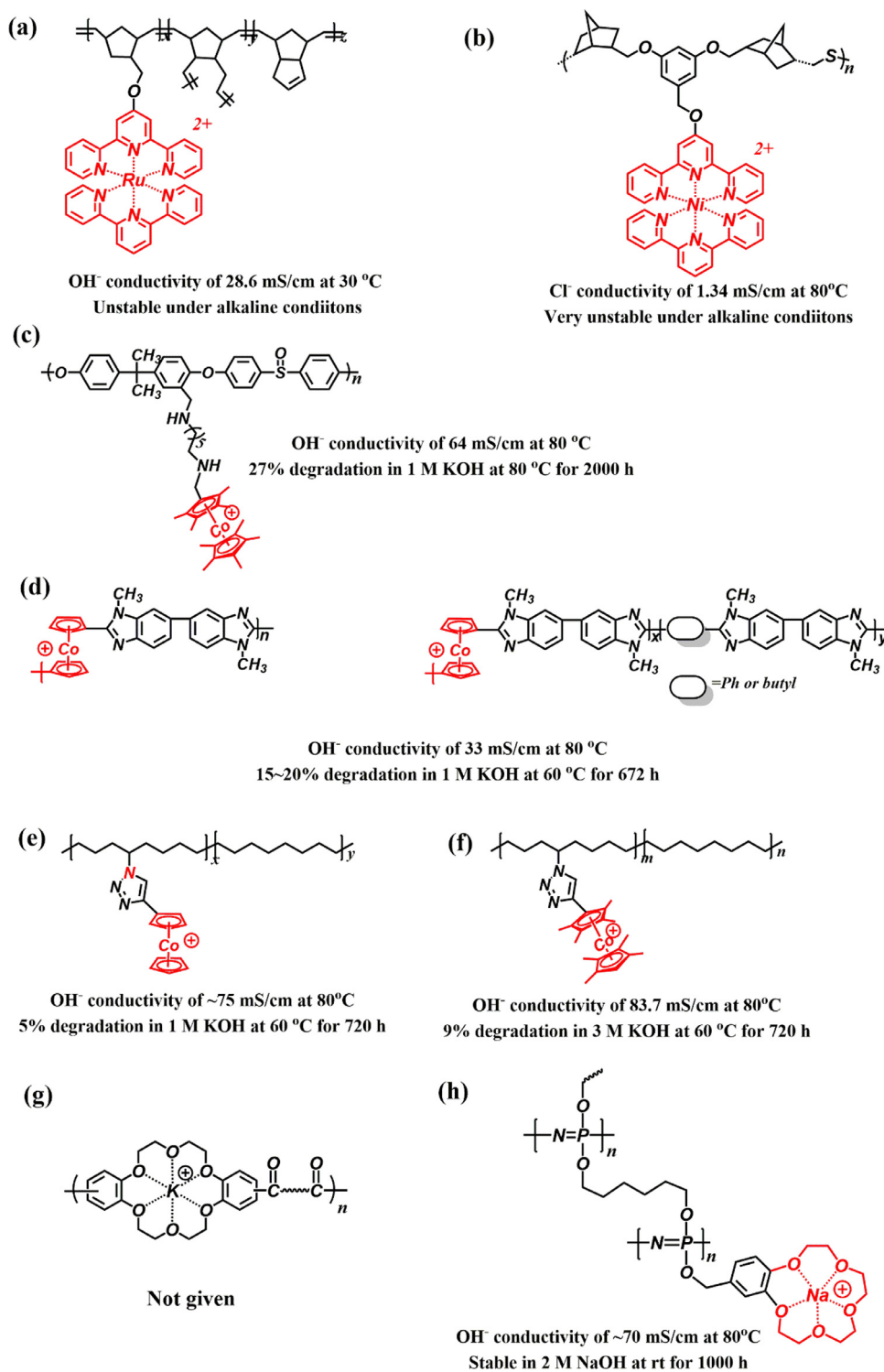


Fig. 15. Summary of organometallic cation-based AEPs with performances comparison in current research [67-70, 160-166].

On the other hand, tertiary sulfonium-based PSF AEPs [66] have been proposed, but exhibited a low ion conductivity of 15.4 mS/cm and poor alkaline stability (Fig. 14(d)).

2.3. Organic metal cation-based AEPs

Tew et al. [67] proposed employing organometallic salts as the cationic groups (Fig. 15(a)), and they presented bis(terpyridine)ruthenium(II)-based AEMs in 2011. Unfortunately,

these AEMs possessed very low ion conductivity (4.4 mS/cm at 30 °C) and were unstable in 1 M NaOH.

After that, Gu et al. [68] prepared a permethyl cobaltocenium (Cp*₂Co⁺)-based PSF (Cp*₂Co⁺-PSf) membrane (Fig. 15(c)). Cp*₂Co⁺ groups were found to be stable (8.5% degradation) in 1 M NaOH/D₂O at 140 °C for 1000 h. The OH⁻ conductivity of Cp*₂Co⁺-PSf membranes reached 64 mS/cm at 80 °C. Chen et al. [69] systematically investigated the effect of substitutions on the alkaline stability of the cobaltocenium groups (Table 1). They found

that 1,1'-dimethylcobaltocenium (DMCp₂Co⁺) with an electron-donating group could significantly improve the alkaline stability of Cp₂Co⁺, while 1,1'-dicarboxycobaltocenium (DCCp₂Co⁺) with an electron-withdrawing group dramatically decreased their alkaline stability. They also prepared a series of cobaltocenium-containing PBI membranes that exhibited ~20% degradation in 1 M KOH at 60 °C for 672 h (Fig. 15(d)).

Tang and co-workers [160,161] also reported a series of cobaltocenium-containing polyethylene membranes (H-AEM₅₀-OH) via ROMP reactions (Fig. 15(e) and 15(f)). These H-AEM₅₀-OH membranes exhibited an increase in ion conductivity (90 mS/cm at 90 °C) and were stable in 1 M NaOH at 80 °C for 30 days. Kwasny et al. [70] prepared a series of crosslinked nickel cation-based AEMs (Fig. 15(b)). However, similar to Ru²⁺-based AEMs, these nickel-based AEMs exhibited very low ion conductivity (Cl⁻ < 2 mS/cm at 80 °C) and were very unstable under alkaline conditions.

Compared with these metal cation groups, cobaltocenium-based AEPs possessed best alkaline stability and acceptable ion conductivity. However, most of the synthesis processes of these AEMs were complicated, such as in the monomer synthesis of Tang and Chen et al.'s work [69,160,161].

On the other hand, Zhuang and co-workers [162] proposed the use of K⁺ or Na⁺-complexing Crown ether as the cationic groups in 2009. Unlike traditional cationic groups, Crown ethers are ring shaped heterocyclic compounds containing several ether groups. They can strongly combine with certain metal cations to form complexes. When metal atoms, such as sodium or potassium, pass through the center of the ring, they can capture the specific metal cations by the exposed oxygen atoms according to the cavity size of the Crown ether [163], so that the metal cation-containing Crown ether can transport OH⁻. For example, 18-Crown-6 ether has a high affinity for K⁺, 15-Crown-5 ether for Na⁺, and 12-Crown-4 ether for Li⁺, respectively. Zhu and co-workers [164] prepared a series of cross-linked Na⁺-15-Crown-5 polyphosphazene membranes. These Crown ether-based membranes were stable in 2 M NaOH for 1000 h along with ion conductivities over 75 mS/cm at 90 °C. Recently, Zheng et al. [165] and Yang et al. [166] also reported on Crown ether-based AEMs. Unfortunately, the complexation between metal cations and Crown ether was an irreversible reaction. Therefore, K⁺ or Na⁺-complexing Crown ethers were unstable in water or low basic concentrations due to the dissociation of metal cations. Therefore, the metal cation-containing Crown ether would be a great candidate for alkaline fuel cell applications when one can find an ideal solution to maintain the basic concentration during fuel cell operation.

2.4. Highly stable polymer backbones

Previously, industrially available poly(aromatic ether)s, such as PEEK, PSF, and PPO [73–78], have been widely developed for AEPs due to their low cost, easy modification, and good mechanical properties. Most of these polymers can be directly obtained from industry, which is beneficial for realizing the near-term commercialization of AEPs. Generally, the popular way to prepare these poly(aromatic ether)-based AEPs is the chloromethylation of phenyl groups or the radical halogenation of benzyl groups in the aryl-ether polymer backbone along with quaternarization. However, aryl ether cleavage reactions in aryl ether polymers were first identified under alkaline conditions by Fujimoto et al. [22] and Arges et al. [26].

In 2017, Bae and co-workers [123] investigated the chemical stability of different polymers. They found that withdrawing groups (such as carbonyl groups and sulfonyl groups) in the polymer backbones could decrease the chemical stability of the polymer backbone, and aryl ether-free polymers such as SEBS and poly(biphenyl alkylene)s exhibited much higher chemical stability

than that of the aryl-ether polymers. This work highlighted the importance of chemical stability of the polymer backbone. Many polymerization methods have been employed to prepare aryl ether-free polymers.

2.4.1. Polyolefins and fluoropolymers by radiation-grafting

Although BTMA-type AEPs have been previously demonstrated to be unstable under alkaline conditions, while the BTMA-type AEPs have currently received many attentions due to the emergence of radiation-grafting AEPs. Typically, in 2014, Varcoe and coworkers [167,168] reported the use of a BTMA-functionalized ethylene-tetrafluoroethylene (BTMA-ETFE) as AEIs by radiation grafting, and the BTMA-ETFE ionomer displayed a remarkable fuel cell performance. Subsequently, Wang et al. [33,169] developed a BTMA-functionalized low-density polyethylene (BTMA-LDPE) membrane (40 ± 5 μm) for AEMs. Combining with BTMA-ETFE ionomer, BTMA-LDPE membrane-based fuel cells exhibited distinguished PPD over 2 W/cm² at 80 °C. Moreover, they found that switching from LDPE to high-density polyethylene (HDPE) could lead to remarkably enhanced fuel cell performance (Fig. 16(a)). The PPD of H₂-O₂ AEMFCs has been advanced to 2.55 W/cm² with BTMA-HDPE membrane and BTMA-ETFE ionomers. Both of BTMA-LDPE and BTMA-HDPE membranes exhibited high OH⁻ conductivity up to 200 mS/cm at 80 °C along with excellent mechanical properties. The key to the success of these BTMA-type AEPs is that these membranes are modified from commercial preforming HDPE (10 μm) and LDPE (15 μm) films that endow them excellent performance. Although the chemical structure of BTMA-LDPE and BTMA-HDPE membranes is very similar, the *in-situ* durability is totally different. HDPE-based cells operated stably at 0.6 A/cm² current density for 440 h at 70 °C along with stable area specific resistance (ASR), while LDPE-based cells displayed a rapid degradation at initial 100 h with an increase in ASR (38 to 52 mΩ cm²). The improved *in-situ* durability has been hypothesized to be due to enhanced water transport characteristics, caused by the change in the nanomorphology/microstructure of the precursor HDPE film. On the other hand, the alkaline stability issues associated with BTMA-ETFE ionomer still have not been well addressed. BTMA-ETFE membrane became brittle and showed severe breakage after being soaked in aqueous NaOH at 80 °C for 28 days accompanied by a color change from light to dark yellow [33].

2.4.2. Polynorbornene by ring-opening metathesis polymerization

Clark et al. [170] proposed a ROMP method to fabricate aryl ether-free polymers by constructing alkyl-alkyl bonds in 2009. They reported a series of QA-based polynorbornene (PNB) membranes via a facile ROMP reaction. These membranes exhibited a high OH⁻ conductivity of 111 mS/cm at 50 °C and acceptable mechanical properties. Recently, PNB-based AEMs have attracted wide attentions due to their incredible power density, as shown in Fig. 16(b). Kohl and co-workers [15,38] have reported a series of side-chain-type PNB copolymers for AEMs by ROMP. The OH⁻ conductivity of these PNB membranes reached to 198 mS/cm² at 80 °C. Subsequently, Huang et al. [97] prepared a series of composite PNB membranes with a PTFE reinforcement (GT64). The PPD of H₂-O₂ AEMFCs was dramatically improved to 3.37 W/cm² at 80 °C along with a 545 h *in-situ* durability under 0.6 A/cm² at 80 °C. They pointed out that high power density was associated with lower water uptake and high mechanical properties. Meanwhile, they [9] reduced the thickness of PTFE-reinforced PNB membranes to 10 μm, and the PPD further increased to 3.5 W/cm² under 9.7 A/cm² current density, along with a lowest ASR of 29 mΩ cm² to date.

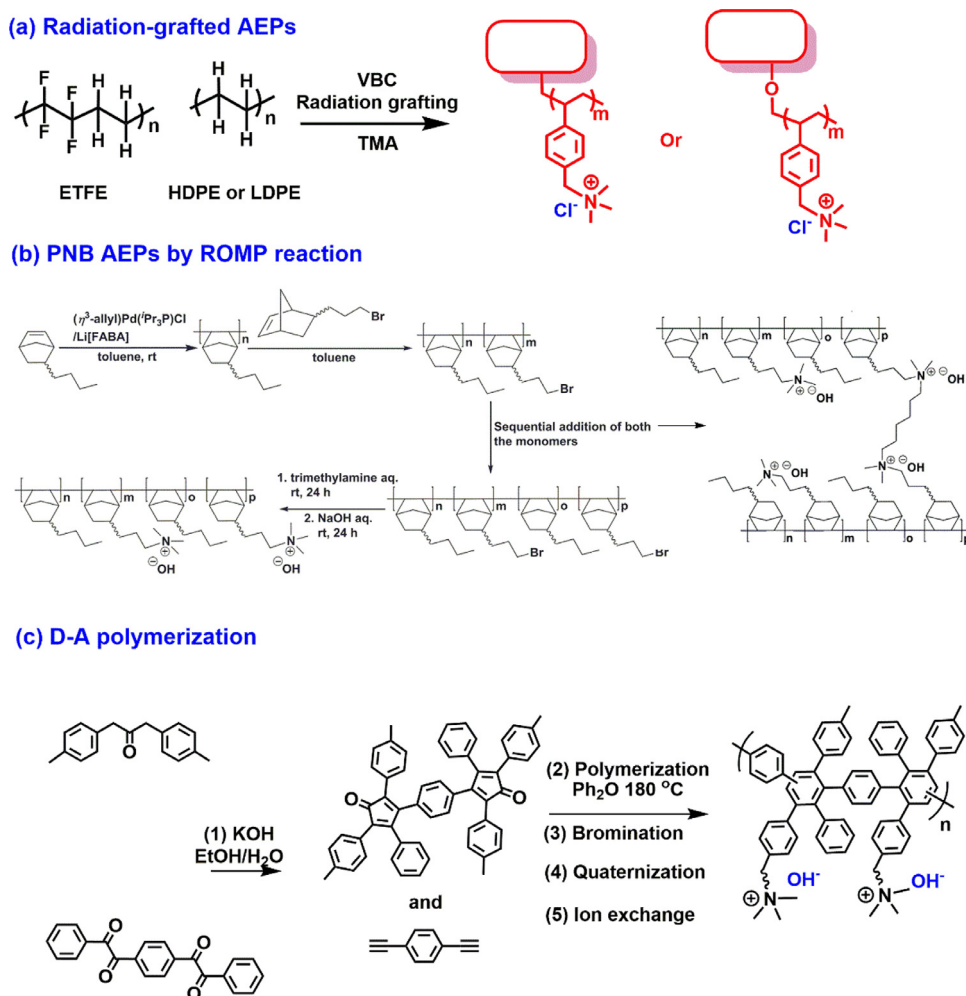


Fig. 16. The general synthesis routines of (a) radiation-grafting AEPs, (b) PNB-based AEPs, (c) D-A polyphenylenes [15,38,97,122,167–169, 171].

2.4.3. Polyphenylene Diels-Alder polymerization

Diels-Alder (D-A) polymerization has been employed to construct aryl-aryl polymers. Hibbs et al. [122,171] presented a BTMA-poly(phenylene) membrane (BTMA-PP) for AEMs by D-A polymerization, as shown in Fig. 16(c). They indicated that the D-A polymerization is conducted by heating equimolar amounts of the bis(cyclopentadienone)s and 1,4-diethynylbenzene with the loss of one carbon monoxide molecule for each D-A reaction accompanying with the formation of a highly stable aromatic ring that makes the polymerization irreversible. Subsequently, aforementioned side-chain-type PP membranes have been widely developed [27,47,172] and exhibited excellent alkaline stability. Kim and co-workers [13] highlighted the advantages of D-A polymerization including (i) metal-free conditions to avoid potential contamination of metals of the resulting materials, (ii) irreversible high molecular weight growth, and (iii) good solubility and thus good processability of the resulting polymer for sequential quaternization. However, the synthesis of these D-A polyphenylenes is complicated and requires multiple reactions (6 steps) to fabricate hydroxide-conducting polymers.

2.4.4. Polyfluorenes by metal-catalyzed coupling reactions

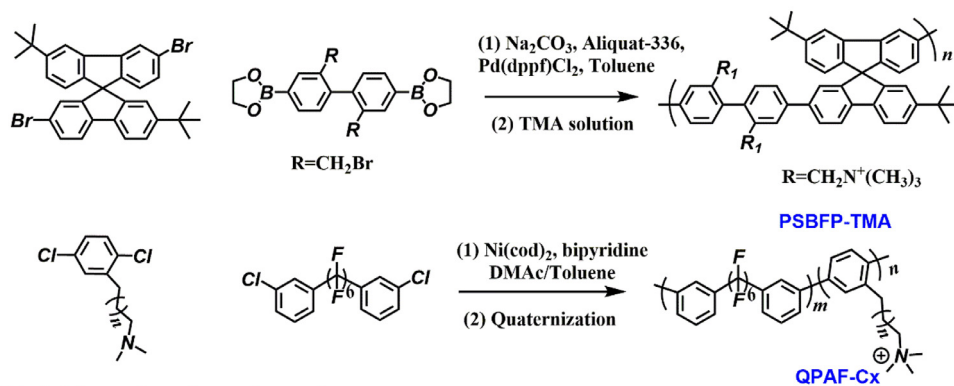
Metal-catalyzed coupling reactions have been also widely used for constructing aryl-aryl polymers [173] (Fig. 17(a)). Recently, Yamaguchi and co-workers [174] prepared a series of BTMA-spirobifluorene ionomers for AEMFCs and water electrolysis by Suzuki-Miyaura coupling reaction. They indicated that typical

PPofen suffered from low solubility and processability because of the strong π - π stacking interactions of the polymer backbone, and that spirobifluorene polymers could improve the solubility and mechanical properties of AEMs due to the twisted polymer backbone and increased chain entanglement. These membranes exhibited a OH^- conductivity of 86.2 mS/cm at 70 °C, and were stable in 1 M NaOH at 80 °C for one week and in Fenton's solution (3 wt% H_2O_2 and 3 ppm FeSO_4) at 80 °C for 8 h.

Nickel-catalyzed coupling reactions have been recognized as a versatile and efficient methods to synthesize polyphenylene polymers. Typically, Miyatake and co-workers [175,176] reported a series of PF-containing polyaromatics (QPAF-C $_x$, where $x = 2-6$) using a nickel-catalyzed coupling reaction. They found that QPAF-C3 exhibited an optimum OH^- conductivity of 99 mS/cm at 80 °C and was stable 1 M KOH at 80 °C for 1000 h.

Compared with two metal-catalyzed coupling reactions, the Suzuki-Miyaura coupling reaction is performed via two steps by employing aromatic boronic acids/boronate esters and aromatic bromide compounds in the presence of a palladium-complex, while the nickel-catalyzed coupling reaction is carried out in one step using aromatic chloride compounds. It seems the nickel-catalyzed coupling reaction is easier and more effective for coupling reactions than the Suzuki-Miyaura coupling reaction due to low temperature and short time. However, polymer prepared by nickel coupling reaction [175] showed a higher polydispersity index (10.2–17.4) than Suzuki coupling (2.1 to 3.3).

(a) Metal-catalyzed coupling reaction



(b) Acid-catalyzed condensation

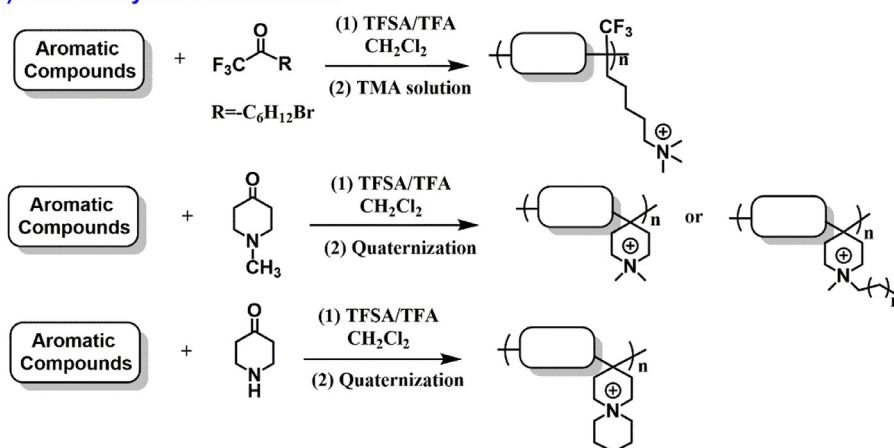


Fig. 17. The general synthesis routines of (a) Metal-catalyzed coupling reaction and (b) acid-catalyzed condensation [86,96,128,134,136,177].

2.4.5. Polyaromatics by acid-catalyzed polycondensation

Super acid-catalyzed polycondensation is another class of reactions to build aryl-alkyl polymers, and this reaction is primarily based on aromatic compounds and specific ketones, as shown in Fig. 17(b). Acid-catalyzed polycondensation provides several advantages such as oxygeninsensitivity, high molecular weight, metal free reaction, and extensive species options. Typically, aforementioned PAPs and some of side-chain-type polyphenylenes were produced by this method. [86,96,128,134,136,177].

2.4.6. SEBS and Tröger's base polymers

SEBS-based AEPs have attracted attentions due to their aryl ether-free backbone (Fig. 18(a)) since the SEBS is commercially available. Gao et al. [59] prepared a BTMA-type SEBS (QASEBS) that exhibited a OH^- conductivity of 100 mS/cm at 80 °C and was stable in 1 M KOH at 60 °C for 1700 h. Subsequently, Mohanty et al. [60] also prepared a series of BA-type SEBS membranes. They indicated that BTMA-type SEBS membrane exhibited the higher ion conductivity (over 100 mS/cm at 60 °C) and water uptake than other large volume BA-type SEBS. Jeon et al. [62] developed a series of side-chain-type and crosslinked SEBS (SEBS-Cn-TMA-x) membranes that displayed acceptable OH^- conductivities at 80 °C (50 to 92 mS/cm) and exhibited a PPD of 520 mW/cm² at 60 °C.

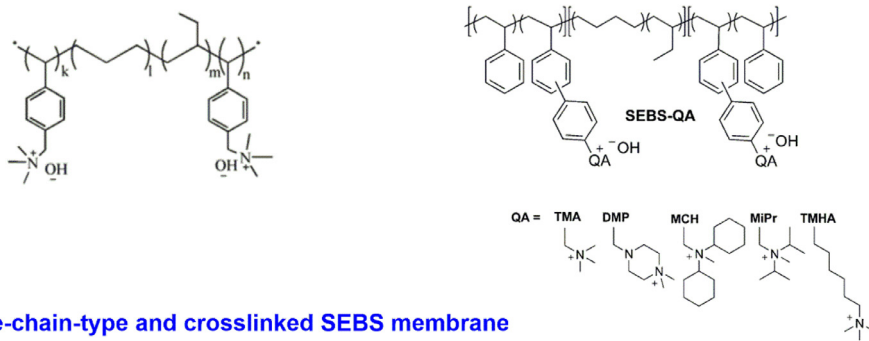
Similar to PBI polymers, Tröger's base (TB) polymers with inflexible bridged bicyclic units attracted attention when Carta et al. [178] rediscovered TB chemistry and first reported on TB polymer membranes for gas separation by acid-catalyzed polymerization via diamine monomers. Later, Yang et al. [179] proposed TB polymers for AEM applications in 2016, as shown in Fig. 18(c). These TB membranes possessed a OH^- conductivity of 164.4 mS/cm at

low IEC of 0.82 mmol/g. They indicated that the high ion conductivity of TB polymers was attributed to their intrinsic microporosity. Unfortunately, gas permeable TB membranes could cause gas crossover issues in AEMFCs. Therefore, TB-based AEPs could be a good candidate for AEIs because of their high gas permeability and ion conductivity. Hu et al. [180] also prepared a series of multi-cation crosslinked TB membranes to improve the film-forming ability and mechanical properties.

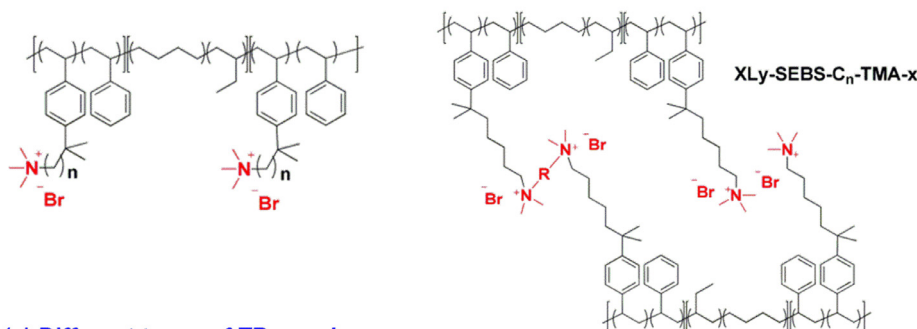
2.5. Outlook for highly stable AEPs

Recently, Pivovar and co-workers [12] have developed a standard method to evaluate the performance AEPs, and measured the Cl^- conductivity, water uptake, IEC and alkaline stability (in 1 M NaOH at 80 °C for 1000 h) of different type AEMs. The results indicated that polyphenylene-type AEMs and some of BTMA-type AEMs displayed an outstanding alkaline stability (*ex-situ* durability) and a relatively higher conductivity. Fig. 19 summarizes the *ex-situ* durability, OH^- conductivity, and water uptake of different types of AEPs reported so far. However, *ex-situ* and *in-situ* durability have been demonstrated to be mismatching. For instance, Li et al. [181] compared the *ex-situ* and *in-situ* alkaline stability of different types of PPO membranes. They found that BTMA-PPO with poor alkaline stability showed acceptable *in-situ* durability under 0.1 A/cm² current density, while side-chain-type PPO exhibited significant voltage loss. Dekel et al. [46,182] investigated the alkaline stability of different cationic groups at low λ values by storing the cationic groups in a K^+ /Crown/DMSO solution. They indicated that the basicity of AEMFCs could be very high in the cathode site, especially in high current density. Their results showed that BTMA groups

(a) BA type SEBS membranes



(b) Side-chain-type and crosslinked SEBS membrane



(c) Different types of TB membranes

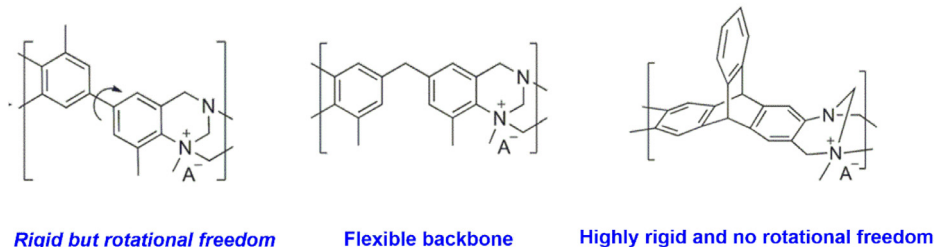


Fig. 18. (a) BTMA-type SEBS, (b) side-chain-type and crosslinked SEBS, and (c) different types of TB membranes [178,179].

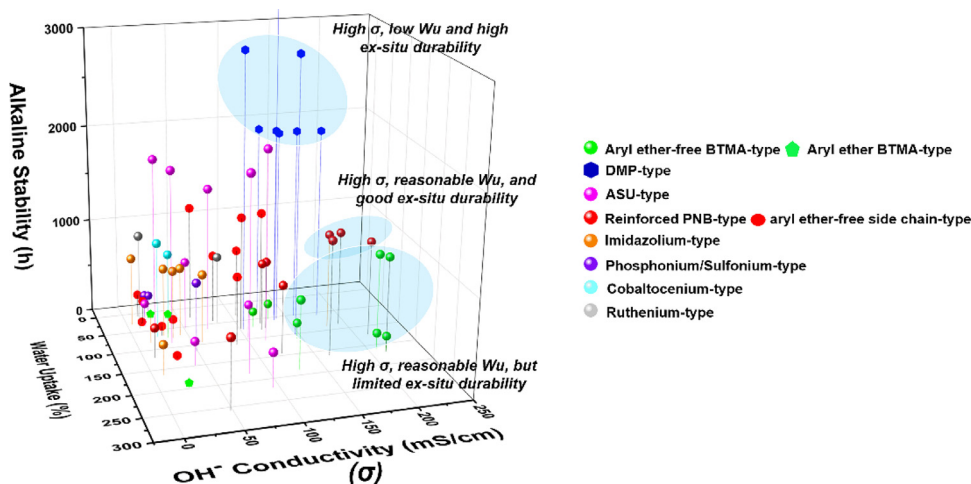


Fig. 19. Comparison between the water uptake (Wu), OH⁻ conductivity (σ), and *ex-situ* stability of typical BTMA-type, DMP-type, ASU-type, side chain type, IM-type, phosphonium/sulfonium-type, cobaltocenium type, and ruthenium-type AEPs reported so far. Recorded Wu corresponds to σ at the same temperature (most AEPs are recorded at 80 °C, but some for the side chain, IM, sulfonium, and ruthenium-type AEPs are plotted at room temperature and 60 °C due to insufficient information). The alkaline stability was recorded based on the temporal stability of AEPs in 1 M NaOH or KOH at 80 °C with degradation lower than 10%, and some of stable AEPs was recorded at more harsh condition due to insufficient information [9,14,33,67-69, 86,96,97,105,129,136,147,155,156,160,161,167-169, 173,177,181,183,217].

presented acceptable alkaline stability in low λ conditions at room temperature, while ASU and large steric hindrance IM groups exhibited rapid degradation when λ was lower than 4. However, the relationship between λ values and current density still has not been revealed by experiments.

3. Strategies to enhance properties of AEPs: importance of morphology and stability

Apart from durability, AEMs must simultaneously possess high OH^- conductivity with qualified mechanical properties and dimensional stability for AEMFCs. In addition, developing a thin AEM ($\sim 30\ \mu\text{m}$) is indeed crucial for AEMFCs to realize high power density. Thin AEMs can endow corresponding MEAs with many merits. For instance, thin AEMs possess a lower mass transfer resistance and are preferable for water back diffusion. However, there is still an underlying challenge between thin membrane and mechanical properties or gas permeability. When the membrane is thin, the mechanical properties and gas tightness of the membrane may dramatically decrease. Moreover, some interesting phenomena also have been found in current research, such as thin membranes exhibit a worse durability than thick membranes, and crosslinked membranes always possess higher alkaline stability than pristine membranes [184]. As a result, membrane reinforcing technology and strategies should be developed to address these issues.

3.1. Microphase separation

Improving the microphase separation of AEPs has been previously considered as a feasible way to boost the physical properties of the AEPs. Typically, Zhuang and co-workers [14] proposed to construct ionic highways in AEPs based on QAPS by optimizing the microphase morphology of the AEPs in 2014. They found that QAPS membranes with enhanced hydrophilic/hydrophobic microphase separation could both effectively promote ion conductivity and improve the chemical stability of the QAPS due to the formation of ionic channels that reduce the ion-transport distance in the AEPs. After this report, a mass of aryl ether AEPs have been designed to improve their microphase separation, including cation remotely-grafted AEPs, ionic-cluster AEPs, and multi-cation side chain AEPs (Fig. 20(a)).

3.1.1. Cation remotely-grafted AEPs

Cation remotely-grafted AEPs have been well discussed in aforementioned side-chain-type AEPs. All of results [9,105,124,125,173,175,185] revealed that side-chain-type AEMs exhibited higher ion conductivity and alkaline stability than pristine BTMA-type AEPs due to the absence of BTMA groups and the improvement of microphase separation. Moreover, the number of alkyl spacers also show significant effect on AEPs performance, and five or six alkyl spacers have been demonstrated to be optimal design for side-chain-type AEPs.

3.1.2. Ionic-cluster AEPs

On the other hand, increasing the aggregation of ionic groups is another way to construct the ion channels in AEPs. As early as 2011, Watanabe and co-workers [186] reported a series of multiblock poly(arylene ether)s membranes (QPE) and investigated the microphase separation and ion-transporting channels in these AEPs. These membranes exhibited much higher OH^- conductivities of 144 mS/cm at 80 °C. Similarly, Lai et al. [187] and He et al. [188] prepared a series of ion cluster-type polyaromatics to increase the cation density, and intended to improve the microphase separation of these AEPs. However, although these ion-clustered AEMs contributed to constructing ion channels and improving the ion

conductivity, the substitution of BTMA groups and the electron-withdrawing effect in local aryl ether bonds were dramatically increased, resulting in the detrimental effect in alkaline stability.

3.1.3. Multi-cation side chain AEPs

Multi-cation side chain AEMs have been widely developed in aryl ether polymers, which is another way to improve the microphase separation of AEMs and reduce the BTMA contents [127,128,189,190]. The merits of these AEMs are that well-organized QA groups in the side chain could effectively adjust the physical properties of AEPs. For instance, compared to BTMA-type AEPs, multi-cation side chain AEPs showed lower water uptake and swelling ratio, but higher ion conductivity in same IEC values, indicating that multi-cation side chain AEPs possessed higher ion-conducting efficiency.

3.1.4. Covalent assembly AEPs

Very recently, Kim et al. [37] developed a series of covalent assembly AEMs and proposed a new concept in ion transport, as shown in Fig. 20(a). These AEMs, containing charge-delocalized pyrazolium cations and homoconjugated triptycenes, exhibited a high conductivity of 111.6 mS/cm at 80 °C with low water uptake (7.9%) and IEC (0.91 mmol/g). They indicated the covalent assembly of repeating ionic segments served as ionic highways that could result in higher conductivity by lowering the activation barriers for ion transport. Importantly, $\text{H}_2\text{-O}_2$ AEMFCs based on covalent assembly AEMs reached a PPD of 0.73 W/cm² at 80 °C and also achieved a 400 h *in-situ* durability under 0.4 A/cm² current density.

3.2. Crosslinking

3.2.1. Conventional crosslinked membranes

The crosslinking method has been regarded as a simple and effective way to enhance the dimensional stability of AEMs. In particular, when AEMs were fabricated into very thin films, the AEMs require high mechanical stability. Since a majority of AEMs were based on halogenated or aminated polymers, the simplest way to prepare a crosslinked membrane was by directly reacting it with diamine or dibromo cross-linkers, such as 1,6-hexanediamine and 1,5-dibromopentane [191]. However, ordinary crosslinked AEMs prepared by hydrophobic crosslinkers possess a lower swelling ratio, higher tensile strength, but restricted ion conductivity compared with pristine membranes due to the reticular crosslinked structure.

3.2.2. Multi-cation crosslinked membranes

Enlightened by the multi-cation side chain strategy, researchers developed a series of multi-cation crosslinked membranes for further optimizing the properties of AEMs. Chen et al. [184] prepared a series of multi-cation crosslinked poly(arylene piperidinium) membranes with 5 alkyl spacers. They found that the OH^- conductivity (155 mS/cm at 80 °C) and dimensional stability of these crosslinked membranes were superior to pristine PAP membranes (102 mS/cm at 80 °C). Moreover, the alkaline stability of these crosslinked membranes also exhibited a slight improvement in 2 M NaOH at 80 °C.

3.2.3. Thiol-ene crosslinked membranes

UV-initiated thiol-ene click chemistry has been considered as a facile and effective method to obtain robust membranes due to the availability of metal catalysts and the solution-free casting method. Hickner and co-workers [192] have reported a series of crosslinked comb-shaped PPO membranes *via* thiol-ene click chemistry. They indicated that the thiol-ene crosslinking method improved the dimensional stability and alkaline stability. The crosslinked membranes retained a higher ion conductivity and alkaline stability in

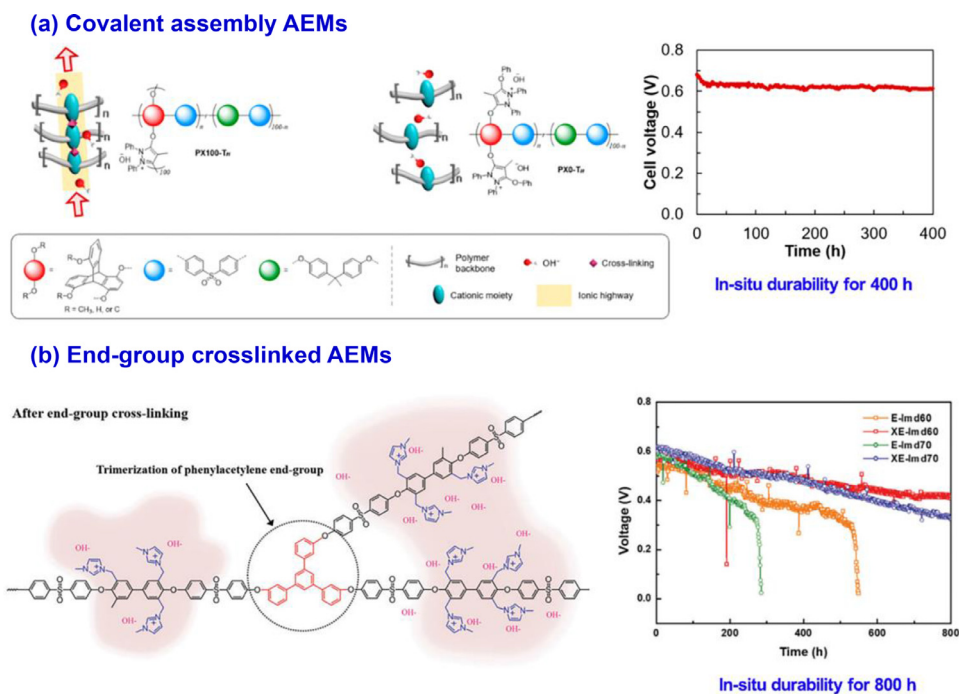


Fig. 20. (a) Covalent assembly AEMs along with in-situ durability. [37], Copyright 2020. Adopted with permission from American Chemical Society. (b) End-group crosslinked AEMs along with *in-situ* durability testing at 0.2 A/cm² at 60 °C. [193], Copyright 2017. Adopted with permission from Royal Society of Chemistry.

both 1 M and 4 M NaOH at 80 °C after 500 h than those of BTMA-PPO membrane.

3.2.4. End-group crosslinked membranes

Lee's group [193] prepared a series of end-group crosslinked PSF membranes by introducing a benzyne group at the end of the PSF polymer chain (Fig. 20(b)). The ion conductivity (107 mS/cm at 80 °C) and dimensional stability of these PSF membranes have been improved after end-group crosslinking. Importantly, after end-group crosslinking, *in-situ* durability of H₂-O₂ AEMFCs has been significantly improved, and the cells were operated under 0.2 A/cm² at 60 °C for 800 h.

3.3. Organic-inorganic composite strategy

Similar to the crosslinking method, the organic-inorganic composite strategy has also been regarded as an efficient and simple way to improve the comprehensive performance of AEMs. Many inorganic materials such as SiO₂ [194], TiO₂ [195], ZrO₂ [196], Al₂O₃ [197], montmorillonite [198], nanotubes [199], and layered double hydroxide (LDH) [200] have been employed as fillers for AEMs.

3.3.1. Traditional composite membranes

The simplest way to prepare a composite membrane is to directly dope inorganic materials into the polymer solution. Li et al. [196], Wu et al. [194], and Chen et al. [201] prepared a series of aryl ether composite membranes for AEMs (Fig. 21(a)). Basically, these results showed similar phenomenon that composite AEMs possessed higher mechanical properties and ion conductivity than pristine AEMs. However, most of inorganic materials were not able to transport OH⁻ ions, and most composite AEMs employed a direct-doping method, resulting in a limited ion conductivity and a poor dispersion of inorganic materials.

3.3.2. New types of composite membranes

(a) Porous-sandwich structure composite membranes. To address the dispersion and utilization issues of inorganic materi-

als, Chen et al. [202] designed a series of LDH/PPO composite membranes with a porous sandwich structure by spraying QA-functionalized LDH (QA-LDH) on the surface of triple-ammonium side chain PPO membranes, as shown in Fig. 21(b). They found that porous QA-LDH layers had a high ion conductivity of 122 mS/cm at 80 °C, which could effectively improve comprehensive performance of PPO membranes.

(b) Aligned composite membranes: Fan et al. [203] designed a series of electric-field oriented LDH/polyphosphazene composite membranes, as shown in Fig. 21(c). They found that LDH nanoplatelets possessed ion-transporting capability in LDH interlayers, and orientated LDH nanoplatelets could take full advantage of the bulk conductivity of the LDH nanoplatelets. Interestingly, the ion conductivity of aligned LDH/polyphosphazene composite membranes showed a 39% improvement compared to normal LDH/polyphosphazene composite membranes.

However, the electrorheological effect of LDH nanoplatelets was still weak under an applied electric field due to the inadequate ionic groups on the LDH. Chen et al. [204] presented a series of magnetic field-oriented ferroferric oxide (Fe₃O₄)/PPO composite membranes (Fig. 21(d)). Based on the surface modification technology, spherical Fe₃O₄ was modified with QA groups, giving QA-Fe₃O₄ composites good ion-transporting capability. After magnetic-field orientation, magnetic QA-Fe₃O₄ nanoparticles were consecutively aligned in PPO membrane and constructed magnetic-field-induced ion channels (MICs). Aligned composite membranes displayed a further 55% increase in ion conductivity compared to normal composite membranes.

3.4. Outlook for performance-enhancing strategies

Many strategies have been introduced to enhance the comprehensive performance of AEPs and to tackle the adverse trade-offs in their properties. Microphase separation of AEPs contributes to improving the ion-conducting efficiency and adjusting dimensional

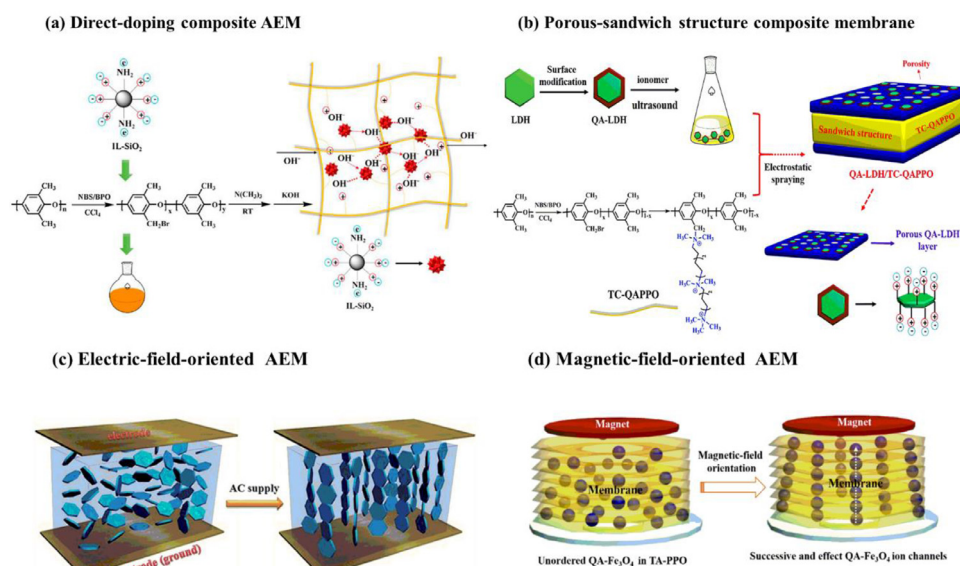


Fig. 21. (a) Directly-doping composite AEMs. [201], Copyright 2017. Adopted with permission from Elsevier Science Ltd. (b) Porous-sandwich structure composite AEMs. [202], Copyright 2018. Adopted with permission from Elsevier Science Ltd. (c) Electric-field-oriented composite AEMs. [203], Copyright 2014. Adopted with permission from Royal Society of Chemistry. (d) Magnetic-field-oriented composite AEMs. [204], Copyright 2019. Adopted with permission from Royal Society of Chemistry.

stability, while crosslinking and inorganic-organic composite methods are mainly employed to enhance the mechanical properties. The majority of the reported AEMs with microphase separation to date are aryl ether polymers or multiblock copolymers. However, many aryl ether-free AEPs, such as PAP and BTMA-HDPE homopolymers, possessed poor microphase separation, but exhibited excellent fuel cell performance. That is, there has been no clear evidence that microphase separation of AEMs is beneficial for the power density and *in-situ* durability of AEMFCs to date.

On the other hand, many crosslinked AEMs cannot be redissolved, thus the AEMs are usually prepared during membrane casting process. Therefore, the thickness of crosslinked AEMs could be increased after adding crosslinkers, such as multi-cation crosslinked AEMs and end-group crosslinked AEMs. In this case, the thickness of crosslinked AEMs should be taken into account when used for AEMFCs. As composite AEMs, they have not attracted research interest so far due to limited fuel cell performance. Nevertheless, PTFE-reinforced composite AEMs recently received many attentions due to the success of PTFE-reinforced PNB membranes in fuel cell performance [9,97].

There has been another underlying methods to enhance the fuel cell performance of AEMs. In 2016, nanocrack-regulated self-humidifying PEMs [3] have proved to be effective to improve the power density and *in-situ* stability of PEMFCs, especially at high temperature and low RH condition. Our recent research demonstrated that the nanocrack-regulated AEMs contributed to enhancing the *in-situ* durability and water retention, particularly in high temperature and low humidity condition, and the details of nanocrack-regulated AEMs will be presented in our future research. Recently, Guiver's group [4,5] presented a series of magnetic-field-oriented PEMs that exhibited higher power density and *in-situ* durability than Nafion® 212 membranes. This magnetic-field-oriented strategy is expected to be promising for AEMs.

4. Recent progress in ionomers

So far, most of researches on AEPs are based on AEM applications. Obviously, AEMs are indeed the most important materials for AEMFCs. Without a qualified membrane, AEMFCs are impossible to reach the same level as PEMFCs. However, ionomer research is still

lacking to date and only a few studies have specifically researched on AEIs, despite that ionomers have already been considered as a crucial material in AEMFCs.

4.1. Importance of ionomer research

4.1.1. Ionomer effects and water transport behavior

TPBs are the important reaction sites for hydrogen oxidation and oxygen reduction in catalyst layers. Here, AEIs act as a binder to mechanically anchor the catalyst particles in the electrode, and to conduct OH^- ions between catalysts and AEMs. Therefore, AEI is a key material to construct effective TPBs. In this case, AEI requires high ion conductivity along with qualified binding capability that is truly related with their chemistry and molecular weight.

Basically, the electrode was fabricated by coating an ionomer-containing catalyst ink solution (*so called catalyst slurry*) onto AEM or a gas diffusion layer (GDL). The key point related to the construction of effective TPBs is that the catalyst slurry should have a good dispersion and fast solidification during coating. Hence, a solvent selected to dissolve ionomers should possess a high dielectric constant and low boiling point at the same time [23]. Typically, isopropanol/deionized water (IPA/DI water) has been well documented to be a good solvent system for catalyst slurries. Generally, AEI requires good solubility in IPA/DI water, while BTMA-ETFE is a special case. BTMA-ETFE with poor solubility can be directly used as AEI after grinding the polymer powder to a small size. Although this grinding method has not been widely applied in other AEIs, this method provides a feasible way for those AEIs with poor solubility.

Compared to PEMFCs, AEMFCs face more complicated water management issues. In PEMFCs, water is only generated at the cathode as a product and not electrochemically consumed. Water is moved to the cathode from the anode by electro-osmotic drag as H^+ is produced by HOR. Thus, removing water from the cathode is the primary concern in the PEMFC to avoid catastrophic electrode flooding. In AEMFCs, two water molecules are consumed in the cathode while four water molecules are generated in the anode, and therefore the speed of water generation is two times faster than the water consumption. That is, the water management between the anode and cathode is important in AEMFCs since the

Table 2
Comparison of performance requirements between AEMs and AELs.

Properties	AEMs	AELs
Ion conductivity (σ)	High IEC and high σ	Suitable IEC and high σ
<i>Ex-situ/in-situ</i> stability	Highly stable	Highly stable
Water behavior	Suitable water uptake with low free water to control dimensional stability	High water permeability
Swelling ratio (SR)	Low SR	Low-intermediate SR
Mechanical properties	Good mechanical properties	No limitation
Gas permeability	Low gas permeability	Good gas permeability
Anchoring capability	No limitation	Good anchoring capability
Solubility	No limitation	Good solubility or good dispersion
Phenyl or ammonium adsorption effect	No limitation	Minimal phenyl and ammonium adsorption effects

ion conduction is actually based on water transport. Omasta et al. [10] indicated the importance of water balancing in the anode and the cathode based on BTMA-ETFE ionomers, and the moderate RH responded positively to address the anode flooding issues. Importantly, the high rate of water back diffusion from the anode toward cathode can naturally prevent from the anode flooding and the cathode dry-out issues.

Currently, the water transport behavior in AEMFCs can be referred to as water flux, water diffusion, or water diffusivity, all of these can be described as water permeability. Recently, Eriksson et al. [35] investigated the water transport behavior in liquid water and water vapor based on commercial Tokuyama A201 membrane. They demonstrated that the water fluxes of liquid water were approximately three times larger than those of water vapor. Besides, water fluxes increased with current density in both anode and cathode, while water in the anode increased quickly in high current density compared to the cathode. Based on modeling of commercial A201 membrane, they calculated the mass transport coefficients for vaporous water (K), liquid water (K_{aq}), and the osmotic drag coefficient (η). They indicated that η can be used to determine the speed of water back diffusion, and when the η is lower than -0.5 , it is good for water back diffusion. Therefore, insufficient water vapor permeability of AELs could be an underlying issue for AEMFCs operating in low RH. The water has different states in AEPs, such as free water (bulk water) and bound water that can be detected by differential scanning calorimetry (DSC). The suitable contents of free water and bound water have considered to be beneficial for fuel cell performance [9].

On the other hand, water transport not only relates with the ion conductivity, but also affects the alkaline stability of AELs and AEMs. Very recently, Dekel et al. [36] indicated that water diffusivity in AEMs has a strong impact on cell durability as well. Superior water diffusivity, which is imperative for increasing water transport from the anode towards the cathode, provides improved levels of hydration.

4.1.2. Difference between AELs and AEMs

Nowadays, many researchers are prone to use similar AEPs both as AEMs and AELs for AEMFCs [175,176]. Indeed, it is a simple and timesaving way to address the compatibility issues between the AEMs and AELs. However, the requirements for the properties of AEMs and AELs are not consistent due to their different roles, as shown in Table 2. There are three points that need to be emphasized. (1) Certainly, both AEMs and AELs require high ion conductivity and alkaline stability to reduce the internal resistance and ensure the long-term *in-situ* stability. AEMs require low water uptake and swelling ratio to maintain dimensional stability and to prevent fuel cross-over. Meanwhile, AELs need high water and gas permeability to reduce the mass transport resistance. Notably, the anode and the cathode may require AELs with different water contents due to the importance of water balancing in two electrodes [10]. To address the anode flooding issues and to control the

water balancing, many parameters have been employed in AEMFCs, such as thin membrane, low RH condition, and high fuel gas flow rate. However, low water contents in the anode and the cathode signify a higher alkalinity (lower λ values) that could be a big challenge for the alkaline stability of AELs, particularly in BTMA-based AEPs. (2) The solubilities of AEMs and AELs are different. Desirable AELs should have good solubility or good dispersion in low-boiling pointsolvents to improve their dispersion in catalyst slurry. A small amount of DI water is necessary to prepare a catalyst slurry since it can prevent from catalyst burning or sparking. On the other hand, AEMs need a restricted solubility to maintain dimensional stability during fuel cell operation. (3) As Kim et al. reported [104–106], AELs should possess minimal interactions (such as phenyl and ammonium adsorptions) with electrocatalysts, particularly in polyaromatics, while AEMs have no limitations in terms of the adsorption effect. Moreover, the state-of-the-art AEMs employed high IEC values over 2 mmol/g or even 3 mmol/g to improve the ion conductivity. However, the high IEC of AELs may cause the anode flooding at high RH and more cation adsorption of aromatic polymer AELs on catalysts can occur.

4.2. Development of ionomers

4.2.1. Preliminary ionomers

In earlier research, most AEPs displayed poor solubility with limited ion conductivity and were difficult to dissolve in low-boiling point solvents. Therefore, it was difficult to obtain an ionomer as a binder at that time. In this context, aqueous KOH and NaOH [111] have been added to the electrodes to increase the ion conductivity. After that, PTFE and Nafion polyelectrolytes were utilized as binders for alkaline membrane fuel cells, even though it is well-known that these two binders are not able to transport OH^- ions or even hinder the transport of OH^- ions. Typically, Scott et al. [205] used a PTFE binder and a cross-linked fluorinated membrane (MORGANE®-ADP, thickness: 150–160 μm , resistance in OH^- form: 0.6 Ω) for DMFCs. The PPD of the cells only reached 10 mW/cm^2 . Subsequently, Coutanceau et al. [206] applied Nafion binder for solid alkaline fuel cells using Ag or Pt-Pd as electrode catalysts, and reached a PPD of 18–20 mW/cm^2 with methanol or ethylene-glycol at 20 $^\circ\text{C}$. Similarly, Scott et al. [207] investigated the effect of temperature, oxidant (air or oxygen), and methanol concentration on DMFC performance using PtRu/C anode and Pt/C cathode with a Nafion binder. However, the PPD of the cells only reached 16 mW/cm^2 at 60 $^\circ\text{C}$.

Considering the success of PFSA ionomers in PEMFCs, Miyazaki et al. [208] proposed to use Nafion polyelectrolyte incorporated with ammonium counterions as binders, and they found that ammonium counterions had a positive effect on the formation of TPBs in MEA. All these preliminary attempts to use PTFE or Nafion binders in the early 2000s displayed relatively poor fuel cell performance since these binders were not able to transport OH^- .

4.2.2. Cationic ionomers

As a result, the development of available cationic ionomers for binders became an urgent demand at that time. To achieve this goal, Varcoe et al. [209] proposed to directly add an insoluble crosslinked-polystyrene AEP to catalyst electrodes. The PPD of H_2/O_2 fuel cells was substantially increased from 1.6 to 55 mW/cm^2 at 50°C after simply adding cationic ionomers. Unfortunately, these crosslinked ionomers could not be dissolved in solvents. After that, Park et al. [191] prepared a series of crosslinked PSF membranes and utilized TMA/TMHDA-aminated PSF as binders. MEA prepared from these aminated PSF polyelectrolytes reached a PPD of 30 mW/cm^2 under H_2/air conditions. Subsequently, Zhang and co-workers [210] synthesized a PVDF-based cationic ionomer using an atom transfer radical polymerization (ATRP) method, realizing a PPD of 55 mW/cm^2 in a direct hydrazine hydrate fuel cell (DHFC). However, PVDF-based polyelectrolytes were easily de-fluorinated under alkaline conditions. Then, Luet al. [211] prepared a methanol-soluble QPSF for AEMs and ionomers, and a H_2-O_2 AEMFC containing Cr-decorated Ni (CDN) anode and Ag cathode showed a PPD of 50 mW/cm^2 at 60°C .

In 2008, semi-commercial AEMs and ionomers appeared on the market. The Tokuyama Corporation reported two types of cationic ionomers (product code: A3Ver2 and AS-4), and Fumatech Corporation also reported a FAA membrane and a Fumion ionomer. Subsequently, Bunazawa and Yamazaki [212] first investigated the effect of the different contents of commercial A3 ionomers on fuel cell performance. They found that the MEA with 45.4% mass ionomer showed the best fuel cell performance with a PPD of 58.9 mW/cm^2 . Before 2008, the PPD of AEMFCs rarely exceeded 60 mW/cm^2 due to the poor performance of AEMs and ionomers. Nevertheless, this situation changed in 2009. Gu et al. [63] developed a soluble TPQPOH ionomer and realized a PPD of 196 mW/cm^2 at 80°C based on a FAA commercial membrane.

Although these preliminary efforts displayed the feasibility and importance of cationic ionomers, the PPD of these reported MEAs was still far away from applications. Due to the development of radiation-grafting techniques, the PPD of AEMFCs was significantly improved around 2012. Scott and co-workers [213] investigated the effect of various parameters, such as catalyst and ionomer loadings, the thickness of the catalyst layer, and fabrication techniques on the fuel cell performance by employing a BTMA-LDPE membrane and TMHDA-functionalized PS ionomers. H_2/air cells showed a PPD of 135 mW/cm^2 at 60°C . Subsequently, Mamlouk and Scott [214] developed a series of LDPE membranes and PS ionomers with different QA groups. A H_2/O_2 fuel cell showed a PPD of 478 mW/cm^2 with a current density of 722 mA/cm^2 , indicative of a further breakthrough in the AEMFCs performance at that time. After that, they emphasized the water management of AEMFCs [215]. They indicated that the main source of performance loss of AEMFCs was caused by the restricted mass transport of water from the anode to the cathode sites. After optimizing the water management, MEA prepared from BTMA-PS ionomers and BTMA-LDPE membrane achieved a PPD of 823 mW/cm^2 at 60°C under H_2/O_2 conditions.

These new advances provided deeper insight into the fundamental issues in AEMFCs such as the water management. However, the *in-situ* stability of AEMFCs was still a big challenge for AEMFCs. On the other hand, PPO-based AEIs have also received attention for AEIs due to their relatively higher chemical stability compared to PEEK and PSF-based AEPs. BTMA-PPO was frequently used as AEIs for PPO-based AEMs due to their acceptable solubility. Zhu et al. [128] presented a series of multi-cation side chain PPO ionomers—D30NC6NC6 (IEC=2.47 mmol/g) and T20NC6NC5N (IEC=2.52 mmol/g). H_2-O_2 AEMFCs employing T20NC6NC5N ionomers and AEMs exhibited a PPD of 364 mW/cm^2 at 60°C . Subsequently, some N-heterocyclic PPOs also have been

developed as AEIs. Chen et al. [131] presented a stable ASU-PPO ionomer with a PPD of 178 mW/cm^2 at 60°C . Li et al. [132,133] also prepared a series of ASU and DMP-functionalized PPO. PPO-ASU ionomer exhibited a PPD of 138 mW/cm^2 by employing a commercial LAM membrane ($80\ \mu\text{m}$, YiChen Technology, China).

4.2.3. Aryl ether-free ionomers

Fig. 22 summarizes current AEIs and Table 3 list the development of current AEMFCs based on different type AEMs and AEIs along with detailed testing conditions. In 2017, Gao et al. [216] reported a QASEBS ionomer for AEMFCs. H_2-O_2 AEMFCs based on QASEBS ionomer reached a PPD of 375 mW/cm^2 at 50°C , and the cells operated almost stably at a current density of 0.1 A/cm^2 for 500 h. Subsequently, they [59] optimized the dew point of electrodes, and the PPD of fuel cells was improved to 721.7 mW/cm^2 at 60°C .

Kim and co-workers investigated the phenyl absorption effect of side-chain-type poly(biphenyl) (BPN) and polyfluorene (FLNs) ionomers [105] on Pt/C and Pt-Ru/C. Rotating disk electrode experiments and DFT calculation study indicated that when phenyl groups have an orientation parallel to the catalyst surface, the activity of alkaline HOR and ORR decreased significantly. Specifically, FLN ionomers with non-rotatable backbone exhibited lower phenyl absorption and higher PPD (1.46 W/cm^2) than BPN and TPN ionomers with rotatable backbone. FLN-based fuel cells exhibited a 550 h *in-situ* durability under 0.6 A/cm^2 at 80°C . Subsequently, Kim's group [106] found that ammonium groups also have a cation-hydroxide-water co-adsorption on catalysts. They designed two different BPN ionomers: (1) introducing symmetric dimethyl groups in the BPN backbone to increase polymer fractional free volume (o-BPN), (2) replacing the alkyl TMA side chain with alkyl triethylammonium (TEA-o-BPN). They found that TEA-o-BPN exhibited the highest PPD over 1.5 W/cm^2 at 80°C due to lower cation adsorption effects. TEA-o-BPN-based fuel cells also exhibited a 100 h *in-situ* durability under 0.6 A/cm^2 .

On the other hand, DMP-type PAP exhibited outstanding fuel cell performance. However, PAP-type AEIs are scarce to date. Only two types of PAP ionomers—poly(biphenyl piperidinium) (PBP) and PTP—have been currently developed. Typically, Li et al. achieved a PPD over 2 W/cm^2 based PTP ionomers and AEMs under H_2-O_2 conditions [183]. On the other hand, PBP ionomers have been employed for high-performance PAP-TP-x membrane and reached a PPD to 0.92 W/cm^2 with a Ag cathode [96] and 1.31 W/cm^2 with Pt/C [99] cathode under H_2 -air conditions at 95°C , respectively, and the cell operated stably at a constant current density of 0.5 A/cm^2 for 300 h. However, PTP and PBP ionomers have been demonstrated to possess high phenyl adsorption on catalysts in Kim and co-workers' reports [105–109]. As a consequence, the power density of these PAP-based cells could be further improved after seeking a preferable ionomer.

On the other hand, BTMA-ETFE ionomers have achieved a lot of progress so far, and exhibited a good compatibility with BTMA-ETFE, BTMA-LDPE and BTMA-HDPE membranes. Typically, in 2018, Omasta et al. [98] presented a PPD of 1.9 W/cm^2 at 60°C under H_2-O_2 based on BTMA-ETFE membrane and ionomers. They emphasized the importance of water management in AEMFCs by a water-visualizing fuel cell system. Furthermore, replacing BTMA-ETFE ionomers to Gen-2 perfluorinated (PF) ionomers, H_2-O_2 AEMFCs reached a PPD to 1.4 W/cm^2 . Similarly, Pivovar and co-workers [217–218] worked on Gen-2 PF ionomers, and investigated the effect of using ionomer dispersions and ionomer solutions on fuel cell performance. They indicated that MEA using an ionomer dispersion exhibited a higher PPD ($>300\text{ mW/cm}^2$) than using an ionomer solution.

Subsequently, BTMA-ETFE ionomers have been combined with high-performance BTMA-HDPE membrane [169]. H_2-O_2 fuel cells

Table 3
Summary of state-of-the-art AEPs and AEMFC performance.

AEMs [thickness (μm)]/ σ_{OH^-} (mS/cm) at 80 °C]	AEIs (IEC-mmol/g, cationic type)	A/C catalysts	A/C DP (°C)	A/C BP (kPa)	A/C FR (L/min) active area	PPD (W/cm ²)	<i>In-situ</i> durability (Voltage loss)	Ref
Aryl ether-free AEMs and AEIs								
GT82–15/PTFE (10/14)	BTMA-ETFE (NG, BTMA)	PtRu/C, 0.7 mg/cm ² ; Pt/C, 0.6 mg/cm ² .	66/75	50/100	1/1(5cm ²)	3.5 (H ₂ -O ₂), ~1.2 (H ₂ -Air) at 80 °C	Stable (100 h, H ₂ /CO ₂ free air, 0.6 A/cm ² , 80 °C)	[9]
GT64–15/PTFE (<20/NG)	BTMA-ETFE (NG, BTMA)	PtRu/C, 0.7 mg/cm ² ; Pt/C, 0.6 mg/cm ² .	67/74	0/0	NG (5cm ²)	3.4 (H ₂ /O ₂) at 80 °C	Stable (545 h, H ₂ /CO ₂ free air, 0.6 A/cm ² , 80 °C)	[97]
HDPE (29±2/214)	BTMA-ETFE (1.9, BTMA)	PtRu/C, 0.7 mg/cm ² ; Pt/C, 0.6 mg/cm ² .	78/78	0/0	1/1 (5cm ²)	2.55 (H ₂ /O ₂) at 80 °C	7% loss (440 h, H ₂ /CO ₂ free air, 0.6 A/cm ² , 70 °C)	[169]
LDPE (28±6/208)	BTMA-ETFE (1.9, BTMA)	PtRu/C, 0.7 mg/cm ² ; Pt/C, 0.6 mg/cm ² .	78/78	0/0	1/1 (5cm ²)	2.01 (H ₂ /O ₂) at 80 °C	Rapid loss (100 h, H ₂ /CO ₂ free air, 0.6 A/cm ² , 70 °C)	[169]
QAPPT (30±5/137)	PTP (2.65, DMP)	PtRu/C, 0.27mgPt/cm ² ; Pt/C, 0.4 mgPt/cm ²	80/80	200/200	1/1 (4cm ²)	2.08/1.5 (H ₂ /O ₂) at 80 °C	Stable (125 h, H ₂ /CO ₂ free air, 0.2A/cm ² , 80 °C)	[129,183]
PAP-TP-85 (25±5/193 at 95 °C)	PBP (3.52, DMP)	PtRu/C, 0.15 mgPt/cm ² ; Ag, 1 mgAg/cm ²	94/95	250/130	0.15/0.95 (5cm ²)	0.92 (H ₂ /CO ₂ -free air) at 95 °C	11.5% (300 h, H ₂ /CO ₂ free air, 0.5 A/cm ² , 95 °C)	[96]
PAP-TP-85 (25±5/193 at 95 °C)	PBP(3.52, DMP)	PtRu/C, 0.15 mgPt/cm ² ; Pt/C, 0.4 mgPt/cm ²	88/97	125/250	1/2 (5cm ²)	1.89 (H ₂ /O ₂) and 1.31 (H ₂ /CO ₂ -free air) at 95 °C	NG	[99]
BTMA-ETFE (>25/132)	BTMA-ETFE (2.01, BTMA)	PtRu/C, 0.48 mgPt/cm ² ; Pt/C, 0.53 mgPt/cm ²	45/46	0/0	1/1 (5cm ²)	1.9 (H ₂ /O ₂) at 60 °C	40% (400 h, H ₂ /O ₂ , 0.6A/cm ² , 60 °C)	[98]
TPN (30/100)	FLN-55 (2.5, alkyl ammonium)	PtRu/C, 0.5 mgPt/cm ² ; Pt/C, 0.6 mgPt/cm ²	80/80	285/285	2/1 (5cm ²)	1.45 (H ₂ /O ₂) and 0.685 (H ₂ /CO ₂ -free air) at 80 °C.	Slight loss (550 h, H ₂ /O ₂ , 0.6 A/cm ² , 80 °C)	[105]
TPN (35/100)	TEA-o-BPN (2.2, alkyl ammonium)	PtRu/C, 0.5 mgPt/cm ² ; Pt/C, 0.6 mgPt/cm ²	80/80	285/285	2/1 (5cm ²)	>1.5 (H ₂ /O ₂) at 80 °C	Stable (120 h, H ₂ /O ₂ , 0.6 A/cm ² , 80 °C)	[106]
TPN (30/100)	BPN (2.6, alkyl ammonium)	PtRu/C, 0.5mgPt/cm ² ; Pt/C, 0.6 mgPt/cm ²	80/80	285/285	2/1 (5cm ²)	1.2 (H ₂ /O ₂) at 80 °C.	NG	[105]
Gen 2 PFAEM (45/122)	BTMA-ETFE (2.01, BTMA)	PtRu/C, 0.48 mgPt/cm ² ; Pt/C, 0.53 mgPt/cm ²	50/53	15/15	1/1 (5cm ²)	1.4 (H ₂ /O ₂) at 60 °C.	NG	[98]
Gen 2 PFAEM (29/55)	BTMA-ETFE (2.01, BTMA)	Pt/Vu, 0.5 mg/cm ² ; Ag/Vu, 1.0 mg/cm ²	50/53	121/121	1/1 (5cm ²)	0.62 (H ₂ /O ₂) at 60 °C.	NG	[217] [218]
M20C9N6NC5N (NG/115)	BTMA-ETFE (2.01, BTMA)	PtRu/C, 0.6 mgPt/cm ² ; Pt/C, 0.6 mgPt/cm ²	NG	0/0	1/1 (5cm ²)	0.94 (H ₂ /O ₂) at 760 °C.	NG	[49]

(continued on next page)

Table 3 (continued)

AEMs [thickness (μm)/ σ_{OH^-} (mS/cm) at 80 °C]	AEIs (IEC-mmol/g, cationic type)	A/C catalysts	A/C DP (°C)	A/C BP (kPa)	A/C FR (L/min) active area	PPD (W/cm ²)	<i>In-situ</i> durability (Voltage loss)	Ref
QASEBS (20/100)	QASEBS (1.36, BMTA)	PtRu/C, 0.3 mgPt/cm ² ; Pt/C, 0.3 mgPt/cm ²	60/50	100/100	1/1 (5cm ²)	0.721(H ₂ /O ₂) at 60 °C.	NG	[216]
XL100-SEBS-C5-TMA-0.8 (60/65)	FLN-55 (2.5, alkyl ammonium)	PtRu/C, 0.5 mgPt/cm ² ; Pt/C, 0.6 mgPt/cm ²	60/60	0/0	2/1 (5cm ²)	0.52(H ₂ /O ₂) at 60 °C.	NG	[62]
AEH9620 (22/35 at 30 °C)	QASEBS (0.21, alkyl ammonium)	Pt/C, 0.5 mgPt/cm ² ; Pt/C, 0.5 mgPt/cm ²	50/50	200/200	0.1/0.2(NG)	0.375 (H ₂ /O ₂) at 50 °C.	0.22 mV/h deg (500 h, H ₂ /O ₂ , 0.1A/cm ² , 50 °C)	[59]
89% HMT-PMBI (34±2/23)	89% HMT-PMBI (2.5, IM)	Pt/C, 0.4 mgPt/cm ² ; Pt/C, 0.4 mgPt/cm ²	60/60	200/200	NG (5cm ²)	0.37 (H ₂ /O ₂) at 60 °C.	Stable (8 h, H ₂ /O ₂ , 0.1 A/cm ² , 60 °C)	[152]
PAImBB (20/82)	BTMA-ETFE (NG, BTMA)	PtRu/C, 0.5 mgPt/cm ² ; Pt/C, 0.5 mgPt/cm ²	70/70	0/0	1/1 (5cm ²)	0.25 (H ₂ /O ₂) at 70 °C.	NG	[154]
Aryl ether AEMs and AEIs								
TMIImPPO (NG/NG)	CBQPPO (NG, alkyl ammonium)	PtRu/C, 0.5 mgPt/cm ² ; Pt/C, 0.5 mgPt/cm ²	70/70	100/100	1/1 (5cm ²)	1.37 (H ₂ /O ₂) at 70 °C.	0.6/cm ² 70 °C<60 h	[41]
aQAPS-S ₈ (50±5/108)	aQAPS-S ₁₄ (1, BTMA)	PtRu/C, 0.4 mgPt/cm ² ; Pt/C, 0.4 mgPt/cm ²	60/60	100/100	0.4/0.4 (4cm ²)	1.0 (H ₂ /O ₂) at 60 °C.	NG	[14]
PX75-T50 (NG/~110)	Crosslinked PS (NG, BTMA)	PtRu/C, 0.5 mgPt/cm ² ; Pt/C, 0.5 mgPt/cm ²	80/80	0/0	1/1 (5cm ²)	0.73 (H ₂ /O ₂) at 80 °C	0.4 A/cm ² 80 °C 400 h	[37]
T20NC6NC5N (34±2/180)	T20NC6NC5N (2.52, alkyl ammonium)	Pt/C, 0.4mgPt/cm ² ; Pt/C, 0.4 mgPt/cm ²	60/60	100/100	0.25/0.25 (4cm ²)	0.36 (H ₂ /O ₂) at 60 °C	NG	[128]
XE-Im d60 (NG/~80)	Tokuyama AS-4 (NG)	Pt/C, 0.5mgPt/cm ² ; Pt/C, 0.5 mgPt/cm ²	80/80	0/0	0.2/0.2 (5cm ²)	0.15 (H ₂ /O ₂) at 80 °C	0.2 A/cm ² 60 °C 800 h, 33% loss/	[193]
Commercial FAA (70/17 at RT)	TPQPOH (1.09, P ⁺)	Pt/C, 0.5mgPt/cm ² ; Pt/C, 0.5 mgPt/cm ²	80/80	250/250	0.2/0.2 (5cm ²)	0.19 (H ₂ /O ₂) at 80 °C	NG	[63]
ASU-TC-PPO (100/96)	ASU-PPO (2.24, ASU)	Pt/C, 0.5mgPt/cm ² ; Pt/C, 0.5 mgPt/cm ²	60/60	100/100	0.3/0.3 (5cm ²)	0.178 (H ₂ /O ₂) at 60 °C.	NG	[131]
Commercial AEMs and AEIs								
Tokuyama A901 (10/38)	Tokuyama AS-4 (NG)	Pt/C, 0.4 mgPt/cm ² ; Pt/C, 0.4 mgPt/cm ²	85/85	250/250	0.2/0.2	0.737 (H ₂ /O ₂) at 80 °C.	NG	[212]
Commercial FAA-(20/40 at 30 °C)	Fumion (NG)	Pt/C, 0.4mgPt/cm ² ; Pt/C, 0.4 mgPt/cm ²	60/60	100/100	0.4/0.4	0.52 (H ₂ /O ₂) at 80 °C.	NG	[T]
AEH9620 (22/35 at 30 °C)	Acta I2 (NG)	Pt/C, 0.5mgPt/cm ² ; Pt/C, 0.5 mgPt/cm ²	50/50	200/200	0.1/0.2	0.125 (H ₂ /O ₂) at 50 °C.	NG	[59]

A/C: anode/cathode; DP: dew point; BP: backpressure; FR: flow rate; T: this work; NG: not given.

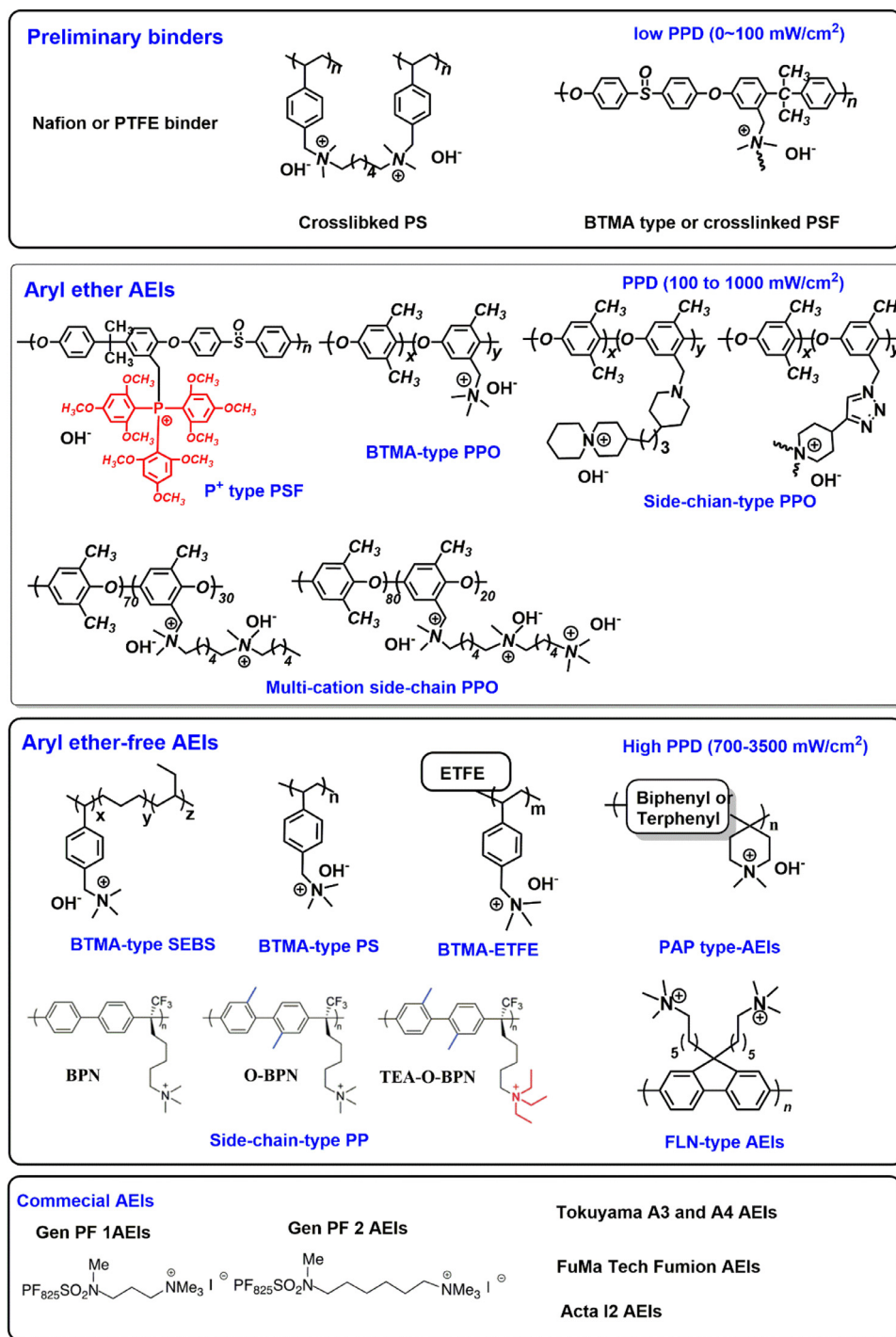


Fig. 22. Summary of AEIs and binders in current research, and these structures are collected from references [14,59,63,96,98,105,106,111,128,131-133, 169,181,191,205-219].

with Ag/C cathode reached a PPD of 1.72 W/cm² at 80 °C. Peng et al. [11] also reported a precious metal free cathode (nitrogen-doped carbon-CoO_x nanohybrids), and the cell reached a PPD over 1 W/cm² along with a 100 h *in-situ* durability based on BTMA-ETFE ionomers and BTMA-LDPE membrane. Meanwhile, the BTMA-ETFE ionomers have been employed for other AEMs. Typically, H₂-O₂ fuel cells based on BTMA-ETFE ionomers and a PTFE-reinforced PNB membrane (GT64-15) reached a PPD over 3 W/cm² at 80 °C, and operated stably under 0.6 A/cm² current density for 545 h [97]. BTMA-ETFE ionomers exhibited excellent compatibility with PTFE-reinforced PNB membranes.

Recently, Fan et al. [154] utilized BTMA-ETFE ionomer for large-hindrance PBI (PALmEE) AEMs. However, H₂-O₂ AEMFCs only reached a PPD of 0.25 W/cm² at 70 °C. Although PALmEE membrane (20 μm) exhibited excellent mechanical properties (tensile strength: 75 MPa and elongation at break: 17%) and acceptable ion conductivity, the fuel cell performance is somehow poor based on current fuel cell technology. Therefore, the compatibility issues between AEIs and AEMs should be noticed and further confirmed. BTMA-ETFE ionomer seems to possess excellent compatibility with flexible polymers (such as PE and PNB), but to mismatch with rigid

polymers (PBI). Therefore, different type AEMs may require matching ionomers, which should be further investigated.

4.3. Outlook for AEPs and fuel cell performance

4.3.1. Structure design of AEMs and AELs

AEMs and AELs play different roles in AEMFCs in some ways, therefore, the structure of AEMs and AELs should be differentiated.

4.3.1.1. For AEMs. Reviewing on Nafion® polyelectrolytes, the flexible and polar perfluorinated side chain (C-C and C-F bonds) increases the entanglement of polymers, resulting in Nafion membranes with excellent mechanical and film-forming properties. Unfortunately, perfluorinated AEMs have not received many attentions because of difficulties with fluorine chemistry and contamination issues in fluorine industry. Definitely, aryl ether-free AEMs are a current mainstream in AEMFCs, that can be briefly divided into two series of backbones: alkyl-alkyl backbones (polyolefin, PNB, polystyrene, or SEBS) and aryl-aryl backbones (PAP, polyphenylene, PBI, or TB). In fact, the state-of-the-art alkyl-alkyl AEMs show higher PPD than aryl-aryl AEMs. However, it is interesting to note that most alkyl-alkyl AEMs are based on commercial pre-formed membranes or reinforced with thin PTFE films, which endow outstanding film-forming and mechanical properties with these AEMs. However, every coin has two sides. Most of alkyl-alkyl AEMs possess poor solubility in many organic solvents. Therefore, the room for modification and optimization of these AEMs is very limited, especially to replace the BTMA groups. A majority of polystyrene or SEBS membranes [132,133] has been demonstrated to possess week mechanical strength (~10 MPa) and high elongation at break (>200%) due to nonpolar and flexible alkyl-alkyl backbones, causing a poor dimensional stability. Similarly, without PTFE reinforcement, crosslinked PNB membranes also exhibited a limited fuel cell performance [38]. On the other hand, aryl-aryl AEMs without reinforcement show excellent mechanical properties. Notice that AEMs require rotatable polymer backbones along with sufficient mechanical strengths. The merits of aryl-aryl AEMs are that the aromatic backbones have strong interactions between each other by π - π stacking. Some rotatable aryl-aryl polymers, such as PAP and PP, can simultaneously possess high tensile strength over 60 MPa along with reasonable elongation at break (10 to 117%). Therefore, the membrane-reinforcing strategies should be considered in the future AEMs.

4.3.1.2. For AELs. Aforementioned reviews reveal that AELs should possess minimal interaction with electrocatalysts, meaning that the AELs require non-rotatable or low phenyl-containing backbones along with suitable IECs, exemplified with BTMA-ETFE and FLN ionomers. Moreover, Matanovic et al. [101] found that polyphenylene ionomers are likely to suffer from the electrochemical oxidation and to produce phenol groups that limited the ORR activity, while FLN ionomers with substituents could alleviate this oxidation. Therefore, the polymer backbone of AELs needs to be carefully designed to fulfill all these requirements. Regarding IEC values, AELs require high ion conductivity and water permeability, but low ammonium adsorption. Current state-of-the-art AELs, such as BTMA-ETFE, FLN, PTP, and PBP ionomers, employ high IEC values over 2 mmol/g along with high water uptake. Therefore, the IECs of AELs should be kept in balance between the water permeability and ammonium adsorption.

On the other hand, Pt-Ru/C anode catalyst has been demonstrated to possess the least phenyl adsorption with AELs [101], and many high-performance AEMFCs are based on the Pt-Ru/C anode, as listed in Table 3. Therefore, different types of cationic groups may also display diverse adsorption behavior on catalysts, while systematical study still has not been performed. Actually, in

our unpublished work, we found that AELs still require reasonable molecular weight to anchor catalysts in the electrode very well, and this property is a fundamental requirement for AELs, which should not be overlooked in AELs.

4.3.2. Comparison of state-of-the-art AELs and AEMs

Table 3 and Fig. 23 summarize the current progress in AEMFCs. Nowadays, BTMA-type, DMP-type, and side chain type (five or six alkyl spacers) AEPs have seen a great progress in current research. Although some other cationic groups also possessed high alkaline stability, the corresponding AEPs, such as ASU, large-hindrance IM and cobaltocenium groups, exhibited a limited ion conductivity and fuel cell performance. Besides, most of high-performance AELs are based on BTMA and alkyl ammonium groups, while other cationic functional groups in the AELs are rare. Therefore, QA group is so far the best cationic group. Overall, DMP-type and side-chain-type AEPs show higher *ex-situ* durability than BTMA-type AEMs. Meanwhile, the alkaline stability of BTMA-type AEMs shows a big difference depending on the commercial pre-forming films. Typically, BTMA-HDPE membrane is more stable than BTMA-ETFE and BTMA-LDPE membranes.

Moreover, the *ex-situ* durability and *in-situ* durability of AEPs have been demonstrated to be mismatching. Some of AEPs exhibited excellent *ex-situ* durability over 5000 h, while no cells to date have been reported to show sufficient *in-situ* durability (~2000 h) at DOE-relevant current densities (0.6 A/cm²) [25], particularly at high temperature and in low humidity condition. Although DMP-type AEPs exhibited outstanding *ex-situ* durability, their long-term *in-situ* durability have reached below 300 h at 0.6 A/cm² so far. On the contrary, BTMA-HDPE membrane and BTMA-ETFE ionomers-based AEMFCs achieved a 440 h *in-situ* durability under 0.6 A/cm². As side-chain-type AEPs, the *in-situ* durability is also limited without reinforcement, while it is dramatically improved to 545 h (under 0.6 A/cm²) after PTFE-reinforcement. Therefore, the mechanical degradation of AEMs should be elaborately investigated during *in-situ* durability testing, and the mechanical properties of AEMs should be seriously taken into account when the AEMs are used for *in-situ* durability testing, particularly in OH⁻ form and at 100% RH. Since the PPD of AEMFCs has reached to an equal level to PEMFCs, the *in-situ* durability should be emphasized in the future research to promote the commercialization of AEMFCs.

5. New challenge of AEMFCs and perspective of AEPs

5.1. Unrealistic testing conditions

Although AEMFCs have advanced rapidly in recent years, however, it is interesting to note that current reported large jumps in AEMFC performance have been based on at least somewhat unrealistic testing conditions, such as high gas flow rates, high purity O₂, and employing Pt-based catalysts rather than non-platinum group catalysts. Moreover, the carbonation of AEPs is a lingering issue in AEMFCs, while that have been mostly overlooked in previous research. It is well known that OH⁻-conducting AEPs can react with CO₂ to produce CO₃²⁻ and/or HCO₃⁻ anions that increase the area-specific resistance since CO₃²⁻ and/or HCO₃⁻ has a lower intrinsic mobility than OH⁻. The carbonation of AEPs has been demonstrated to have a severe reduction in the operating cell voltage as high as 400 mV [219]. Researchers have hypothesized that the carbonation of AEPs increased the internal resistance and could be self-purging during operation at a current density higher than 1 A/cm². However, in 2019, Mustain et al. [220] investigated the CO₂ effects on fuel cell performance, and demonstrated that both of two assertions are not correct. They found that the concentrations of CO₃²⁻ in the anode is higher than in the cathode and AEMs. The resulting CO₃²⁻ concentration gradient makes

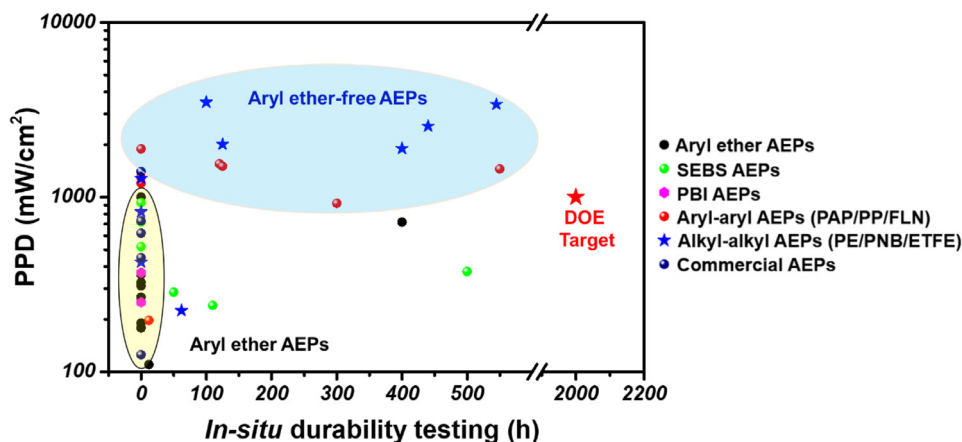


Fig. 23. Summary of PPD and *in-situ* durability testing of representative AEPs in current research [9,14,24–27, 37,59,63,96,98,105,106,111,128,131–139, 167–172, 181,191,205–219].

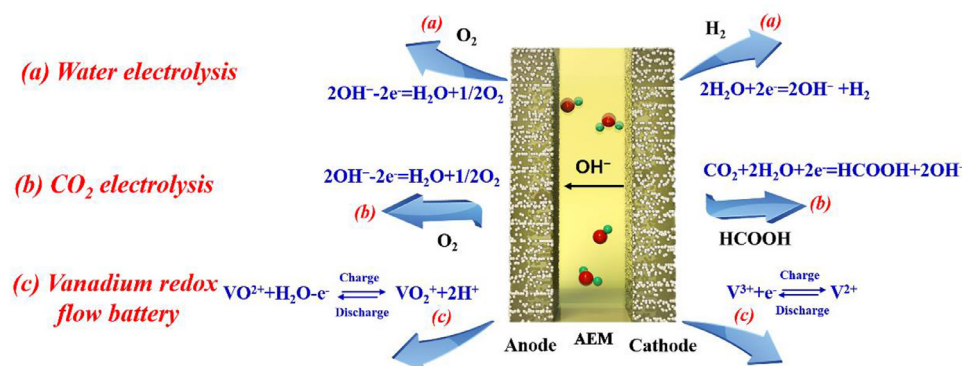


Fig. 24. Future applications of AEMs in water electrolysis, CO₂ electrolysis and vanadium redox flow batteries.

CO₃²⁻ accumulate within the anode, which decreases the local pH, leading to an increase in the anode potential. Besides, CO₃²⁻ in the anode effectively shuts off catalyst sites, causing an increase in charge transfer resistance due to a lack of availability of reacting OH⁻ anions. They indicated that even at 5 ppm CO₂ showed a significant loss in fuel cell performance.

5.2. Potential applications of AEPs

Because of the significant progress in AEMFCs, AEPs can be applied in other fields, such as water electrolysis, CO₂ electroreduction and vanadium redox flow batteries (VRFBs). Nevertheless, the performance requirements of AEPs used in different fields are slightly different depending on the operating conditions, as shown in Fig. 24.

5.2.1. Water electrolysis

AEPs are very promising for hydrogen production in electricity-driven water splitting, so called water electrolysis. Actually, water electrolysis is a reverse reaction relative to that of AEMFCs, and the structure of the water electrolysis device is very similar to AEMFCs. Consequently, the function and challenge of AEMs and AEPs used in water electrolysis are similar to AEMFCs, especially in terms of alkaline stability and ion conductivity. Very recently, Kim and coworkers [221] reported a stable and non-adsorbing ionomer for an AEM electrolyser that operated without the supporting NaOH/KOH electrolyte and used inexpensive catalysts. They pointed out that AEPs were easy to oxidation in the anode due to high potential, and phenolic compounds would be produced in some aromatic AEPs after oxidation. These phenolic compounds can

be detrimental to AEM electrolyser performance because they neutralize the alkaline charge carriers in the polymer [222].

5.2.2. CO₂ electrolysis

Actually, AEPs can be used for CO₂ electrolysis. Wang et al. [223] prepared a series of AEMs based on composite poly(vinyl alcohol) for CO₂ electroreduction to formate. They indicated that these AEMs produced higher CO₂ electroreduction efficiencies (67.6% to 68.6%) than Nafion 212 membrane (57.6%), implying that the use of AEMs in CO₂ electroreduction is feasible.

5.2.3. Vanadium redox flow battery

On the other hand, AEPs have potential applications in vanadium redox flow batteries (VRFBs). Here, a reduction in vanadium permeability through the membrane is very important to minimize self-discharge and to obtain a high Coulombic efficiency (CE). Chen et al. [224–226] prepared a series of TMA-based poly(flourenyl ether) AEMs to prevent vanadium crossover and capacity fade in VRFBs. Moreover, they remarked that VRFBs employing an AEM exhibited 100% CE under various current densities for VRFB applications.

6. Conclusion and future perspective

In summary, AEPs have been recognized with unprecedented achievements in AEMFCs in the past three years, especially in OH⁻ conductivity, *ex-situ* durability, and fuel cell performance, making low-cost AEMFCs practical in the near future. This review systematically and comprehensively summarized the development of

AEPs and highlighted the importance of durability, ionomer research, and the difference between AEMs and ionomers by comparing the advantages and disadvantages of the state-of-the-art AEMs and ionomers to accurately guide the direction of the future research on AEMFCs.

The major conclusions are as follows:

Years of study have developed a lot of cationic species and polymer backbones to address durability issues. Among them, QA is so far the most-studied cationic group due to their high ion conductivity and *ex-situ* durability. For the polymer backbone, aryl ether-free AEPs have been demonstrated to be superior for AEMFCs than aryl ether AEPs. Typically, BTMA-type, side-chain-type, and DMP-type AEPs have seen great progress in ion conductivity (~200 mS/cm) and power density (PPD to 3.5 W/cm²). Some of these AEPs will probably realize the commercial stage in the near future.

Many different strategies have been employed to enhance the comprehensive properties and performance of AEPs, such as microphase separation, crosslinking, inorganic-organic strategies, and commercial substrates. All these methods seem promising for further improvement of the performance of AEPs. Additionally, the durability issue of AEPs is still severe. Although a few AEPs exhibited high PPD, *in-situ* durability (~500 h) is still far from future requirements (2020 DOE: 0.6 A/cm² for 2000 h). Moreover, *ex-situ* durability does not match with *in-situ* durability. Therefore, it is important that *ex-situ* and *in-situ* durability evaluation systems should be further exploited and an effective method of evaluating durability should be developed in the near future.

Currently, most AEPs are used for AEMs, and AELs research is still lacking to date. This review comprehensively introduces the development of AELs, and emphasizes the deferent structural design between AELs and AEMs. The property requirements of AEMs and AELs are different in several aspects. BTMA-ETEF and FLN ionomers have proved to be good candidates for AELs. Importantly, the compatibility issues between AEMs and AELs should be noticed, and the mismatch between AEMs and ionomers may cause undetectable performance loss in AEMFCs.

Nowadays, some new challenges should be noticed in current research, which could hinder the future development of AEMFCs, such as electrochemical oxidation of AELs and the mechanical failure of AEMs during fuel cell operation, the carbonation of AEMFCs, and unrealistic testing conditions.

This review is expected to give a better understanding of AEMs and AELs, and provides an insight into the design of AEMs and AELs to reveal the limitations and challenges of AEMFCs. With these design strategies in mind, it is recommended to seek satisfactory AEMs and AELs in other applications, such as water electrolysis, CO₂ reduction, and flow batteries. We believe that the present review timely contributes to promoting the realization of AEMFCs in the near future.

Declaration of Competing Interest

No conflict of interest exists in the submission of this manuscript, and manuscript is approved by all authors for publication. The manuscript has not been submitted or considered for publication elsewhere.

Acknowledgement

This research was supported by the Technology Development Program to Solve Climate Change through the National Research Foundation of Korea (NRF) funded by the Ministry of Science and ICT (NRF-2018M1A2A2061979) and by the Technology Innovation Program (20010955, Development of fuel cell module technology using polymer electrolyte membrane for hydrocarbon-based fuel

cell) through the Korea Evaluation Institute of Industrial Technology (KEIT) funded by the Ministry of Trade, Industry & Energy (MOTIE) of South Korea.

References

- [1] Lee YM. Fuel cells: operating flexibly. *Nature Energy* 2016;1:16136/1-2.
- [2] Chen NJ, Chuan H, Wang HH, Kim SP, Kim HM, Lee WH, Bae JY, Park JH, Lee YM. Poly(alkyl-terphenyl piperidinium) ionomers and membranes with outstanding alkaline membrane fuel cell performance of 2.58 W cm². *Angew Chem Int Ed* 2021. doi:10.1002/ange.202013395.
- [3] Park CH, Lee SY, Hwang DS, Shin DW, Cho DH, Lee KH, Kim TW, Kim TW, Lee M, Kim DS, Doherty CM, Thornton AW, Hill AJ, Guiver MD, Lee YM. Nanocrack-regulated self-humidifying membranes. *Nature* 2016;532:480-3.
- [4] Liu X, Zhang J, Zheng C, Xue J, Huang T, Yin Y, et al. Oriented proton-conductive nano-sponge-facilitated polymer electrolyte membranes. *Energy Environ Sci* 2020;13:297-309.
- [5] Liu X, Li Y, Xue J, Zhu W, Zhang J, Yin Y, et al. Magnetic field alignment of stable proton-conducting channels in an electrolyte membrane. *Nat Commun* 2019;10:1-13.
- [6] Lee SH, Kasaiah JC. Proton transfer and the mobilities of the H⁺ and OH⁻ ions from studies of a dissociating model for water. *J Chem Phys* 2011;135:124505-15.
- [7] Guiver MD, Lee YM. Polymer rigidity improves microporous membranes. *Science* 2013;339:284-5.
- [8] Lopez-Haro M, Guetaz L, Printemps T, Morin A, Escribano S, Jouneau PH, et al. Three-dimensional analysis of Nafion layers in fuel cell electrodes. *Nat Commun* 2014;5:1-6.
- [9] Mandal M, Huang G, Hassan N U, Peng X, Gu T, Brooks-Starks AH, Bahar B, Mustain W E, Kohl P A. The importance of water transport in high conductivity and high-power alkaline fuel cells. *J Electrochem Soc* 2019;167:054501/1-11.
- [10] Omasta TJ, Wang L, Peng X, Lewis CA, Varcoe JR, Mustain WE. Importance of balancing membrane and electrode water in anion exchange membrane fuel cells. *J Pow Sourc* 2018;375:205-13.
- [11] Peng X, Omasta TJ, Magliocca E, Wang LQ, Varcoe JR, Mustain WE. Nitrogen-doped carbon-CoO_x nanohybrids: a precious metal free cathode that exceeds 1.0 Wcm⁻² peak power and 100 h life in anion exchange membrane fuel cells. *Angew Chem Int Ed* 2019;131:1058-63.
- [12] Meeke KM, Antunesa CM, Strassera DJ, Owczarczyka ZR, Yang-Neyerlina AC, Pivovar BS. High-throughput anion exchange membrane characterization at NREL. *ECS Trans* 2019;92:723-31.
- [13] Park EJ, Kim YS. Quaternized aryl ether-free polyaromatics for alkaline membrane fuel cells: synthesis, properties, and performance—a topical review. *J Mater Chem A* 2018;6:15456-77.
- [14] Pan J, Chen C, Li Y, Wang L, Tan L, Li G, et al. Constructing ionic highway in alkaline polymer electrolytes. *Energy Environ Sci* 2014;7:354-60.
- [15] Mandal M, Huang G, Kohl PA. Highly conductive anion-exchange membranes based on cross-linked poly (norbornene): vinyl addition polymerization. *ACS Appl Energy Mater* 2019;2(4):2447-57.
- [16] Wang Y, Wang G, Li G, Huang B, Pan J, Liu Q, Han J J, Xiao L, Lu J T, Lin Z. Pt-Ru catalyzed hydrogen oxidation in alkaline media: oxophilic effect or electronic effect? *Energy Environ Sci* 2015;8:177-81.
- [17] Wang YJ, Qiao J, Baker R, Zhang J. Alkaline polymer electrolyte membranes for fuel cell applications. *Chem Soc Rev* 2013;42:5768-87.
- [18] Shin DW, Guiver MD, Lee YM. Hydrocarbon-based polymer electrolyte membranes: importance of morphology on ion transport and membrane stability. *Chem Rev* 2017;117:4759-05.
- [19] Dekel DR. Review of cell performance in anion exchange membrane fuel cells. *J Pow Sourc* 2018;375:158-69.
- [20] Luo T, Abdu S, Wessling M. Selectivity of ion exchange membranes: a review. *J Membr Sci* 2018;555:429-54.
- [21] Zhou J, Zuo P, Liu Y, Yang Z, Xu T. Ion exchange membranes from poly(2,6-dimethyl-1,4-phenylene oxide) and related applications. *Sci China Chem* 2018;61:1062-87.
- [22] Fujimoto C, Kim DS, Hibbs M, Wroblewski D, Kim YS. Backbone stability of quaternized polyaromatics for alkaline membrane fuel cells. *J Membr Sci* 2012;423:438-49.
- [23] Shin MS, Byun YJ, Choi YW, Kang MS, Park JS. On-site crosslinked quaternized poly (vinyl alcohol) as ionomer binder for solid alkaline fuel cells. *Int J Hydro Energy* 2014;39:16556-61.
- [24] Couture G, Alaaeddine A, Boschet F, Ameduri B. Polymeric materials as anion-exchange membranes for alkaline fuel cells. *Progress Polym Sci* 2011;36:1521-57.
- [25] Thompson ST, Peterson D, Ho D, Papageorgopoulos D. Perspective—the next decade of AEMFCs: near-term targets to accelerate applied R&D. *J Electrochem Soc* 2020;167:084514/1-6.
- [26] Arges CG, Ramani V. Two-dimensional NMR spectroscopy reveals cation-triggered backbone degradation in polysulfone-based anion exchange membranes. *Proc Natl Acad Sci* 2013;110:2490-5.
- [27] Park EJ, Maurya S, Hibbs MR, Fujimoto CH, Kreuer K-D, Kim YS. Alkaline stability of quaternized diels-alder polyphenylenes. *Macromolecules* 2019;52:5419-28.

- [28] Lee W-H, Mohanty AD, Bae C. Fluorene-based hydroxide ion conducting polymers for chemically stable anion exchange membrane fuel cells. *ACS Macro Lett* 2015;4:453–7.
- [29] Chempath S, Boncella JM, Pratt LR, Henson N, Pivovar BS. Density functional theory study of degradation of tetraalkylammonium hydroxides. *J Phys Chem C* 2010;114:11977–83.
- [30] Navlani-García M, Mori K, Kuwahara Y, Yamashita H. Recent strategies targeting efficient hydrogen production from chemical hydrogen storage materials over carbon-supported catalysts. *NPG Asia Mater* 2018;10:277–92.
- [31] Yu L, Zhu Q, Song S, McElhenny B, Wang D, Wu C, Qin Z, Bao J, Yu Y, Chen S, Ren Z. Non-noble metal-nitride based electrocatalysts for high-performance alkaline seawater electrolysis. *Nat Commun* 2019;10:1–10.
- [32] Zhu H, Sun Z, Chen N, Cao H, Chen M, Li K, Cai Y, Wang F. A non-precious-metal catalyst derived from a $\text{Cp}_2\text{-Co}^+\text{-PBI}$ composite for cathodic oxygen reduction under both acidic and alkaline conditions. *Chem Electro Chem* 2017;4:1117–23.
- [33] Wang L, Brink JJ, Liu Y, Herring AM, Ponce-González J, Whelligan DK, Varcoe JR. Non-fluorinated pre-irradiation-grafted (peroxidated) LDPE-based anion-exchange membranes with high performance and stability. *Energy Environ Sci* 2017;10:2154–67.
- [34] You W, Noonan KJT, Coates GW. Alkaline-stable anion exchange membranes: a review of synthetic approaches. *Progress Polym Sci* 2019;100 101177/1–13.
- [35] Eriksson B, Grimmler H, Carlson A, Ekström H, Wreland Lindström R, Lindbergh G, Lagergren C. Quantifying water transport in anion exchange membrane fuel cells. *Int J Hydro Energy* 2019;44:4930–9.
- [36] Yassin K, Rasin IG, Brandon S, Dekel DR. Quantifying the critical effect of water diffusivity in anion exchange membranes for fuel cell applications. *J Membr Sci* 2020;608 118206/1–6.
- [37] Kim Y, Wang Y, France-Lanord A, Wang Y, Wu YM, Lin S, Li YF, Grossman JC, Swager TM. Ionic highways from covalent assembly in highly conducting and stable anion exchange membrane fuel cells. *J Am Chem Soc* 2019;141:18152–9.
- [38] Mandal M, Huang G, Kohl PA. Anionic multiblock copolymer membrane based on vinyl addition polymerization of norbornenes: applications in anion-exchange membrane fuel cells. *J Membr Sci* 2019;570:394–402.
- [39] Gupta G, Scott K, Mamlouk M. Soluble polystyrene-*b*-poly(ethylene/butylene)-*b*-polystyrene based ionomer for anion exchange membrane fuel cells operating at 70 °C. *Fuel Cells* 2018;18:137–47.
- [40] Pasquini L, Wacrenier O, Vona MLD, Knauth P. Hydration and ionic conductivity of model cation and anion-conducting ionomers in buffer solutions (Phosphate, Acetate, Citrate). *J Phys Chem B* 2018;122:12009–16.
- [41] Liang X, Shehzad MA, Zhu Y, Wang L, Ge X, Zhang J, Wu L, Varcoe JR, Xu T. Ionomer cross-linking immobilization of catalyst nanoparticles for high performance alkaline membrane fuel cells. *Chem Mater* 2019;31:7812–20.
- [42] Choi J, Kim M-H, Han JY, Chae JE, Lee WH, Lee YM, Lee SY, Jang JH, Henkensmeier D, Yoo SJ, Sun Y-E, Kim H-J. Application of spirobiindane-based micro-porous poly(ether sulfone)s as polymeric binder on solid alkaline exchange membrane fuel cells. *J Membr Sci* 2018;568:67–75.
- [43] Yang Z, Zhou J, Wang S, Hou J, Wu L, Xu T. A strategy to construct alkali-stable anion exchange membranes bearing ammonium groups via flexible spacers. *J Mater Chem A* 2015;3:15015–19.
- [44] Ran J, Wu L, He Y, Yang Z, Wang Y, Jiang C, et al. Ion exchange membranes: new developments and applications. *J Membr Sci* 2017;522:267–91.
- [45] Willdorf-Cohen S, Mondal AN, Dekel DR, Diesendruck CE. Chemical stability of poly(phenylene oxide)-based ionomers in an anion exchange-membrane fuel cell environment. *J Mater Chem A* 2018;6:22234–9.
- [46] Dekel DR, Willdorf S, Ash U, Amar M, Pusara S, Dhara S, Srebniak S, Diesendruck CE. The critical relation between chemical stability of cations and water in anion exchange membrane fuel cells environment. *J Pow Sour* 2018;375:351–60.
- [47] Lee W-H, Park EJ, Han J, Shin DW, Kim YS, Bae C. Poly(terphenylene) anion exchange membranes: the effect of backbone structure on morphology and membrane property. *ACS Macro Lett* 2017;6:566–70.
- [48] Wang C, Mo B, He Z, Shao Q, Pan D, Wujick E, Guo J, Xie X, Xie X, Guo Z. Crosslinked norbornene copolymer anion exchange membrane for fuel cells. *J Membr Sci* 2018;556:118–25.
- [49] Zhu L, Yu X, Peng X, Zimudzi TJ, Saikia N, Kwasny MT, Song S, Kushner DI, Fu Z, Tew GN, Mutain WE, Yandrasits MA, Hickner MA. Poly(olefin)-based anion exchange membranes prepared using Ziegler-Natta polymerization. *Macromolecules* 2019;52:4030–41.
- [50] Zhu L, Yu X, Hickner MA. Exploring backbone-cation alkyl spacers for multi-cation side chain anion exchange membranes. *J Pow Sour* 2018;375:433–41.
- [51] Chen N, Lu C, Li Y, Long C, Zhu H. Robust poly(aryl piperidinium)/N-spirocyclic poly(2,6-dimethyl-1,4-phenyl) for hydroxide-exchange membranes. *J Membr Sci* 2019;572:246–54.
- [52] Chen N, Long C, Li Y, Wang D, Lu C, Zhu H, Yu JH. Three-decker strategy based on multifunctional layered double hydroxide to realize high-performance hydroxide exchange membranes for fuel cell applications. *ACS Appl Mater Interfaces* 2018;10:18246–56.
- [53] Akiyama R, Yokota N, Miyatake K. Chemically stable, highly anion conductive polymers composed of quinquophenylene and pendant ammonium groups. *Macromolecules* 2019;52:2131–8.
- [54] Akiyama R, Yokota N, Nishino E, Asazawa K, Miyatake K. Anion conductive aromatic copolymers from dimethylaminomethylated monomers: synthesis, properties, and applications in alkaline fuel cells. *Macromolecules* 2016;49:4480–9.
- [55] Wang Z, Li Z, Chen N, Lu C, Wang F, Zhu H. Crosslinked poly(2,6-dimethyl-1,4-phenylene oxide) polyelectrolyte enhanced with poly(styrene-*b*-(ethylene-co-butylene)-*b*-styrene) for anion exchange membrane applications. *J Membr Sci* 2018;564:492–500.
- [56] Ziv N, Dekel DR. A practical method for measuring the true hydroxide conductivity of anion exchange membranes. *Electrochem Commun* 2018;88:109–13.
- [57] Liu FH, Yang Q, Gao XL, Wu HY, Zhang QG, Zhu AM, Liu QL. Anion exchange membranes with dense N-spirocyclic cations as side-chain. *J Membr Sci* 2020;595 117560/1–9.
- [58] Hao J, Gao X, Jiang Y, Zhang H, Luo J, Shao Z, Yi BL. Crosslinked high-performance anion exchange membranes based on poly(styrene-*b*-(ethylene-co-butylene)-*b*-styrene). *J Membr Sci* 2018;551:66–75.
- [59] Gao X, Yu H, Qin B, Jia J, Hao J, Xie F, Shao ZG. Enhanced water transport in AEMs based on poly(styrene-ethylene-butylene-styrene) triblock copolymer for high fuel cell performance. *Polym Chem* 2019;10:1894–903.
- [60] Mohanty AD, Ryu CY, Kim YS, Bae C. Stable elastomeric anion exchange membranes based on quaternary ammonium-tethered polystyrene-*b*-poly(ethylene-co-butylene)-*b*-polystyrene triblock copolymers. *Macromolecules* 2015;48:7085–95.
- [61] Hugar KM, You W, Coates GW. Protocol for the quantitative assessment of organic cation stability for polymer electrolytes. *ACS Energy Lett* 2019;4:1681–6.
- [62] Jeon J Y, Park S, Han J, Maurya S, Mohanty A D, Tian D, Saikia N, Hickner, Ryu CY, Tuckerman ME, Paddison SJ, Kim YS, Bae C. Synthesis of aromatic anion exchange membranes by Friedel-Crafts bromoalkylation and cross-linking of polystyrene block copolymers. *Macromolecules* 2019;52:2139–2147.
- [63] Gu S, Cai R, Luo T, Chen Z, Sun M, Liu Y, He GH, Yan YS. A soluble and highly conductive ionomer for high-performance hydroxide exchange membrane fuel cells. *Angew Chem Int Ed* 2009;48:6499–502.
- [64] Han H, Ma H, Yu J, Zhu H, Wang Z. Preparation and performance of novel tetraphenylphosphonium-functionalized polyphosphazene membranes for alkaline fuel cells. *Eur Polym J* 2019;114:109–17.
- [65] Noonan KJ, Hugar KM, Kostalik HAT, Lobkovsky EB, Abruna HD, Coates GW. Phosphonium-functionalized polyethylene: a new class of base-stable alkaline anion exchange membranes. *J Am Chem Soc* 2012;134:18161–4.
- [66] Zhang B, Gu S, Wang J, Liu Y, Herring AM, Yan Y. Tertiary sulfonium as a cationic functional group for hydroxide exchange membranes. *RSC Adv* 2012;2:12683–5.
- [67] Zha Y, Disabb-Miller ML, Johnson ZD, Hickner MA, Tew GN. Metal-cation-based anion exchange membranes. *J Am Chem Soc* 2012;134:4493–6.
- [68] Gu S, Wang J, Kaspar RB, Fang Q, Zhang B, Coughlin EB, Yan Y. Permethylobaltocenium (Cp^*_2Co) as an ultra-stable cation for polymer hydroxide-exchange membranes. *Sci Rep* 2015;5 11668/1–11.
- [69] Chen N, Zhu H, Chu Y, Li R, Liu Y, Wang F. Cobaltocenium-containing polybenzimidazole polymers for alkaline anion exchange membrane applications. *Polym Chem* 2017;8:1381–92.
- [70] Kwasny MT, Zhu L, Hickner MA, Tew GN. Utilizing thiol-ene chemistry for crosslinked nickel cation-based anion exchange membranes. *J Polym Sci Part A Polym Chem* 2018;56:328–39.
- [71] Marino MG, Kreuer KD. Alkaline stability of quaternary ammonium cations for alkaline fuel cell membranes and ionic liquids. *ChemSusChem* 2015;8:513–23.
- [72] Huang T, He G, Xue J, Otoo O, He X, Jiang H, et al. Self-crosslinked blend alkaline anion exchange membranes with bi-continuous phase separated morphology to enhance ion conductivity. *J Membr Sci* 2020;597 117769/1–10.
- [73] Wu X, Chen W, Yan X, He G, Wang J, Zhang Y, Zhu X. Enhancement of hydroxide conductivity by the di-quaternization strategy for poly(ether ether ketone) based anion exchange membranes. *J Mater Chem A* 2014;2:12222–31.
- [74] Han KW, Ko KH, Abu-Hakme K, Bae C, Sohn YJ, Jang SS. Molecular dynamics simulation study of a polysulfone-based anion exchange membrane in comparison with the proton exchange membrane. *J Phys Chem C* 2014;118:12577–87.
- [75] Pan Y, Zhang Q, Yan X, Liu J, Xu X, Wang T, Hamouti IE, Ruan X, Hao C, He GH. Hydrophilic side chain assisting continuous ion-conducting channels for anion exchange membranes. *J Membr Sci* 2018;552:286–94.
- [76] Ge Q, Ran J, Miao J, Yang Z, Xu T. Click chemistry finds its way in constructing an ionic highway in anion-exchange membrane. *ACS Appl Mater Interfaces* 2015;7:28545–53.
- [77] Chen Y, Li Z, Chen N, Li R, Zhang Y, Li K, Wang F, Zhu H. A new method for improving the conductivity of alkaline membrane by incorporating TiO_2 -ionic liquid composite particles. *Electrochimica Acta* 2017;255:335–46.
- [78] Li Y, Zhou W, Wang H, Xie L, Liang Y, Wei F, Idrobo J-C, Pennycook SJ, Dai HJ. An oxygen reduction electrocatalyst based on carbon nanotube-graphene complexes. *Nat Nanotechnol* 2012;7:394–400.
- [79] Wang Y, Yang Y, Jia S, Wang X, Lyu K, Peng Y, Zheng Y, Wei X, Ren H, Xiao L, Wang J, Muller DA, Abruña HD, Hwang BJ, Lu JT, Zhuang L. Synergistic Mn-Co catalyst outperforms Pt on high-rate oxygen reduction for alkaline polymer electrolyte fuel cells. *Nat Commun* 2019;10:1–8.
- [80] Pan J, Zhu L, Han J, Hickner MA. Mechanically tough and chemically stable anion exchange membranes from rigid-flexible semi-interpenetrating networks. *Chem Mater* 2015;27:6689–98.
- [81] Li N, Wang L, Hickner M. Cross-linked comb-shaped anion exchange membranes with high base stability. *Chem Commun (Camb)* 2014;50:4092–5.

- [82] Lin B, Xu F, Su Y, Han J, Zhu Z, Chu F, Ren Y, Zhu L, Ding J. Ether-free polybenzimidazole bearing pendant imidazolium groups for alkaline anion exchange membrane fuel cells application. *ACS Appl Energy Mater* 2019;1:1089–1098.
- [83] Olsson JS, Pham TH, Jannasch P. Poly(N,N-diallylazacycloalkane)s for anion-exchange membranes functionalized with N-spirocyclic quaternary ammonium cations. *Macromolecules* 2017;50:2784–93.
- [84] Olsson JS, Pham TH, Jannasch P. Poly(arylene piperidinium) hydroxide ion exchange membranes: synthesis, alkaline stability, and conductivity. *Adv Funct Mater* 2018;28:1702758/1–10.
- [85] Olsson JS, Pham TH, Jannasch P. Tuning poly(arylene piperidinium) anion-exchange membranes by copolymerization, partial quaternization and crosslinking. *J Membr Sci* 2019;578:183–95.
- [86] Zhuang Y, Seong JG, Do YS, Lee WH, Lee MJ, Cui Z, Lozano AE, Guiver MD, Lee YM. Soluble, microporous, Troger's Base copolyimides with tunable membrane performance for gas separation. *Chem Commun (Camb)* 2016;52:3817–20.
- [87] Han J, Zhu L, Pan J, Zimudzi TJ, Wang Y, Peng Y, Hickner MA, Zhuang L. Elastic long-chain multication cross-linked anion exchange membranes. *Macromolecules* 2017;50:3323–32.
- [88] Miyaniishi S, Fukushima T, Yamaguchi T. Synthesis and property of semicrystalline anion exchange membrane with well-defined ion channel structure. *Macromolecules* 2015;48:2576–84.
- [89] Su Z, Kole S, Harden LC, Palakkal VM, Kim C, Nair G, Arges CG. Peptide-modified electrode surfaces for promoting anion exchange ionomer microphase separation and ionic conductivity. *ACS Mater Lett* 2019;1:467–75.
- [90] Park AM, Wycisk RJ, Ren X, Turley FE, Pintauro PN. Crosslinked poly(phenylene oxide)-based nanofiber composite membranes for alkaline fuel cells. *J Mater Chem A* 2016;4:132–41.
- [91] Zhang X, Cao Y, Zhang M, Wang Y, Tang H, Li N. Olefin metathesis-crosslinked, bulky imidazolium-based anion exchange membranes with excellent base stability and mechanical properties. *J Membr Sci* 2020;598:117793/1–11.
- [92] Zhang Y, Chen W, Yan X, Zhang F, Wang X, Wu X, Peng B, Wang J, He GH. Ether spaced N-spirocyclic quaternary ammonium functionalized crosslinked polysulfone for high alkaline stable anion exchange membranes. *J Membr Sci* 2020;598:117650/1–10.
- [93] Cheng X, Wang J, Liao Y, Li C, Wei Z. Enhanced conductivity of anion-exchange membrane by incorporation of quaternized cellulose nanocrystal. *ACS Appl Mater Interfaces* 2018;10:23774–82.
- [94] Zhang H, Shi B, Ding R, Chen H, Wang J, Liu J. Composite anion exchange membrane from quaternized polymer spheres with tunable and enhanced hydroxide conduction property. *Indust Eng Chem Res* 2016;55:9064–76.
- [95] Feng T, Lin B, Zhang S, Yuan N, Chu F, Hickner MA, Wang C, Zhu L, Ding J. Imidazolium-based organic-inorganic hybrid anion exchange membranes for fuel cell applications. *J Membr Sci* 2016;508:7–14.
- [96] Wang J, Zhao Y, Setzler BP, Rojas-Carbonell S, Ben Yehuda C, Amel A, Page M, Wang L, Hu K, Shi L, Gottesfeld S, Xu B J, Yan Y. Poly(aryl piperidinium) membranes and ionomers for hydroxide exchange membrane fuel cells. *Nature Energy* 2019;4:392–8.
- [97] Huang G, Mandal M, Peng X, Yang-Neyerlin AC, Pivovar BS, Mustain WE, Kohl PH. Composite poly(norbornene) anion conducting membranes for achieving durability, water management and high power (3.4 W/cm²) in hydrogen/oxygen alkaline fuel cells. *J Electrochem Soc* 2019;166:F637–FF44.
- [98] Omasta TJ, Park AM, LaManna JM, Zhang Y, Peng X, Wang L, Jacobson DL, Varcoe JR, Hussey DS, Pivovar BS, Mustain WE. Beyond catalysis and membranes: visualizing and solving the challenge of electrode water accumulation and flooding in AEMFCs. *Energy Environ Sci* 2018;11:551–8.
- [99] Omasta TJ, Zhang Y, Park AM, Peng X, Pivovar B, Varcoe JR, Mustain W E. Strategies for reducing the PGM loading in high power AEMFC anodes. *J Electrochem Soc* 2018;165:F710–F7.
- [100] Wang L, Bellini M, Miller HA, Varcoe JR. A high conductivity ultrathin anion-exchange membrane with 500+ h alkali stability for use in alkaline membrane fuel cells that can achieve 2 W cm⁻² at 80 °C. *J Mater Chem A* 2018;6:15404–12.
- [101] Matanovic I, Chung HT, Kim YS. Benzene adsorption: a significant inhibitor for the hydrogen oxidation reaction in alkaline conditions. *J Phys Chem Lett* 2017;8:4918–24.
- [102] Valade D, Boschet F, Ameduri B. Grafting polymerization of styrene onto alternating terpolymers based on chlorotrifluoroethylene, hexafluoropropylene, and vinyl ethers, and their modification into ionomers bearing ammonium side-groups. *J Polym Sci Part A Polym Chem* 2010;48:5801–11.
- [103] Lee CH, Lee SY, Lee YM, McGrath JE. Chemically tuned anode with tailored aqueous hydrocarbon binder for direct methanol fuel cells. *Langmuir* 2009;25:8217–25.
- [104] Li D, Matanovic I, Lee AS, Park EJ, Fujimoto C, Chung HT, Kim Y S. Phenyl oxidation impacts the durability of alkaline membrane water electrolyzer. *ACS Appl Mater Interfaces* 2019;11:9696–701.
- [105] Maurya S, Noh S, Matanovic I, Park EJ, Narvaez Villarrubia C, Martinez U, Han J, Bae C, Kim YS. Rational design of polyaromatic ionomers for alkaline membrane fuel cells with >1 W cm⁻² power density. *Energy Environ Sci* 2018;11:3283–91.
- [106] Park EJ, Maurya S, Lee AS, Leonard DP, Li D, Jeon JY, Bae C, Kim Y S. How does a small structural change of anode ionomer make a big difference in alkaline membrane fuel cell performance. *J Mater Chem A* 2019;7:25040–6.
- [107] Valade D, Boschet Fdr, Améduri B. Synthesis and modification of alternating copolymers based on vinyl ethers, chlorotrifluoroethylene, and hexafluoropropylene. *Macromolecules* 2009;42:7689–700.
- [108] Valade D, Boschet F, Rouldès S, Ameduri B. Preparation of solid alkaline fuel cell binders based on fluorinated poly(diallyldimethylammonium chloride)s [poly(DADMAC)] or poly (chlorotrifluoroethylene-co-DADMAC) copolymers. *J Polym Sci Part A Polym Chem* 2009;47:2043–58.
- [109] Guinot SSE, Penneub JF, Fauvarque JF. A new class of PEO-based SPEs: structure, conductivity and application to alkaline secondary batteries. *Electrochimica Acta* 2000;43:1163–70.
- [110] Owens BB. A new class of high-conductivity solid electrolytes: tetraalkylammonium iodide-silver iodide double salts. *J Electrochem Soc* 1970;117:1536/1–4.
- [111] Agel E, Bouet J, Fauvarque JF. Characterization and use of anionic membrane for alkaline fuel cells. *J Pow Sour* 2001;101:267–74.
- [112] Sun Z, Pan J, Guo J, Yan F. The alkaline stability of anion exchange membrane for fuel cell applications: the effects of alkaline media. *Adv Sci* 2018;5:1800065/1–11.
- [113] Lee B, Yun D, Lee J-S, Park CH, Kim T-H. Development of highly alkaline stable OH⁻conductors based on imidazolium cations with various substituents for anion exchange membrane-based alkaline fuel cells. *J Phys Chem C* 2019;123:13508–18.
- [114] Liu Y, Wang J, Yang Y, Brenner TM, Seifert S, Yan Y, Liberatore MW. Anion transport in a chemically stable, sterically bulky α -C modified imidazolium functionalized anion exchange membrane. *J Phys Chem C* 2014;118:15136–45.
- [115] Long H, Pivovar B. Hydroxide degradation pathways for imidazolium cations: a DFT study. *J Phys Chem C* 2014;118:9880–8.
- [116] Pan J, Han J, Zhu L, Hickner MA. Cationic side-chain attachment to poly(phenylene oxide) backbones for chemically stable and conductive anion exchange membranes. *Chem Mater* 2017;29:5321–30.
- [117] Ponce-González J, Wheligan DK, Wang L, Bance-Souahli R, Wang Y, Peng Y, Peng H, Apperley DC, Sarode HN, Pendey TP, Divekar AG, Seifert S, Herring AM, Zhuang L, Varcoe JR. High performance aliphatic-heterocyclic benzyl-quaternary ammonium radiation-grafted anion-exchange membranes. *Energy Environ Sci* 2016;9:3724–35.
- [118] Wang L, Magliocca E, Cunningham EL, Mustain WE, Poynton SD, Escudero-Cid R, Nasef MM, Ponce-González J, Bance-Souahli R, Slade RCT, Wheligan DK, Varcoe JR. An optimised synthesis of high performance radiation-grafted anion-exchange membranes. *Green Chem* 2017;19:831–43.
- [119] Danks TN, Slade RCT, Varcoe JR. Comparison of PVDF- and FEP-based radiation-grafted alkaline anion-exchange membranes for use in low temperature portable DMFCs. *J Mater Chem* 2002;12:3371–3.
- [120] Choe Y-K, Fujimoto C, Lee K-S, Dalton LT, Ayers K, Henson NJ, Kim YS. Alkaline stability of benzyl trimethyl ammonium functionalized polyaromatics: a computational and experimental study. *Chem Mater* 2014;26:5675–5682.
- [121] Pham TH, Jannasch P. Aromatic polymers incorporating bis-N-spirocyclic quaternary ammonium moieties for anion-exchange membranes. *ACS Macro Lett* 2015;4:1370–5.
- [122] Hibbs MR. Alkaline stability of poly(phenylene)-based anion exchange membranes with various cations. *J Polym Sci Part B Polym Phys* 2013;51:1736–42.
- [123] Mohanty AD, Tignor SE, Krause JA, Choe Y-K, Bae C. Systematic alkaline stability study of polymer backbones for anion exchange membrane applications. *Macromolecules* 2016;49:3361–72.
- [124] Zhang Z, Wu L, Varcoe J, Li C, Ong AL, Poynton S, Xu T. Aromatic polyelectrolytes via polyacylation of pre-quaternized monomers for alkaline fuel cells. *J Mater Chem A* 2013;1:2595–601.
- [125] Dang H-S, Jannasch P. Exploring different cationic alkyl side chain designs for enhanced alkaline stability and hydroxide ion conductivity of anion-exchange membranes. *Macromolecules* 2015;48:5742–51.
- [126] Nuñez SA, Capparelli C, Hickner MA. N-alkyl interstitial spacers and terminal pendants influence the alkaline stability of tetraalkylammonium cations for anion exchange membrane fuel cells. *Chem Mater* 2016;28:2589–98.
- [127] Pan J, Li Y, Han J, Li G, Tan L, Chen C, Lu J, Zhuang L. A strategy for disentangling the conductivity-stability dilemma in alkaline polymer electrolytes. *Energy Environ Sci* 2013;6:2912–15.
- [128] Zhu L, Pan J, Wang Y, Han J, Zhuang L, Hickner MA. Multication side chain anion exchange membranes. *Macromolecules* 2016;49:815–24.
- [129] Peng H, Li Q, Hu M, Xiao L, Lu J, Zhuang L. Alkaline polymer electrolyte fuel cells stably working at 80 °C. *J Pow Sour* 2018;390:165–7.
- [130] Pham TH, Olsson JS, Jannasch P. N-spirocyclic quaternary ammonium ionenes for anion-exchange membranes. *J Am Chem Soc* 2017;139:2888–91.
- [131] Chen N, Long C, Li Y, Lu C, Zhu H. Ultraprecise and high ion-conducting polyelectrolyte based on six-membered N-spirocyclic ammonium for hydroxide exchange membrane fuel cell applications. *ACS Appl Mater Interfaces* 2018;10:15720–32.
- [132] Chu X, Liu L, Huang Y, Guiver MD, Li N. Practical implementation of bis-six-membered N-cyclic quaternary ammonium cations in advanced anion exchange membranes for fuel cells: synthesis and durability. *J Membr Sci* 2019;578:239–50.
- [133] Wang X, Sheng W, Shen Y, Liu L, Dai S, Li N. N-cyclic quaternary ammonium-functionalized anion exchange membrane with improved alkaline stability enabled by aryl-ether free polymer backbones for alkaline fuel cells. *J Membr Sci* 2019;587:117135/1–10.
- [134] Pham TH, Olsson JS, Jannasch P. Poly(arylene alkylene)s with pendant N-spirocyclic quaternary ammonium cations for anion exchange membranes. *J Mater Chem A* 2018;6:16537–47.

- [135] Zhu H, Li Y, Chen N, Lu C, Long C, Li Z, Liu Q. Controllable physical-crosslinking poly(arylene 6-azaspiro[5.5] undecanium) for long-lifetime anion exchange membrane applications. *J Membr Sci* 2019;590:117307/1-10.
- [136] Pham TH, Olsson JS, Jannasch P. Effects of the N-alicyclic cation and backbone structures on the performance of poly(terphenyl)-based hydroxide exchange membranes. *J Mater Chem A* 2019;7:15895-906.
- [137] Lin B, Qiu L, Lu J, Yan F. Cross-linked alkaline ionic liquid-based polymer electrolytes for alkaline fuel cell applications. *Chem Mater* 2010;22:6718-25.
- [138] Guo M, Fang J, Xu H, Li W, Lu X, Lan C, Li K. Synthesis and characterization of novel anion exchange membranes based on imidazolium-type ionic liquid for alkaline fuel cells. *J Membr Sci* 2010;362:97-104.
- [139] Thomas OD, Soo KJWY, Peckham TJ, Kulkarni MP, Holdcroft S. Anion conducting poly(dialkyl benzimidazolium) salts. *Polym Chem* 2011;2:1641-3.
- [140] Araya SS, Zhou F, Liso V, Sahlin SL, Vang JR, Thomas S, Gao X, Jeppesen C, Kær SK. A comprehensive review of PBI-based high temperature PEM fuel cells. *Int J Hydro Energy* 2016;41:21310-44.
- [141] Bose S, Kula T, Nguyen TXH, Kim NH, Lau K-t, Lee JH. Polymer membranes for high temperature proton exchange membrane fuel cell: recent advances and challenges. *Progress Polym Sci* 2011;36:813-43.
- [142] Kraysberg A, Ein-Eli Y. Review of advanced materials for proton exchange membrane fuel cells. *Energy & Fuels* 2014;28:7303-30.
- [143] Peighambaroust SJ, Rowshanzamir S, Amjadi M. Review of the proton exchange membranes for fuel cell applications. *Int J Hydro Energy* 2010;35:9349-84.
- [144] Rosli RE, Sulong AB, Daud WRW, Zulkifley MA, Husaini T, Rosli MI, Majlan EH. A review of high-temperature proton exchange membrane fuel cell (HT-PEMFC) system. *Int J Hydro Energy* 2017;42:9293-314.
- [145] Henkensmeier D, Kim H-J, Lee H-J, Lee DH, Oh I-H, Hong S-A, Nam S-W, Lim T-H. Polybenzimidazolium-based solid electrolytes. *Macromol Mater Eng* 2011;296:899-908.
- [146] Henkensmeier D, Cho H-R, Kim H-J, Nunes Kirchner C, Leppin J, Dyck A, Jang JH, Cho E, Nam S-K, Lim T-H. Polybenzimidazolium hydroxides-Structure, stability and degradation. *Polymer Degradation and Stability* 2012;97:264-72.
- [147] Thomas OD, Soo KJ, Peckham TJ, Kulkarni MP, Holdcroft S. A stable hydroxide-conducting polymer. *J Am Chem Soc* 2012;134:10753-6.
- [148] Lin B, Dong H, Li Y, Si Z, Gu F, Yan F. Alkaline stable C2-substituted imidazolium-based anion-exchange membranes. *Chem Mater* 2013;25:1858-67.
- [149] Gu F, Dong H, Li Y, Si Z, Yan F. Highly stable N3-substituted imidazolium-based alkaline anion exchange membranes: experimental studies and theoretical calculations. *Macromolecules* 2013;47:208-16.
- [150] Price SC, Williams KS, Beyer FL. Relationships between structure and alkaline stability of imidazolium cations for fuel cell membrane applications. *ACS Macro Lett* 2014;3:160-5.
- [151] Hugar KM, Kostalik HAT, Coates GW. Imidazolium cations with exceptional alkaline stability: a systematic study of structure-stability relationships. *J Am Chem Soc* 2015;137:8730-7.
- [152] Wright AG, Fan J, Britton B, Weissbach T, Lee H-F, Kitching EA, Peckham TJ, Holdcroft S. Hexamethyl-p-terphenyl poly(benzimidazolium): a universal hydroxide-conducting polymer for energy conversion devices. *Energy Environ Sci* 2016;9:2130-42.
- [153] Fan J, Wright AG, Britton B, Weissbach T, Skalski TJJ, Ward J, Peckham TJ, Holdcroft S. Cationic polyelectrolytes, stable in 10 M KOH at 100 °C. *ACS Macro Lett* 2017;6:1089-93.
- [154] Holdcroft S, Fan J. Sterically-encumbered ionenes as hydroxide ion-conducting polymer membranes. *Curr Opin Electrochem* 2019;18:99-105.
- [155] You W, Hugar KM, Coates GW. Synthesis of alkaline anion exchange membranes with chemically stable imidazolium cations: unexpected cross-linked macrocycles from ring-fused ROMP monomers. *Macromolecules* 2018;51:3212-18.
- [156] You W, Padgett E, MacMillan SN, Muller DA, Coates GW. Highly conductive and chemically stable alkaline anion exchange membranes via ROMP of trans-cyclooctene derivatives. *Proc Natl Acad Sci U S A* 2019;116:9729-34.
- [157] Bauer B, Strathmann H, Effenberger F. Anion-exchange membranes with improved alkaline stability. *Desalination* 1990;79:125-44.
- [158] Robertson NJ, Kostalik HA IV, Clark TJ, Mutolo PF, Abruña HD, Coates GW. Tunable high performance cross-linked alkaline anion exchange membranes for fuel cell applications. *J Am Chem Soc* 2010;132:3400-4.
- [159] Zhang B, Kaspar RB, Gu S, Wang J, Zhuang Z, Yan Y. A new alkali-stable phosphonium cation based on fundamental understanding of degradation mechanisms. *ChemSusChem* 2016;9:2374-9.
- [160] Zhu T, Sha Y, Firouzaie HA, Peng X, Cha Y, Dissanayake D, et al. Rational synthesis of metallo-cations toward redox- and alkaline-stable metallo-polyelectrolytes. *J Am Chem Soc* 2020;142:1083-9.
- [161] Zhu T, Xu S, Rahman A, Dogdibegovic E, Yang P, Pageni P, Kabir MP, Zhou X-D, Tang C-B. Cationic metallo-polyelectrolytes for robust alkaline anion-exchange membranes. *Angew Chem Int Ed Engl* 2018;57:2388-92.
- [162] Hou HY. Recent research progress in alkaline polymer electrolyte membranes for alkaline solid fuel cells. *Acta Phys-Chim Sin* 2014;30:1393-407.
- [163] Ge X, He Y, Guiver MD, Wu L, Ran J, Yang Z, Xu T. Alkaline anion-exchange membranes containing mobile ion shuttles. *Adv Mater* 2016;28:3467-72.
- [164] Chen Y, Li Z, Chen N, Zhang Y, Wang F, Zhu H. Preparation and characterization of cross-linked polyphosphazene-crown ether membranes for alkaline fuel cells. *Electrochimica Acta* 2017;258:311-21.
- [165] Yang Q, Li L, Gao XL, Wu HY, Liu FH, Zhang QG, Zhu AM, Zhao CH, Liu QL. Crown ether bridged anion exchange membranes with robust alkaline durability. *J Membr Sci* 2019;578:230-8.
- [166] Zheng XY, Song SY, Yang JR, Wang JL, Wang LL. 4-formyl dibenzo-18-crown-6 grafted polyvinyl alcohol as anion exchange membranes for fuel cell. *Eur Polym J* 2019;112:581-90.
- [167] Gonçalves Biancolli AL, Herranz D, Wang L, Stehlíková G, Bance-Soualhi R, Ponce-González J, Ocón P, Ticianelli E A, Whelligan DK, Varcoe JR, Santiago EI. ETFE-based anion-exchange membrane ionomer powders for alkaline membrane fuel cells: a first performance comparison of head-group chemistry. *J Mater Chem A* 2018;6:24330-41.
- [168] Poynton SD, Slade RCT, Omasta TJ, Mustain WE, Escudero-Cid R, Ocón P, Varcoe JR. Preparation of radiation-grafted powders for use as anion exchange ionomers in alkaline polymer electrolyte fuel cells. *J Mater Chem A* 2014;2:5124-30.
- [169] Wang L, Peng X, Mustain WE, Varcoe JR. Radiation-grafted anion-exchange membranes: the switch from low- to high-density polyethylene leads to remarkably enhanced fuel cell performance. *Energy Environ Sci* 2019;12:1575-9.
- [170] Clark TJ, Robertson NJ, Kostalik IVHA, Lobkovsky EB, Mutolo PF, Abruña HD, Coates GW. A ring-opening metathesis polymerization route to alkaline anion exchange membranes: development of hydroxide-conducting thin films from an ammonium-functionalized monomer. *J Am Chem Soc* 2009;131:12888-9.
- [171] Hibbs MR, Fujimoto CH, Cornelius CJ. Synthesis and characterization of poly(phenylene)-based anion exchange membranes for alkaline fuel cells. *Macromolecules* 2009;42:8316-21.
- [172] Maurya S, Lee AS, Li D, Park EJ, Leonard DP, Noh S, Bae C, Kim YS. On the origin of permanent performance loss of anion exchange membrane fuel cells: electrochemical oxidation of phenyl group. *J Pow Sourc* 2019;436:226866/1-9.
- [173] Yokota N, Shimada M, Ono H, Akiyama R, Nishino E, Asazawa K, Miyake J, Watanabe M, Miyatake K. Aromatic copolymers containing ammonium-functionalized oligophenylene moieties as highly anion conductive membranes. *Macromolecules* 2014;47:8238-46.
- [174] Miyayoshi S, Yamaguchi T. Highly durable spirobifluorene-based aromatic anion conducting polymer for a solid ionomer of alkaline fuel cells and water electrolysis cells. *J Mater Chem A* 2019;7:2219-24.
- [175] Mahmoud AMA, Elsaghier AMM, Otsuji K, Miyatake K. High hydroxide ion conductivity with enhanced alkaline stability of partially fluorinated and quaternized aromatic copolymers as anion exchange membranes. *Macromolecules* 2017;50:4256-66.
- [176] Ono H, Kimura T, Takano A, Asazawa K, Miyake J, Inukai J, Miyatake K. Robust anion conductive polymers containing perfluoroalkylene and pendant ammonium groups for high performance fuel cells. *J Mater Chem A* 2017;5:24804-12.
- [177] Lee W-H, Kim YS, Bae C. Robust hydroxide ion conducting poly(biphenyl alkylene)s for alkaline fuel cell membranes. *ACS Macro Lett* 2015;4:814-18.
- [178] Carta M, Malpass-Evans R, Croad M, Rogan Y, Jansen JC, Bernardo P, McKeown NB. An efficient polymer molecular sieve for membrane gas separations. *Science* 2013;339:303-7.
- [179] Yang Z, Guo R, Malpass-Evans R, Carta M, McKeown NB, Guiver MD, Wu L, Tu X. Highly conductive anion-exchange membranes from microporous troger's base polymers. *Angew Chem Int Ed Engl* 2016;55:11499-502.
- [180] Hu C, Zhang Q, Lin C, Lin Z, Li L, Soyekwo F, Zhu A, Liu Q. Multi-cation crosslinked anion exchange membranes from microporous Tröger's base copolymers. *J Mater Chem A* 2018;6:13302-11.
- [181] Liu L, Chu X, Liao J, Huang Y, Li Y, Ge Z, Hickner MA, Li N. Tuning the properties of poly(2,6-dimethyl-1,4-phenylene oxide) anion exchange membranes and their performance in H₂/O₂ fuel cells. *Energy Environ Sci* 2018;11:435-46.
- [182] Diesendruck CE, Dekel DR. Water-A key parameter in the stability of anion exchange membrane fuel cells. *Curr Opin Electrochem* 2018;9:173-8.
- [183] Li Q, Peng H, Wang Y, Xiao L, Lu J, Zhuang L. The comparability of Pt to Pt-Ru in catalyzing the hydrogen oxidation reaction for alkaline polymer electrolyte fuel cells operated at 80 °C. *Angew Chem Int Ed Engl* 2019;58:1442-6.
- [184] Chen N, Lu C, Li Y, Long C, Li Z, Zhu H. Tunable multi-cations-crosslinked poly(arylene piperidinium)-based alkaline membranes with high ion conductivity and durability. *J Membr Sci* 2019;588:117120/1-10.
- [185] Dang H-S, Jannasch P. Alkali-stable and highly anion conducting poly(phenylene oxide)s carrying quaternary piperidinium cations. *J Mater Chem A* 2016;4:11924-38.
- [186] Tanaka M, Fukasawa K, Nishino E, Yamaguchi S, Yamada K, Tanaka H, Bae B, Miyatake K, Watanabe M. Anion conductive block poly(arylene ether)s: synthesis, properties, and application in alkaline fuel cells. *J Am Chem Soc* 2011;133:10646-54.
- [187] Lai AN, Guo D, Lin CX, Zhang QG, Zhu AM, Ye ML, Liu QL. Enhanced performance of anion exchange membranes via crosslinking of ion cluster regions for fuel cells. *J Pow Sourc* 2016;327:56-66.
- [188] He Y, Ge X, Liang X, Zhang J, Shehzad MA, Zhu Y, Yang Z, Wu L, Xu T. Anion exchange membranes with branched ionic clusters for fuel cells. *J Mater Chem A* 2018;6:5993-8.
- [189] He Y, Zhang J, Liang X, Shehzad MA, Ge X, Zhu Y, Hu M, Yang Z, Wu L, Xu T. Achieving high anion conductivity by densely grafting of ionic strings. *J Membr Sci* 2018;559:35-41.
- [190] Ge Q, Liang X, Ding L, Hou J, Miao J, Wu B, Yang Z, Xu T. Guiding the self-assembly of hyperbranched anion exchange membranes utilized in alkaline fuel cells. *J Membr Sci* 2019;573:595-601.
- [191] Park J-S, Park S-H, Yim S-D, Yoon Y-G, Lee W-Y, Kim C-S. Performance of solid alkaline fuel cells employing anion-exchange membranes. *J Pow Sourc* 2008;178:620-6.

- [192] Zhu L, Zimudzi TJ, Li N, Pan J, Lin B, Hickner MA. Crosslinking of comb-shaped polymer anion exchange membranes via thiol-ene click chemistry. *Polym Chem* 2016;7:2464–75.
- [193] Lee KH, Cho DH, Kim YM, Moon SJ, Seong JG, Shin DW, Sohn J-Y, Kim J-F, Young ML. Highly conductive and durable poly(arylene ether sulfone) anion exchange membrane with end-group cross-linking. *Energy Environ Sci* 2017;10:275–85.
- [194] Wu Y, Wu C, Varcoe JR, Poynton SD, Xu T, Fu Y. Novel silica/poly(2,6-dimethyl-1,4-phenylene oxide) hybrid anion-exchange membranes for alkaline fuel cells: effect of silica content and the single cell performance. *J Pow Sourc* 2010;195:3069–76.
- [195] Chu Y, Chen Y, Chen N, Wang F, Zhu H. A new method for improving the ion conductivity of anion exchange membranes by using TiO₂ nanoparticles coated with ionic liquid. *RSC Adv* 2016;6:96768–77.
- [196] Li X, Yu Y, Meng Y. Novel quaternized poly(arylene ether sulfone)/Nano-ZrO₂ composite anion exchange membranes for alkaline fuel cells. *ACS Appl Mater Interfaces* 2013;5:1414–22.
- [197] Yang C-C, Chiu S-J, Chien W-C, Chiu S-S. Quaternized poly(vinyl alcohol)/alumina composite polymer membranes for alkaline direct methanol fuel cells. *J Pow Sourc* 2010;195:2212–19.
- [198] Liao X, Ren L, Chen D, Liu X, Zhang H. Nanocomposite membranes based on quaternized polysulfone and functionalized montmorillonite for anion-exchange membranes. *J Pow Sourc* 2015;286:258–63.
- [199] Shi B, Li Y, Zhang H, Wu W, Ding R, Dang J, Wang J. Tuning the performance of anion exchange membranes by embedding multifunctional nanotubes into a polymer matrix. *J Membr Sci* 2016;498:242–53.
- [200] Gong C, Zhao S, Tsen W-C, Hu F, Zhong F, Zhang B, Liu H, Zheng G, Qin C, Wen S. Hierarchical layered double hydroxide coated carbon nanotube modified quaternized chitosan/polyvinyl alcohol for alkaline direct methanol fuel cells. *J Pow Sourc* 2019;441:227176/1–10.
- [201] Chen N, Liu Y, Long C, Li R, Wang F, Zhu H. Enhanced performance of ionic-liquid-coated silica/quaternized poly(2,6-dimethyl-1,4-phenylene oxide) composite membrane for anion exchange membrane fuel cells. *Electrochimica Acta* 2017;258:124–33.
- [202] Chen N, Long C, Li Y, Wang D, Zhu H. High-performance layered double hydroxide/poly(2,6-dimethyl-1,4-phenylene oxide) membrane with porous sandwich structure for anion exchange membrane fuel cell applications. *J Membr Sci* 2018;552:51–60.
- [203] Fan J, Zhu H, Li R, Chen N, Han K. Layered double hydroxide-polyphosphazene-based ionomer hybrid membranes with electric field-aligned domains for hydroxide transport. *J Mater Chem A* 2014;2:8376–85.
- [204] Chen N, Wang D, Long C, Li Y, Lu C, Wang F, Zhu H. Magnetic field-oriented ferroferric oxide/poly(2,6-dimethyl-1,4-phenylene oxide) hybrid membranes for anion exchange membrane applications. *Nanoscale* 2018;10:18680–9.
- [205] Yu E. Development of direct methanol alkaline fuel cells using anion exchange membranes. *J Pow Sourc* 2004;137:248–56.
- [206] Coutanceau C, Demarconay L, Lamy C, Léger JM. Development of electrocatalysts for solid alkaline fuel cell (SAFC). *J Pow Sourc* 2006;156:14–19.
- [207] Scott K, Yu E, Vlachogiannopoulos G, Shivare M, Duteanu N. Performance of a direct methanol alkaline membrane fuel cell. *J Pow Sourc* 2008;175:452–7.
- [208] Miyazaki K, Sugimura N, Kawakita K I, Abe T, Nishio K, Nakanishi H, Ogumi Z. Aminated perfluorosulfonic acid ionomers to improve the triple phase boundary region in anion-exchange membrane fuel cells. *J Electrochem Soc* 2010;157:A1153/1–4.
- [209] Varcoe JR, Slade RC, Lam How Yee E. An alkaline polymer electrochemical interface: a breakthrough in application of alkaline anion-exchange membranes in fuel cells. *Chem Commun (Camb)* 2006:1428–9.
- [210] Zhang F, Zhang H, Qu C, Ren J. Poly(vinylidene fluoride) based anion conductive ionomer as a catalyst binder for application in anion exchange membrane fuel cell. *J Pow Sourc* 2011;196:3099–103.
- [211] Pan J, Lu S, Li Y, Huang A, Zhuang L, Lu J. High-Performance alkaline polymer electrolyte for fuel cell applications. *Adv Funct Mater* 2010;20:312–19.
- [212] Bunazawa H, Yamazaki Y. Influence of anion ionomer content and silver cathode catalyst on the performance of alkaline membrane electrode assemblies (MEAs) for direct methanol fuel cells (DMFCs). *J Pow Sourc* 2008;182:48–51.
- [213] Mamlouk M, Wang X, Scott K, Horsfall JA, Williams C. Characterization and application of anion exchange polymer membranes with non-platinum group metals for fuel cells. *Proc Inst Mech Eng Part A J Power and Energy* 2011;225:152–60.
- [214] Mamlouk M, Scott K. Effect of anion functional groups on the conductivity and performance of anion exchange polymer membrane fuel cells. *J Pow Sourc* 2012;211:140–6.
- [215] Mamlouk M, Horsfall JA, Williams C, Scott K. Radiation grafted membranes for superior anion exchange polymer membrane fuel cells performance. *Int J Hydro Energy* 2012;37:11912–20.
- [216] Gao X, Yu H, Jia J, Hao J, Xie F, Chi J, Qin B, Fu L, Song W, Shao Z. High performance anion exchange ionomer for anion exchange membrane fuel cells, 7. *RSC Advances*; 2017. p. 19153–61.
- [217] Parka AM, Owczarczyka ZR, Garnera LE, Yang-Neyerlina AC, Longa H, Antunesa CM, Sturgeona R, Lindellb MJ, Hamrockb SJ, Yandrasitsb MA, Pivovar BS. Synthesis and characterization of perfluorinated anion exchange membranes. *ECS Trans* 2017;80:957–66.
- [218] PivovarBS. Advanced ionomers & MEAs for alkaline membrane fuel cells. DOE Hydrogen and Fuel Cells Program Review Project #FC147. https://www.hydrogen.energy.gov/pdfs/review18/fc147_pivovar_2018_o.pdf (33 pp). 2018;[accessed Jun 2018].
- [219] Ziv N, Mustain W E, Dekel D R. The effect of ambient carbon dioxide on anion-exchange membrane fuel cells. *ChemSusChem* 2018;11:1136–50.
- [220] Zheng Y, Omasta TJ, Peng X, Wang L, Varcoe JR, Pivovar BS, et al. Quantifying and elucidating the effect of CO₂ on the thermodynamics, kinetics and charge transport of AEMFCs. *Energy Environ Sci* 2019;12:2806–19.
- [221] Li D, Park EJ, Zhu W, Shi Q, Zhou Y, Tian H, et al. Highly quaternized polystyrene ionomers for high performance anion exchange membrane water electrolyzers. *Nature Energy* 2020;5:367–85.
- [222] Mustain WE, Kohl PA. Improving alkaline ionomers. *Nature Energy* 2020;5:359–60.
- [223] Wang M, Preston N, Xu N, Wei Y, Liu Y, Qiao J. Promoter effects of functional groups of hydroxide-conductive membranes on advanced CO₂ electroreduction to formate. *ACS Appl Mater Interfaces* 2019;11:6881–9.
- [224] Ahn Y, Kim D. Anion exchange membrane prepared from imidazolium grafted poly(arylene ether ketone) with enhanced durability for vanadium redox flow battery. *J Indust Eng Chem* 2019;71:361–8.
- [225] Chen D, Hickner MA, Agar E, Kumbur EC. Selective anion exchange membranes for high coulombic efficiency vanadium redox flow batteries. *Electrochem Commun* 2013;26:37–40.
- [226] Leung P, Shah AA, Sanz L, Flox C, Morante JR, Xu Q, et al. Recent developments in organic redox flow batteries: a critical review. *J Pow Sourc* 2017;360:243–83.